SHAPE AND SIZE ANALYSIS OF INTERFACES IN PARTICULATE MATERIALS

by
SANTOSH KUMAR

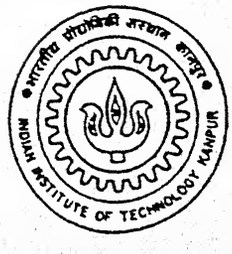

DEPARTMENT OF MATERIALS AND METALLURGICAL ENGINEERING
INDIAN INSTITUTE OF TECHNOLOGY KANPUR
APRIL, 1998

SHAPE AND SIZE ANALYSIS OF INTERFACES IN PARTICULATE MATERIALS

A Thesis Submitted
in partial fulfilment of the requirements
for thr degree of
MASTER OF TECHNOLOGY

by
SANTOSH KUMAR

To the
DEPARTMENT OF MATERIALS AND METALLURGICAL ENGINEERING
INDIAN INSTITUTE OF TECHNOLOGY KANPUR
APRIL, 1998

.....dedicated to

My Parents

and

BABA

CERTIFICATE

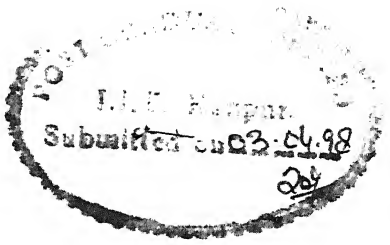

This is to certify that the work in this thesis entitled "*SHAPE AND SIZE ANALYSIS OF INTERFACES IN PARTICULATE MATERIALS.*" has been carried by SANTOSH KUMAR under my supervision and that it has not been submitted elsewhere for a degree.

(Dr. Sandeep Sangal)
Associate Professor

Department of Materials and Metallurgical Engineering
Indian Institute of Technology, Kanpur -208016

ACKNOWLEDGMENTS

I wish to express my gratitude and indebtedness to my supervisor Dr. Sandeep Sangal for his inspiration, encouragement and guidance throughout my thesis work. His constant advises made this work very interesting.

I would like to acknowledge the help, I got from Malikarjun and Shailesh throughout my work. I would also like to thank Kanchan for her cooperation at various stages.

I owe my thanks to my friends Telu, Navneet, Satyajeet, Yogendra.....who made my stay here a memorable one.

Santosh Kumar
Santosh Kumar

ACKNOWLEDGMENTS

I wish to express my gratitude and indebtedness to my supervisor Dr. Sandeep Sangal for his inspiration, encouragement and guidance throughout my thesis work. His constant advises made this work very interesting.

I would like to acknowledge the help, I got from Malikarjun and Shailesh throughout my work. I would also like to thank Kanchan for her cooperation at various stages.

I owe my thanks to my friends Telu, Navneet, Satyajeet, Yogendra.....who made my stay here a memorable one.

Santosh Kumar
Santosh Kumar

CONTENTS

LIST OF TABLES

LIST OF FIGURES

LIST OF SYMBOLS

θ	Angle between Z-axis and normal of the disc
ϕ	Angle between X-axis and projection of normal of the disc in XY plane.
R	Radius of the circular disc
a	Semi-major axis
b	Semi-minor axis
k	Shape factor (Ratio of the semi-minor axis to the semi-major axis)
R_S	Radius of the sphere
H	Tangent diameter
S_v	Surface area per unit volume
N_V	Number per unit volume
μ	Mean
σ^2	Variance
$\bar{l}$	Mean value of line lengths
$(\frac{\bar{1}}{l})$	Harmonic mean of line lengths

ABSTRACT

Interfaces between particles in particulate materials produce a microstructure consisting of line segments of varying lengths on the plane of polish. The interfaces between particles can have variuous sizes and shapes. In this work a stereological analysis has been conducted on circular and elliptical interfaces. Relationships between some stereological parameters, such as, mean tangent diameter and mean size of interfaces. and the length of segments have been derived. Stereological methods have been developed to unfold the shape and size distribution of inter-particle interfaces from the distribution of line lengths (which can be measured from observed microstructures).

In order to test the validity of the above analysis microstructures were generated by simulating discs of circular or elliptical shapes (discs represent the interfaces between particles) and various sizes distributed in 3-D space. This 3-D space was then sectioned by a random plane (which simulates the plane of polish) to obtain a microstructure consisting of line segments (intersections between discs and the random plane). Using the above methods, the line length distribution obtained from these microstructures was analyzed to extract information on the shape and size distribution of discs.

From the above it has been concluded that the stereological relationships and the methods developed for the transformation of line length distribution to disc size distribution are valid. It has also been shown that it is also possible to shed some light on the shape of the interfaces.

CHAPTER 1

INTRODUCTION

The structure of materials consists of several components such as grain-boundaries, interfaces, precipitates etc. The geometrical characteristics, such as size, shape etc., of these components have profound influence on mechanical properties. One of the well established correlation between microstructure and properties is the Hall-Petch [1] relationship between strength and grain size of metals and alloys. Size and size distribution of particles and grains have also been shown by many researchers to have an influence on various mechanical properties.

Figure 1.1 shows an example of a microstructure in a fully annealed polycrystalline specimen of 3% silicon iron. The sample shows many grain-boundaries or interfaces between the grains. These interfaces are planes in 3-dimensional structure and have different shapes and sizes. Figure 1.2 illustrates an SEM micrograph of a Ti-Al alloy. In the microstructure the particles of $TiAl_3$ have precipitated out from the alloy. The 2-D profile of the particles visible in the plane of polish[a] , shown in this figure are actually sections of 3-D polyhedra.

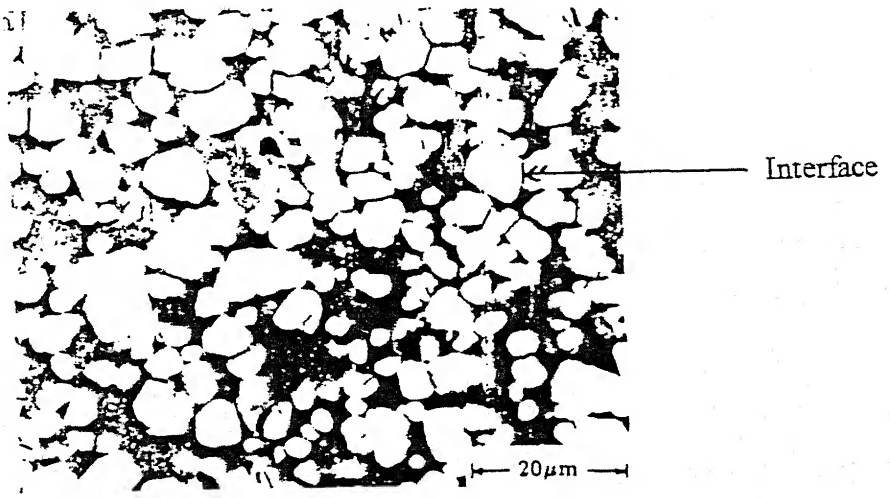

Figure 1.1 : SEM micrograph of Ti-Al alloy showing particles of $TiAl_3$

[a] A plane which intersects a sample to reveal its 2-D information, is called a plane of polish.

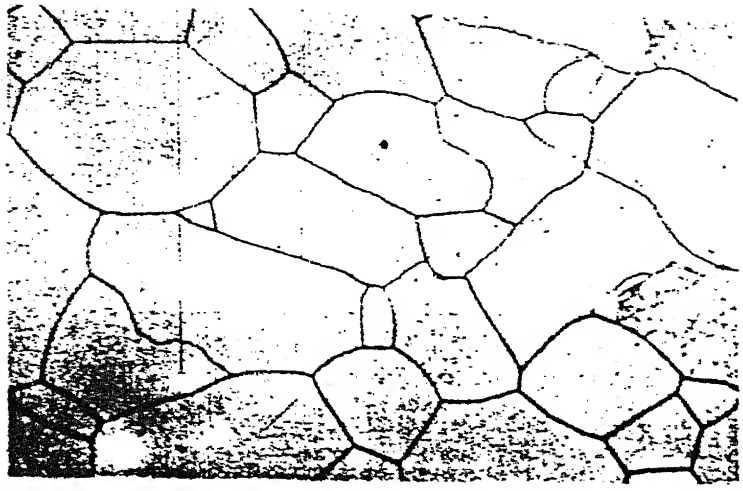

Figure 1.2 : Fully annealed polycrystalline specimen of 3% silicon iron, etched to reveal grain-boundaries.

In powder processing, powder is compacted and sintered for manufacturing purpose. At the beginning of compaction, the powder has a density approximately equal to apparent density. For a loose powder there is an excess of void space, no strength and a low coordination number. As the pressure is applied, the first response is rearrangement of the particles with filling of large pores, giving a higher packing coordination. Increasing pressure provides better packing and leads to decreasing porosity with the formation of new particle interfaces contacts [3]. During the initial stage of sintering a rapid growth of the interparticle necks or bonds is observed. In the intermediate stage, the pore structure become smoother and has interconnected cylindrical necks. In the latter stage of sintering, grain growth occurs, giving a larger average grain size with fewer grains. Figure 1.3 shows the progressive densification and grain growth during sintering. The interfaces between powder particles formed in the initial stage of sintering are converted into grain-boundaries in the final stage of sintering. In the following, the formation of snow as an example of a particulate material is briefly discussed.

The process of compaction, sintering and subsequent densification occurs in nature during the formation of snow. Snow is basically a granular material consisting of ice particles which are bonded to their immediate neighbours through inter-particle bonds. Pile-up of snow on the ground undergoes sintering under pressure generally at temperatures close to its melting point. The deformation behaviour of snow on application of pressure can be described in the following manner:

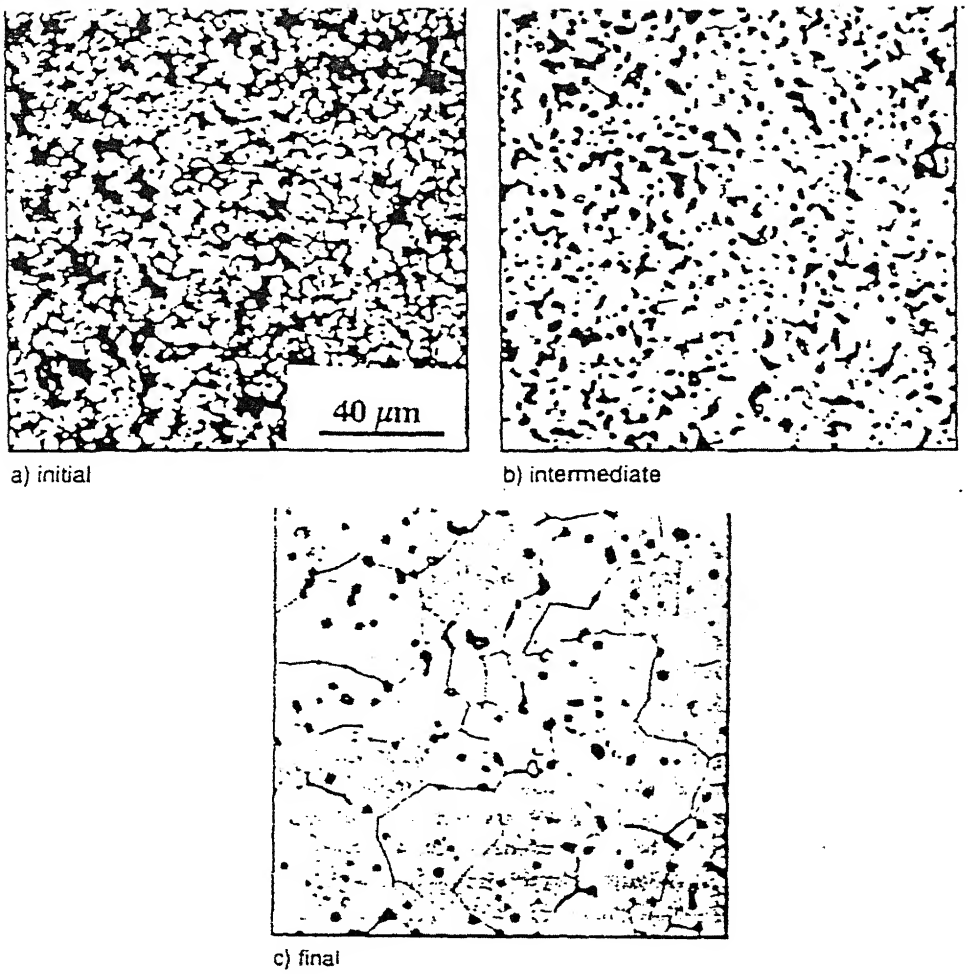

Figure 1.3 : The progressive densification and grain growth during sintering.

Bonds established between coordinating particles in a loose pack of snow are not capable of withstanding high loads. Many bonds between ice particles, therefore, undergo an immediate fracture on the application of external load. Fracture of a majority of initial bonds provide an opportunity for more efficient packing of particles by their readjustment and the mass now occupies a smaller volume. The extent of bond fracture and particle readjustments, however, depends on the initial particle arrangement and the magnitude of the externally applied load. Fracture of bonds and readjustment is called stage I of deformation of snow.

From stage II onwards the structure deforms without any further readjustment of its particles. Under these conditions, the irreversible deformation of snow continues to occur by the time dependent growth of inter-particle bonds. The strain rate in stage II keeps decreasing as the deformation proceeds because the effective pressure on inter-particle bonds decreases as their total area on a given particle increases. Soon the strain rate reaches a steady state and at this point, stage II of deformation terminates. Figure 1.4 shows the vertical snow profile of microstructure immediately after mechanical processing. The ice particles are shown in white while the pores appear black. The pore volume can be reduced by further applying pressure or by increasing the time of mechanical processing [5].

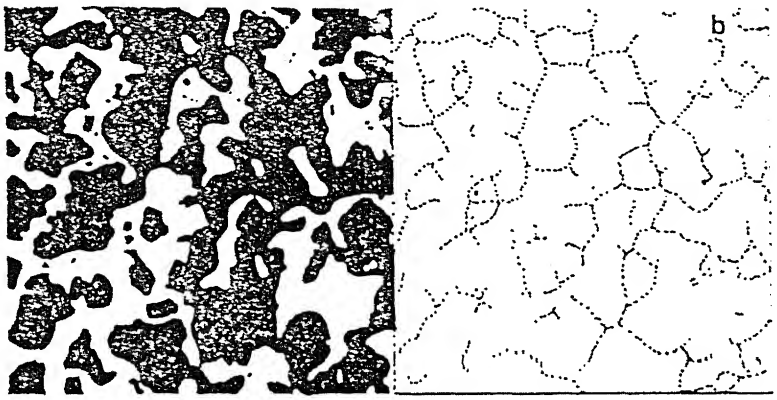

Figure 1.4 : Verticle snow profile of microstructure after mechanical processing.
(a) binary image of microstructure (b) grain skeleton

In the formation of snow from ice particles, Kry [7] assumed the bonds between ice particles to have the shape of circular discs. In snow structure, it is necessary to find out the bond radius between two grains because during deformation the largest stress concentrations occur at the bond since the cross-sectional area is smaller than that of associated grains. Owing to the increased stress concentration through the neck region, any plastic flow which occurs will generally occur in the necks rather than in the grain bodies. These necks, therefore, play a major role in determining the behavior during loading. The changes in the neck sizes can be used to measure the plastic flow.

Another significant factor controlling the mechanical behavior of snow is the number of bonds per grain (3-dimensional coordination number). As the number of bonds per grain increases, more load can be supported, thereby providing a mechanism for reducing the stress concentration in a given bond. If, for a given loading, the stress in a bond can be reduced, then the probability of its breaking will be reduced. If the stress is reduced in a large enough number of bonds, the overall load-bearing capacity of the snow can be increased [8].The degree of bonding between grains and the pore length (or the mean free distance between grains) is considered to control the mechanical properties. Connected with these are the number of grains and bonds per unit volume as well as the free grain surface area per unit volume. Larger the number of bonds and/or bigger the radius, the higher the resistance the material offers to the deformation and higher will thus be the modulus as shown in figure 1.5.

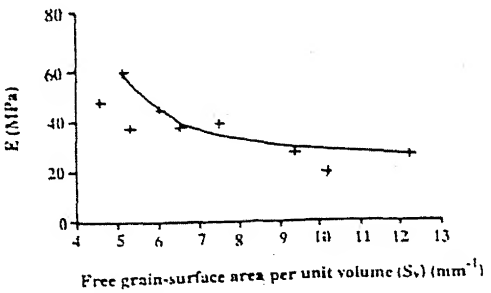

Figure 1.5 : Dependence of Young's modulus on free grain-surface area per unit volume.

The mean 3-dimensional bond radius is a significant parameter for pressure sintering as for bond strength and fracture. The bond radius comes out to be significant parameter for the deformation of snow. However, it turns out that instead of individual bond areas formed on a single particle, it is the

ratio of total bond area and the initial free surface area of a grain which plays a critical role in affecting the deformation of snow. The variation of this ratio i.e. S_b/S_0, during deformation of snow has been shown in figure 1.6..

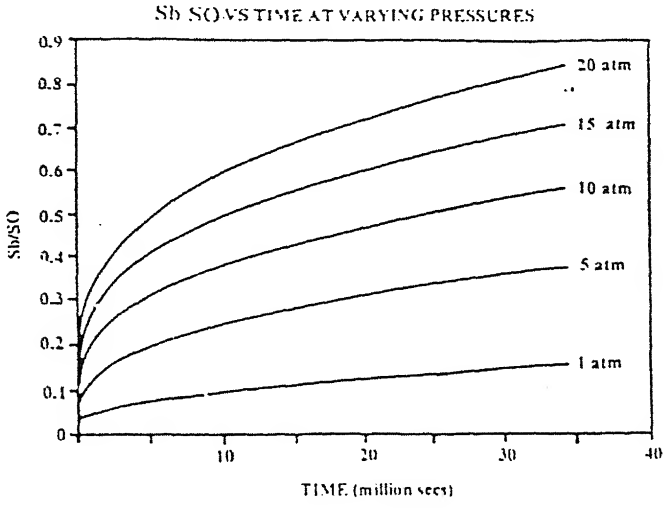

Figure 1.6 : S_b S_o versus time at varying pressures.

This study attempts to analyze the size and shape of interfaces between particles, grains etc. and also thin discs like precipitates in multi-phase and particulate materials. The present study focuses on the shape and size analysis of interfaces/grain-boundaries in particulate materials but is restricted only to circular and elliptical shapes. In this study, the interfaces between particles appear as lines when such a 3-D structure is intersected by a sectioning plane (i.e., plane of polish). these lines have varying lengths as can be observed in figure 3.1. From the distribution of these line lengths it is possible to find the shape and distribution of interfaces/grain-boundaries in 3-dimensional structure by taking various assumptions into account.

In this work, an attempt is made to develop analyses techniques for the line length distribution to obtain the following objectives.

1. To develop relationships for some basic stereological parameters, such as, surface area / volume (S_V), Number of interfaces / volume (N_V), Number of intercepts / length (N_L), Number of profiles / area (N_A), Length of profile / area (L_A) and average value of line lengths.

2. To develop a transform for estimating the distribution of circular and elliptical disc sizes in the 3-D structure from the measurement of the line lengths distribution.

3. To analyze the shape of the discs or the interfaces.

In the next chapter, some basic principles of stereology which have been used in subsequent analyses, are discussed.

CHAPTER 2

FUNDAMENTAL CONCEPTS IN STEREOLOGY

Stereology is a body of mathematical methods relating 3-dimensional parameters defining the structure to 2-dimensional measurements obtainable on sections of the structure. Using stereology it is possible to give quantitative interpretation of 2-dimensional observations in terms of 3-dimensional observations. Mathematical methods have been developed which allow observations made on sections to be interpreted in terms of spatial structure of the specimen [11].

This chapter deals with some of the fundamental concepts in stereology, which are discussed in the subsequent sections.

2.1 Random Sectioning

Figure 2.1 shows a specimen intersected by a plane of polish. The plane of polish is a plane which cuts the specimen to provide a surface for microstructural observations. The orientation (θ,ϕ), of the sectioning plane is defined by its normal which makes an angle θ with z axis and whose projection on XY plane makes an angle ϕ with x-axis.

Consider a line OA which is normal to the section plane and passes through the origin as shown in Figure 2.1. The section plane T is defined by the distance from the origin at which the plane makes an intersection with the specimen. The distance from the origin to the section plane in the direction (θ,ϕ) is given by r with range $\{-\infty < r < \infty\}$. Thus the plane T is uniquely defined by $T = T(\theta,\phi,r)$. Here θ and ϕ have the range $\{0 \le \theta \le \pi,\ 0 \le \phi \le 2\pi\}$. In order to find a random plane

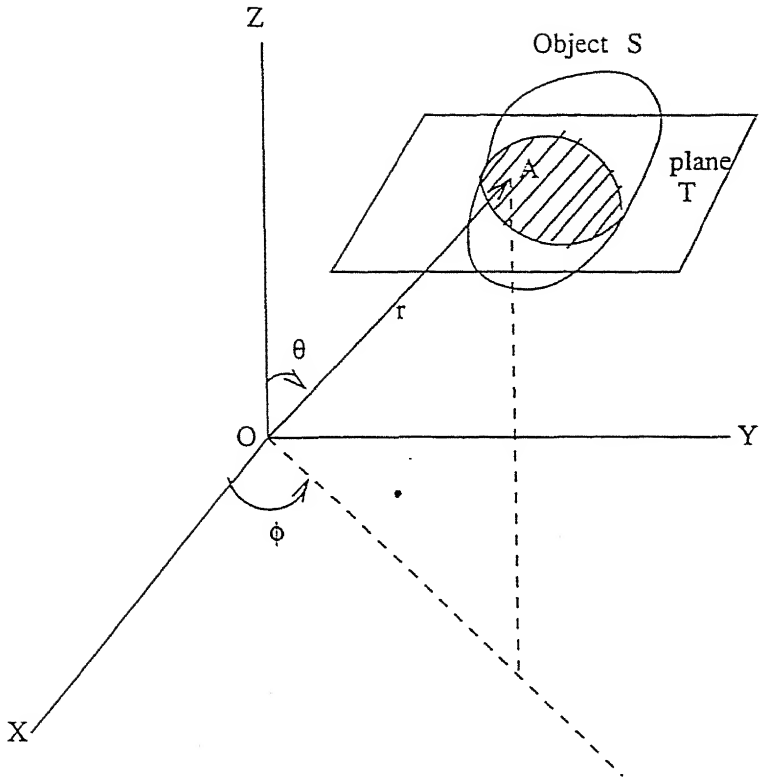

Figure 2.1 : Intersection of specimen and plane of polish.

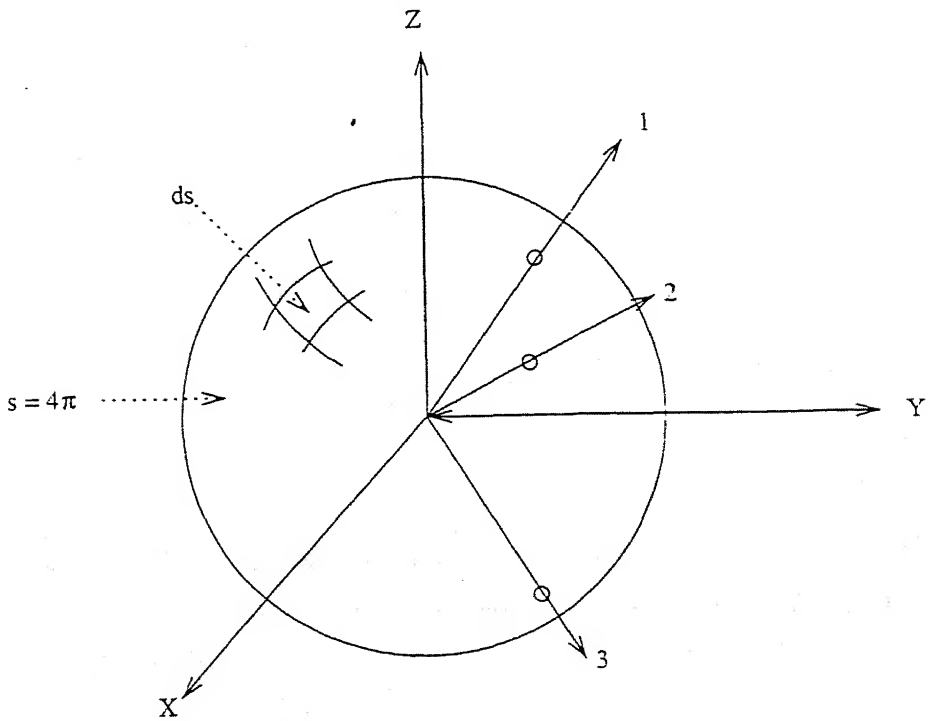

Figure 2.2 : Intersection of lines on sphere surface.

which intersects the specimen S, assign random values to θ,ϕ and r within their specified ranges. By assigning random values to θ,ϕ and r, one can obtain `Isotropic Uniform Random' (IUR) planes [12].

2.2 Averaging with Respect to Orientation

Consider a sphere of unit radius with centre at the origin of XYZ coordinate, as shown in figure 2.2. This figure shows three rays 1, 2 and 3 which are emanating from the origin. For random orientation the intersecting points between the rays and the sphere must be homogeneously dispersed over the sphere surface. The sphere surface can be subdivided into a large number of very small units of area 'ds'. Now, the probability that a ray crosses one of these units `ds' can be written as

$$P_r = \frac{ds}{Surface.area.of.sphere} = \frac{ds}{4\pi} \tag{2.1}$$

Figure 2.3 shows a line whose orientation is defined by two angles θand ϕ, where θ is the angle between the line and z-axis and ϕ is the angle between the x-axis and the projection of the line onto x-y plane. The range of variation of angles θ and ϕ is 0 to π and 0 to 2π respectively. In order to find out the probability that a line will have orientation (θ,ϕ), i.e. it will lie in the range {θ/(θ+dθ); ϕ/(ϕ+dϕ)}, a small quadrangular on the sphere surface is made by sweeping angles dθ and dϕ around the line OA in figure 2.3. The area of this quadrangular at a particular orientation (θ,ϕ) is given by

$$(sin\theta . d\theta).d\phi \tag{2.2}$$

The area of this small quadrangular is not equal but is different for different orientations. This wedge-shaped region tapers to width 0 as the line approaches to z-axis. i.e. as θ→0.

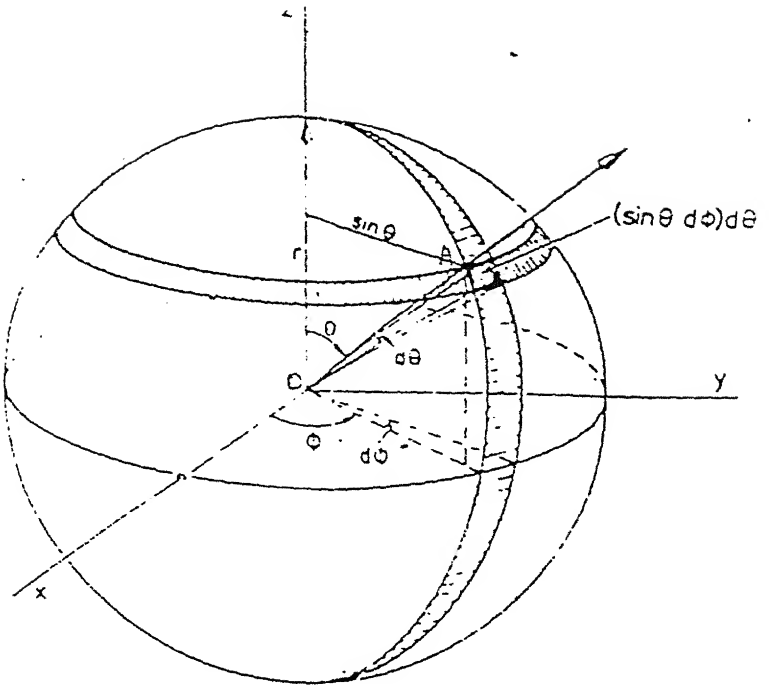

Figure 2.3 : Orientation in 3-dimensional space [13].

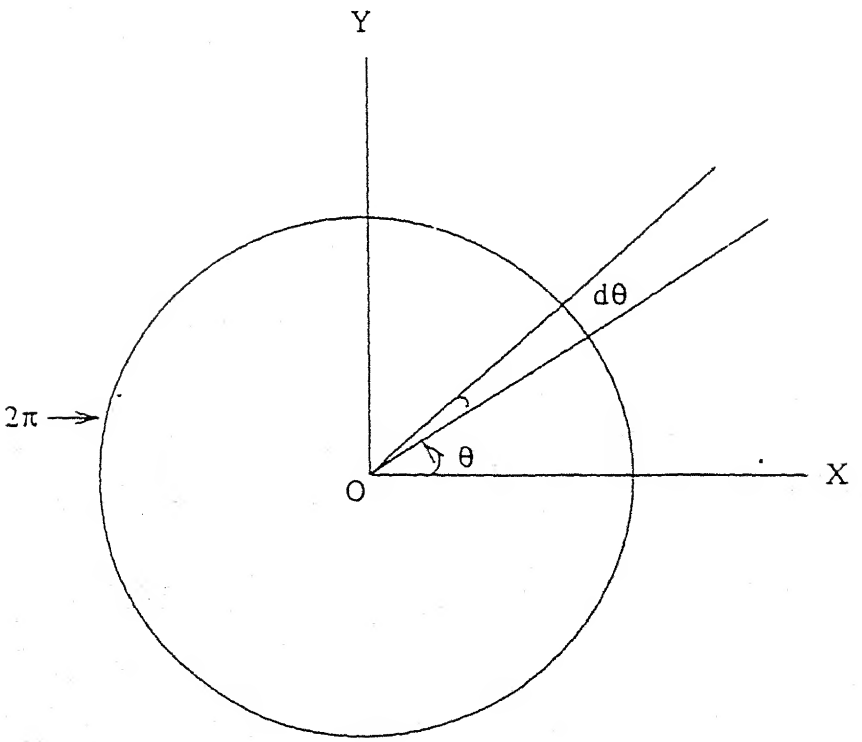

Figure 2.4 : Orientation in 2-dimensional space.

Probability of a line oriented in the range $\{\theta/(\theta+d\theta);\ \phi/(\phi+d\phi)\}$ can now be defined as the ratio of the area of the small quadrangular shape region to the area of the sphere and is given by

$$P_r(\theta,\phi) = \frac{\sin\theta.d\theta.d\phi}{4\pi} \tag{2.3}$$

The random orientations are uniformly distributed over the orientation sphere with probability density given by equation (2.1).

In order to find the average value of any parameter $p_m(\theta,\phi)$ which varies with orientation, integrate the product of parameter and probability over the whole range of θ and ϕ. Thus, the average value of parameter $P_m(\theta,\phi)$ is given by

$$\overline{p}_m = \frac{1}{4\pi}\int_o^{2\pi}\int_o^{\pi} p_m(\theta,\phi).\sin\theta.d\theta.d\phi \tag{2.4}$$

Averaging with respect to orientation in 2-dimension follows a procedure which is analogous to that in 3-dimension. Consider a circle of unit radius with centre at the origin of XY coordinates as shown in figure 2.4. The orientation of a line in 2-dimension is defined by only one angle θ which the line makes with x-axis. as shown in figure 2.4. Probability of finding a line in the range $\{\theta/(\theta+d\theta)\}$ is given by

$$P(\theta) = \frac{d\theta}{2\pi} \tag{2.5}$$

The mean value of any parameter $p_m(\theta)$ is given by the integration of the product of parameter and probability $P(\theta)$ over the whole range of θ, i.e., 0 to 2π :

$$\overline{p}_m = \frac{1}{2\pi}\int_o^{2\pi} p_m(\theta)\,d\theta \tag{2.6}$$

2.3 General Conditions for the Validity of Stereological Principles:

In order to choose a random point from the sample S from which the random plane passes, it is necessary to identify a sufficiently large number of uniformly distributed points in S. Then, one of these points is selected randomly. It is also necessary to ensure that the section plane is randomly oriented i.e. it has random values of θ, ϕ and r.

Very often, however, the specimen S is itself a sample from a much larger body W and the area of the section used for microscopic study is very small compared to the size of W. It is called as "extended case". For the extended case, where the section is cut from an IUR random sample of the very large specimen, arbitrary sections yield unbiased ratio estimators.

The analogous conditions prevail with respect to "cutting" the specimen with a test line. In the extended case arbitrary line sections of the sample S out of the specimen W yield unbiased ratio estimators, provided S is an IUR sample of W [14].

2.4 Basic Stereological Parameters

For every structure, there are two types of parameters. The parameters such as 'surface area of second phase particles per unit volume and number of particles per unit volume, which describe the properties of 3-D structures . While other parameters such as number of intercepts per unit length and length per unit area' termed as 2-D parameters, describe the properties of microstructure observed on the plane of polish. There is a certain relationship between the 2-D and 3-D parameters. Some of the basic relations are discussed in the following subsections.

2.4.1 Surface density, S_V

Consider a cube of dimension `l'. The cube contains second phase particles, as shown in Figure 2.5. The second phase particles are randomly oriented in the cube. Suppose the surface of the second phase particles is represented by a polyhedral surface formed of very small polygons of equal area 'ds', as shown in figure 2.6. If 'N' is the number of polygons covering the surface then the total surface area S_T of the particle is given by

$$S_T = N.ds \tag{2.7}$$

The surface of the second phase particle is assumed to be isotropic, i.e. that the surface elements 'ds' takes all possible orientations in space. Choose randomly one of these surface elements and suspend it in the cube as shown in figure 2.7 . Section this structure with a test line parallel to z-axis. The probability that a random test line parallel to z-axis will intersect the surface element 'ds' will be given by the ratio of the area of the orthogonal projection of 'ds', denoted as A_p, to the orthogonal projection of cube, which is l^2 :

$$P_{r1}(I) = \frac{A_p(\theta,\phi)}{l^2} \tag{2.8}$$

and the average probability of intersection is given by

$$P_r(I) = \frac{\overline{A_p}}{l^2} \tag{2.9}$$

where $\overline{A_p}$ is the projected area averaged over all the orientation.

It is clear from figure 2.7 that the projected area $A_p(\theta,\phi)$ is independent of angle o and depends only on the angle θ. therefore. the value of $A_p(\theta,\phi)$ is given by

$$A_p(\theta,\phi) = ds.cos\theta \tag{2.10}$$

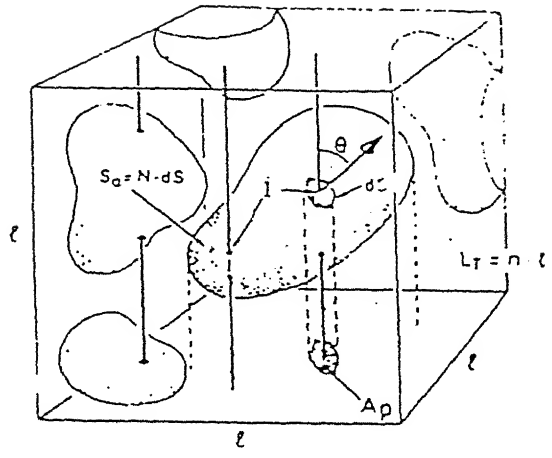

Figure 2.5 : Surface density estimation from intersection count on test lines [15].

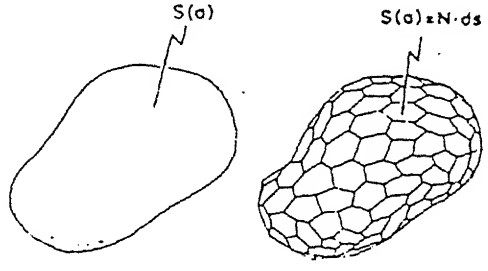

] Figure 2.6 : Polyhedral approximation of smooth surface [15].

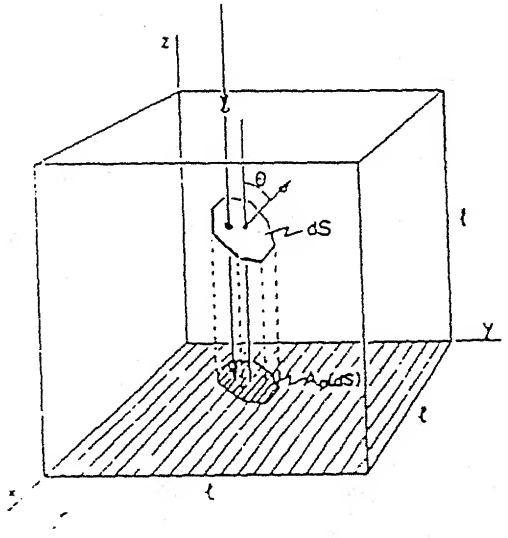

Figure 2.7 : Probability of hitting a surface element and its dependance on θ and ϕ [15].

The average value of $A_p(\theta)$ is given by the integration of the product of $A_p(\theta,\phi)$ with the orientation probability density $P_r(\theta,\phi)$ over the entire range of θ and ϕ. Thus, from equations (2.4) and (2.10), the average projected area is given by

$$\overline{A_p} = \frac{1}{4\pi} \int_0^{2\pi} \int_0^{\pi} ds.cos.\theta.sin\theta.d\theta.d\phi = \frac{1}{2} ds \qquad (2.11)$$

From equations (2.9) and (2.11) the probability of intersection between the surface element and one of the test lines is given by

$$P_r(I) = \frac{I}{2} \frac{ds}{l^2} \qquad (2.12)$$

In the case of n test lines each of length L the expected number of intersections E(I), between test lines and particle becomes

$$E(I) = P_r(I).N.n = \frac{I}{2} \frac{ds}{l^2} N.n = \frac{I}{2} S \frac{L}{l^3}$$

or,

$$\frac{E(I)}{L} = \frac{1}{2} \frac{S}{V}$$

From above

$$S_V = 2.N_L \qquad (2.13)$$

where S_V is the surface area of second phase particles per unit volume = S/V and N_L is the number of intercepts made by test lines per unit length = E(I)/L .

2.4.2 Boundary Density L_A

In the figure 2.8a profile boundaries form a curve of length L, if the curve is smooth it can be cut into infinitesimal straight line segments of equal length 'dL' such that

$$L = \int_{Over.the.curve} .. dL = n.dL \qquad (2.14)$$

where, n is the number of infinitesimal line segments. The curve is assumed to be isotropic such that all the orientations of the segment dL are equally likely. A grid of parallel equidistant test lines are placed onto the section plane, as shown in figure 2.8b. The distance between the test lines (d) is kept greater than the length of line segment in order to avoid more than one intersections of a line segment with test lines. Suppose N is the number of intersections made by line segments on to the test lines. The probability of intersection of a line segment with a test line T_1 is given by

$$P_r\{dL / T_1\} = N / n \qquad (2.15)$$

The value of m, the projection of dL onto the orthogonal complement to the grid is given by

$$m = dL \cos\theta \qquad (2.16)$$

The probability that the element dL intersects a test line T_1 of the grid is given by

$$P_r\{dL / T_1\} = m / d = \frac{dL.\cos\theta}{d} \qquad (2.17)$$

For isotropic orientation of dL, θ must vary uniformly over the range $\{0 < \theta < 2\pi\}$ and the average probability of intersection is given by (using equation (2.6))

$$P_r\{dL / T_1\} = \frac{1}{2\pi}\int_0^{2\pi} P_r\{dL / T_1\}\, d\theta \qquad (2.18)$$

From equations (2.15), (2.17) and (2.18):

$$\frac{2.dL}{\pi.d} = N / n \qquad (2.19)$$

From equations (2.14) and (2.19),the length, L of the boundary in figure 2.8a is given by

$$L = \frac{\pi}{2} N.d \qquad (2.20)$$

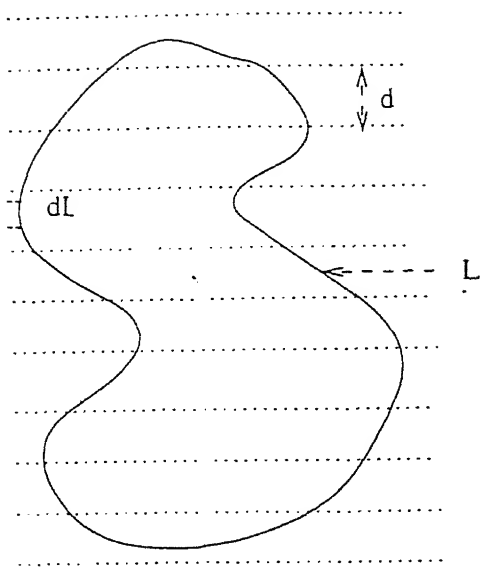

Figure 2.8 (a) : Profile boundary placed on grid of lines.

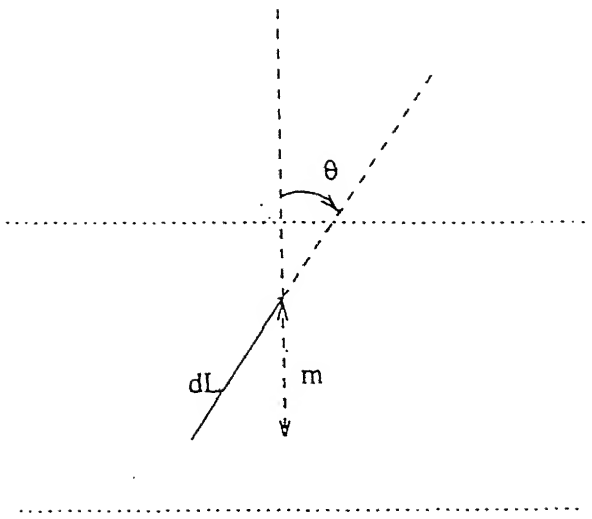

Figure 2.8 (b) : Probability that line segment intersects grid of lines.

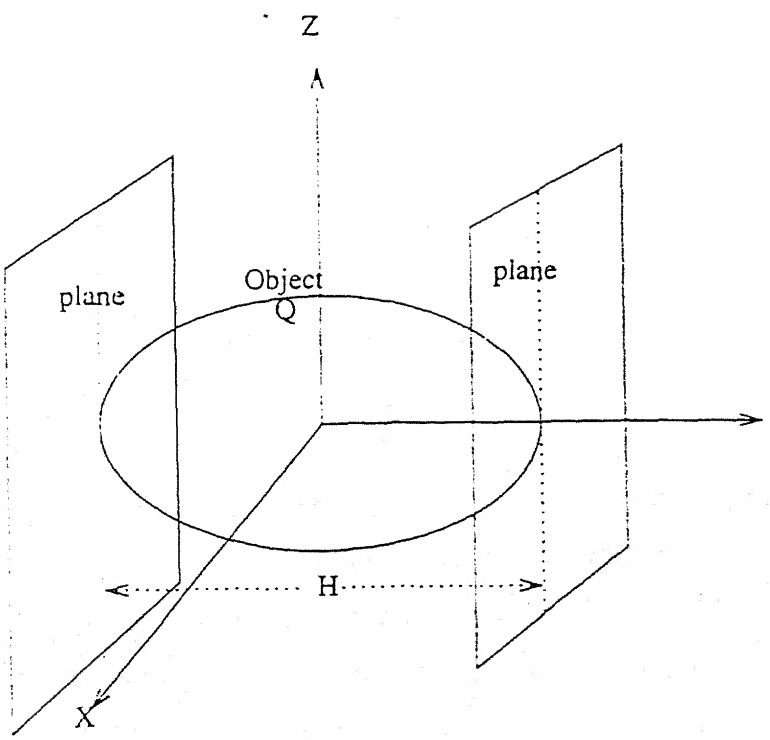

Figure 2.9 : Tangent diameter.

If both the curve and the test grid T_1 are enclosed in an area A, the length of test line is : L_1 = A/d. Substituting the value of d in equation(2.20) the following relationship between the curve length density, L_A and the number of intersections per unit test line length, N_L is obtained as:

$$L_A = \frac{L}{A} = \frac{\pi}{2}.\frac{N}{L_l} = \frac{\pi}{2} N_L \qquad (2.21)$$

2.4.3 Relationship between Surface Density in 3-D Space and Length Density in 2-D Space.

It is clear that on combining equations (2.13) and (2.21), one gets the following relationships between length density L_A and surface density S_V :

$$S_V = \frac{4}{\pi} L_A \qquad (2.22)$$

Stereological relations given by equations (2.13), (2.21) and (2.22) are statistically exact relationships. These relationships are orientation independent and consequently do not depend on the shape of the objects. However, there are other stereological parameters which can be estimated only if the shape of the objects are known. Some of these parameters are discussed in the following sections.

2.5 Tangent Diameter

"Tangent diameter of a particle in a particular direction is the distance between two parallel planes having their normals in the same direction and are tangent to the particle", as shown in figure 2.9. Suppose Q is a particle whose centre coincides with the origin of the XYZ coordinate. The distance between two parallel planes tangent to the particle is denoted as the tangent diameter H, as shown in the figure 2.9. The notation for tangent diameter in a particular direction (θ,o) is given by $H(\theta,\phi)$.

2.5.1 Average Tangent Diameter

Average tangent diameter means the average of all the tangent diameters found along different directions (θ,ϕ) . Therefore, the average tangent diameter, $\overline{H}$ is given by (using equation (2.4)):

$$\overline{H} = \frac{1}{4\pi}\int_o^{2\pi}\int_o^{\pi} H(\theta,\phi)\, \sin\theta\, d\theta\, d\phi \qquad (2.23)$$

It is clear from above discussion that the average tangent diameter is dependent on the shape of the particle.

The value of average tangent diameter for some particles are given below [16]

Table 2.1: Average Tangent Diameters, $\overline{H}$

Particle Shape	Characteristic Dimension	Average Tangent Diameter
Sphere	radius R	2 R
Cylinder	length l, radius r	(l + pR)/2
Hemisphere	radius R	(1 + p/4)R
Parallelepiped	edge lengths: a,b,c	(a + b + c)/2
Cube	edge length: a	3a/2

2.6 Numerical Density of Particles

In this section the relationship between the number of profiles seen on a random section and the number of objects can be established [17]. The objects in this case are discrete particles which are contained in the unit volume of the structure, as shown in the figure 2.10 . Assume a large number of particles (n_o) to be enclosed in a very large space (V_T) such that the numerical density of the particles(N_v) is given by

$$N_V = n_o / V_T \tag{2.24}$$

As shown in figure 2.10, the sample is sectioned by a test plane of area A_T. On this n_p number of particle profiles are observed which have their centers within A_T. The numerical density of profiles N_A is given by

$$N_A = n_P / A_T \tag{2.25}$$

In order to find a relationship between N_A and N_V, the following conditions need to be specified.

1. The particles must be convex solids, so that a plane intersecting the particle at any orientation will produce one profile only.

2. The particles must be randomly oriented within the space and their number must be so large that all orientations between particle and test plane are equally likely.

3. The size of the sample space should be such that the number of particles it contains is very large.

The sample space is randomly sectioned by a plane parallel to X-Z plane and is defined by a cube of volume $V_T = l^3$, so that the section Area is given by

$$A_T = l^2 \tag{2.26}$$

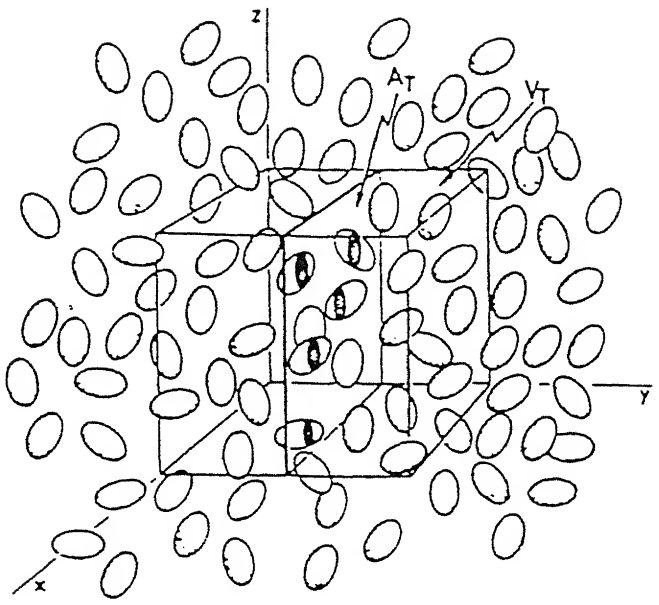

Figure 2.10 : Sectioning of randomly oriented particles by a section plane [18].

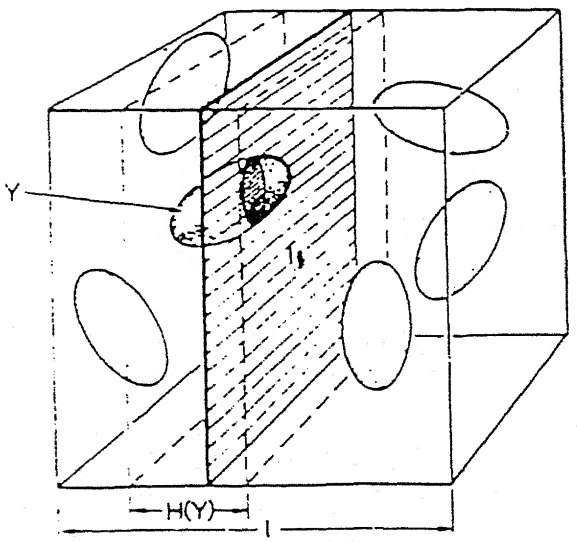

Figure 2.11 : Probability of cutting a random particle [18].

Probability of cutting a single particle Y by the random section plane is given by the ratio of the projections of both particles and containing space on to the orthogonal complement to the section plane as shown in figure 2.11 .

$$P_r\{Y / T_1\} = H(Y) / l \tag{2.27}$$

Considering all possible orientations the probability to cut any one of the particles is given by

$$P_r\{Particle / T_1\} = \overline{H} / l \tag{2.28}$$

The expected number of profiles on section T_1 can be written as

$$n_p = n_{0.} \overline{H} / l \tag{2.29}$$

Dividing both sides by l^2

$$n_p / l^2 = n_{0.} \overline{H} / l^3 \tag{2.30}$$

Numerical density, N_A, of particles on 2-D section can be related to the numerical density of particles, N_V, in 3-D space using equations (2.24), (2.25) and (2.30) :

$$N_A = N_V . \overline{H} \tag{2.31}$$

If the particle population represents a mixture of different sizes and shapes of particles, one can specify $\overline{H}_j$ for each size and shape class and the relative frequency f_j for each class. The total numerical density N_V is the sum of the numerical densities of the particles belonging to each class (N_{vj}).

$$N_V = \sum_j N_{V_j} \tag{2.32}$$

For each class the numerical profile density is given by

$$N_{A_j} = N_{V_j} . \overline{H}_j \tag{2.33}$$

And the total profile density can be written as

$$N_A = \sum_j N_{A_j} = \sum_j N_{V_j} . \overline{H}_j \tag{2.34}$$

or,

$$N_A = N_V . [\sum_j f_j . \overline{H}_j] \tag{2.35}$$

where, $f_j = N_{V_j} / N_V$, is the frequency of the j^{th} class of particles. The term in the bracket of equation (2.35) represents the weighted average of the mean tangent diameters.

2.7 Size Distribution of Section Profiles when Spheres are Randomly Sectioned

The intersection of a sphere with a plane produces a circle on the section plane. The size of the profile (circle) depends on the distance of plane from the centre of sphere. The maximum size of profile is obtained when the plane passes through the centre of sphere. For a sphere of radius R_s ,the profile size can have radius between 0 and R_s depending on the distance of the plane from the centre of sphere.

2.7.1 Spheres of Constant Size

Figure 2.12 shows a sphere of radius R_s placed in the XYZ coordinate system with its centre at the origin. A plane perpendicular to the z-axis makes an intersection with this sphere. Each section will produce a circular profile whose radius r will depend on the position of the section plane with respect to Z-axis . The value of radius r of a circular profile obtained by intersecting a sphere of radius R_s at a height z from the origin by a section plane is given by

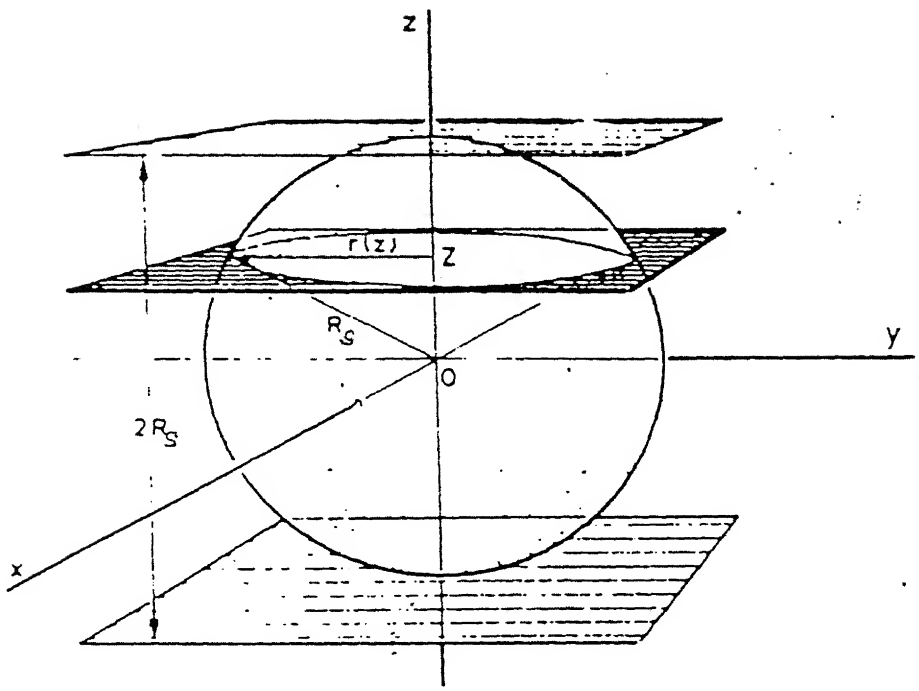

Figure 2.12 : Sectioning of sphere of radius R_s by a plane at height z from the origin.

$$r = \sqrt{R_s^2 - z^2} \tag{2.36}$$

Differentiating the above equation with respect to r gives:

$$dz = \frac{r}{\sqrt{R_s^2 - r^2}} dr \tag{2.37}$$

Probability of cutting a sphere of radius R_s between height z to z+dz by a random horizontal section plane is given by

$$P_r(z) = \frac{dz}{2R_s} \tag{2.38}$$

where $2R_s$ is the tangent diameter of the sphere of radius R_s as shown in Figure 2.12. The radii of circular profiles, obtained from intersection of sphere and plane at a height in between z and z+dz, will vary from r+dr to r respectively. Since same size circular profiles will also be obtained in between -z and -z+dz, the probability of radius of circular profiles lying between r and r+dr will be given by

$$P_r(z) = \frac{dz}{R_s} \tag{2.39}$$

From equations (2.37) and (2.39):

$$P(r) = \frac{r\,dr}{R_s\sqrt{R_s^2 - r^2}} \tag{2.40}$$

The probability density of radii of circular profiles can be written as

$$p(r) = \frac{r}{R_s\sqrt{R_s^2 - r^2}} \tag{2.41}$$

The mean value of radii of circular profiles is given by

$$\bar{r} = \int_0^{R_s} r.p(r)\,dr = \frac{1}{4}\pi R_s \tag{2.42}$$

2.7.2 Derivation of Sphere size Distribution from a Measured Distribution of Profile Sizes

Suppose that the spheres are distributed inside a cube and the size of the spheres vary from 0 to R_{smax}. Let the probability distribution of radius R_s have density $N_V(R_s)$, so that $N_V(R_s)\, dR_s$ is the number of spheres per unit volume whose radii lie in the range (R_s /R_s+dR_s). The probability distribution of profile radii have density $N_A(r)$ so that $N_A(r)\, dr$ is the number of circles per unit area, whose radii lie in the range (r/ r+dr). The relationship between $N_A(r)$ and $N_V(R_s)$ is given by

$$N_A(r)\, dr = \int_r^{R_{smax}} N_V(R_s).P_{R_s}\ P_{(r)}\ dr\ dR_s \qquad (2.43)$$

From equation (2.31):

$$N_A = N_V .2.\overline{R}_s \qquad (2.44)$$

where $\overline{R}_s$ is the mean radius of all spheres.

Hence from equations (2.43) and (2.44):

$$f(r) = \frac{r}{\overline{R}_s} \int_r^{R_{smax}} \frac{F(R_s)\, dR_s}{\sqrt{R_s^2 - r^2}} \qquad (2.45)$$

where $f(r) = N_A(r)/N_A$ is the probability density of profiles and $F(R_s) = N_V(R_s)/N_V$ is the probability density of spheres.

Equation (2.45) is an Abel's Integral equation whose solution is given by

$$F(R_s) = \frac{4\ \overline{R}_s\ R_s}{\pi} \int_{R_s}^{R_{smax}} \frac{r \dfrac{d(.f(r)/r)}{dr} dr}{(r^2 - R_s^2)^{1/2}} \qquad (2.46)$$

f(r) is the experimentally measurable distribution from the microstructure obtained on the plane of polish. Equation (2.46) can then be used to unfold the distribution of spherical particles dispersed in the bulk of a material. However, the above analysis is limited to the spherical shape of particles. For non-spherical shapes the solutions become extremely complex and often there is no solution.

CHAPTER 3

APPROACH

Interfaces between particles or grains when cut by the plane of polish yield line segments in 2-D microstructure as shown in figure 3.1 . Transformation from 3-D to 2-D results in the loss of some information (typically shape and size distribution) . In some special cases such as spherical particles, a complete description of the 3-D structure can be obtained from an analysis of 2-D microstructure, as already discussed in section (2.7). However, in most cases this is not possible without making any assumptions regarding shape or size distribution of microstructural components.

In the subsequent chapters, an analysis of the 2-D microstructure obtained from a 3-D structure consisting of circular and elliptical interfaces has been done. These interfaces can also be regarded as circular or elliptical discs of zero or near zero thickness (thin discs). All such interfaces (or 2-D particles) will simply constitute as lines in the 2-D microstructure. The interfaces are assumed to be randomly distributed in 3-D space (this assumption is generally true for structures in most real materials). The line length distribution is the only experimentally measurable parameter. Using principles of stereology, basic stereological parameters describing the 3-D spatial structure have been developed in the present work.

A rigorous analysis of basic stereological parameters has been carried out in order to develop the relationships between various 2-D and 3-D parameters. Stereological analyses of discs of circular and elliptical shapes of constant and varying sizes have also been carried out. Practical methods have been proposed to extract information about the 3-D structure of these discs from 2-D measurements.

In order to test the validity of various relationships, a distribution of circular as well as elliptical discs were generated in 3-D space. This structure is then sectioned to obtain the 2-D microstructures. An example of such a structure is shown in figure (3.1). The figure shows that for the case of spatial

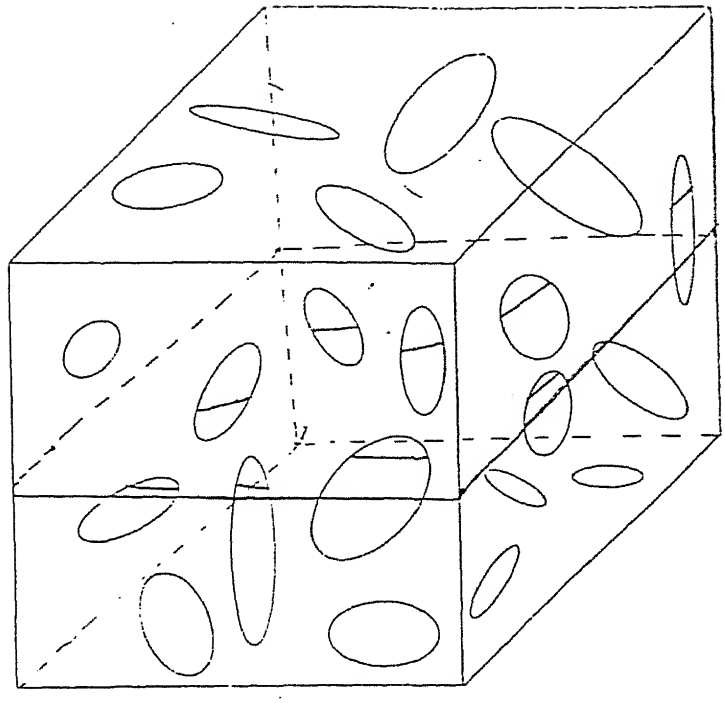

Figure 3.1 (a) : Circular discs (interfaces) of various sizes inside a cubic volume.

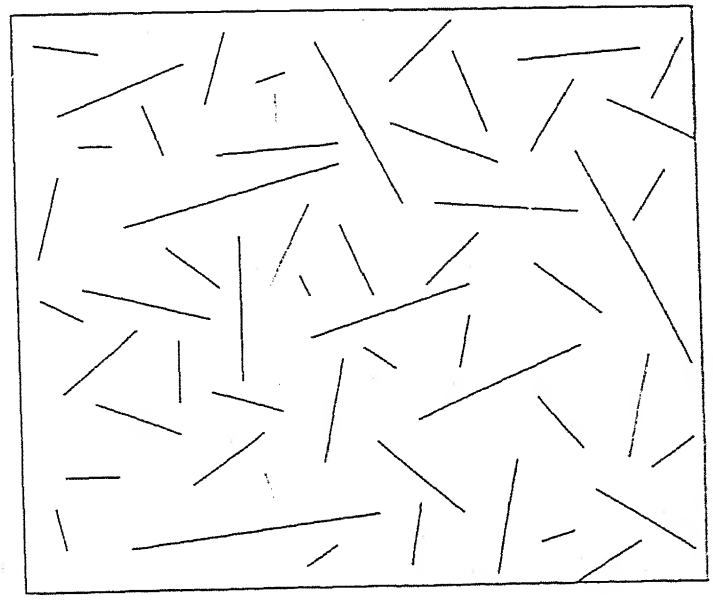

Figure 3.1 (b) : Lines obtained from intersection of circular discs (interfaces) of various sizes by a plane of polish.

distribution of circular discs of various size, the 2-D microstructure consists of a distribution of line lengths. Detailed methodology of such simulations has been discussed in chapter 5.

From the above mentioned simulated microstructures the following "measurements" were made:

1. Number of intercepts per unit length , N_L
2. Total length of lines per unit area in the microstructure, L_A
3. Number of lines per unit area, N_A
4. Line length distribution and computation of statistical parameters, such as, average line length and standard deviation of line lengths.

The above "measurements" on the 2-D section are used to obtain some standard 3-D stereological parameters such as, surface area per unit volume, S_V and number of discs per unit volume, N_V. The calculated values can then be compared to the actual values used in the simulation. These comparisons were used as a test for the validity of the simulations (derived in chapter 5). Correlation between the line length distribution to the disc shape and size distributions have also been developed in the subsequent chapters.

CHAPTER 4

ANALYSIS OF DISCS

As stated earlier, when the discs are intersected by the plane of polish, lines of different lengths are obtained. as shown in figure 3.1(b). In this chapter an analysis of the distribution of the line lengths has been developed to obtain size, size distribution and shape of discs in the 3-D spatial. The present study is restricted only to circular and elliptical discs. For both types of discs several stereological relationships have been established. Practical methods have also been developed for the analysis of the experimentally measurable parameters of microstructures.

4.1 Circular Discs

All the discs are assumed to have a circular shape. The expressions for various parameters (tangent diameter, probability of cutting etc.) are obtained from a circular disc. The expressions are used to derive the relationship between the distribution of line lengths and the distribution of circular discs. First, discs of constant size have been analyzed and then the analysis has been extended to discs of varying sizes.

4.1.1 Discs of Constant Size

Let the radius of the constant size discs is 'R'. The discs are randomly oriented in 3-D space. Figure 4.1 shows a circular disc whose orientation is defined by the angles θ and ω.

4.1.1.1 Average tangent diameter

In order to determine the average tangent diameter, the tangent planes are kept parallel to the XY plane and the disc is permitted to take all possible orientations, as shown in figure 4.1. From this figure it is clear that there is no effect of angle ϕ on the value of tangent diameter $H(\theta,\phi)$ because changing angle ϕ simply results in the rotation of disc around the Z-axis. $H(\theta,\phi)$ can be expressed by the following relation :

$$H(\theta,\phi) = 2R|cos(\theta - 90)| = 2R|sin(\theta)| \qquad (4.1)$$

Averaging over all orientations, the average tangent diameter can be written as: (using equation (2.23))

$$\overline{H} = \frac{4R}{\pi} \qquad (4.2)$$

4.1.1.2 Probability of cutting a disc by the plane of polish

Consider the discs to be contained in a cubic volume, as shown in figure 3.1(a). From equation (2.28), probability of cutting a randomly oriented circular disc of radius 'R' by a horizontal plane of polish within the cube of dimension 'L' is given by

$$P_r = \frac{\overline{H}}{L} \qquad (4.3)$$

Substituting $\overline{H}$ from equation (4.2) in the above expression gives the probability of cutting as :

$$P_r = \frac{4R}{\pi L} \qquad (4.4)$$

4.1.1.3 Average length of lines on the 2-D section

On the plane of polish. lines of different lengths are obtained as shown in figure 3.1. Figure 4.2 shows that the line "mn" is obtained from the intersection of a horizontal plane at a height z from the origin and a circular disc of radius 'R' and orientation (θ,o). 'O' is the origin of XYZ coordinate system and also the centre of the circular disc. 'op' is the

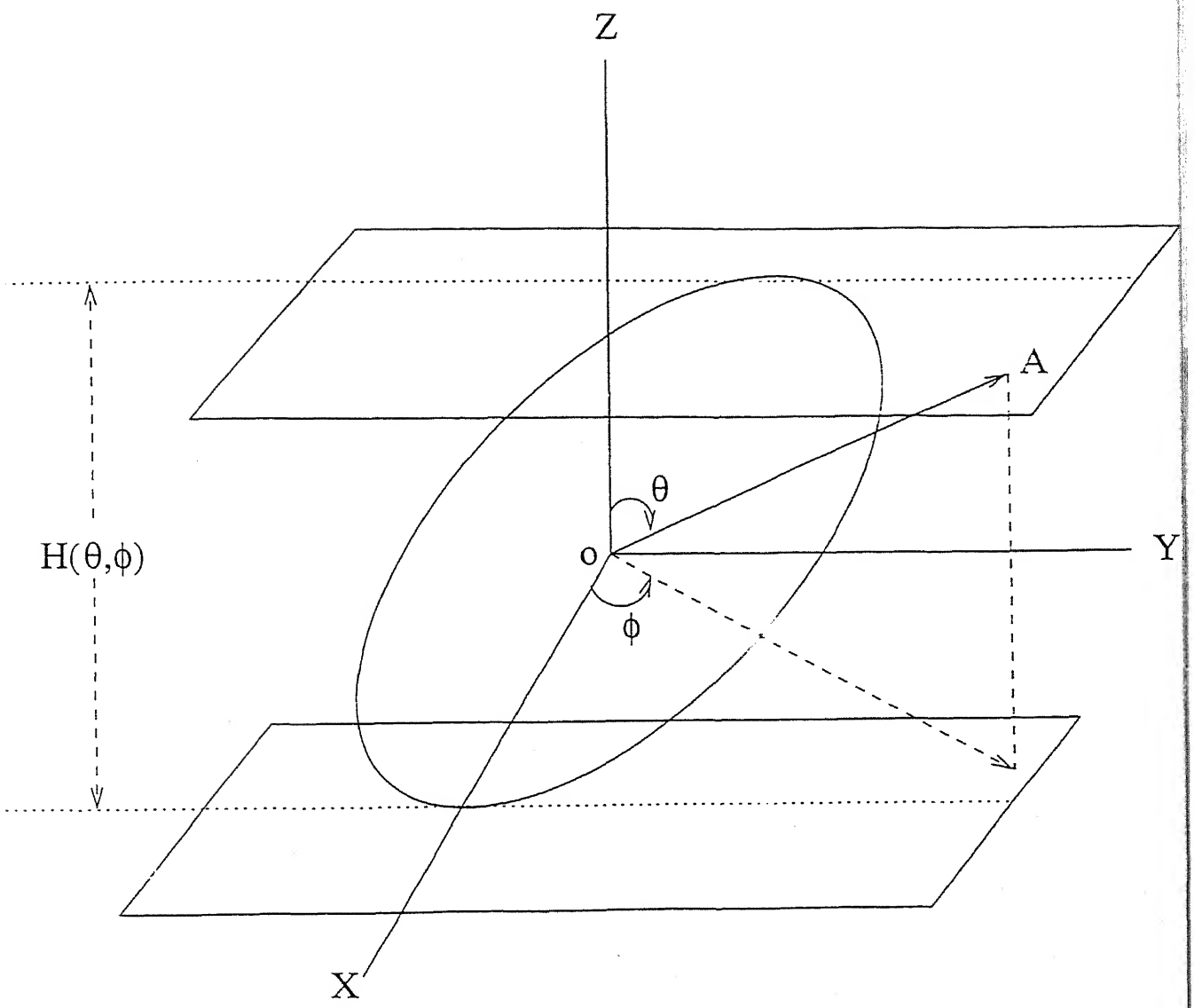

Figure 4.1 : Tangent diameter of a circular disc at a particular orientation (θ,ϕ).

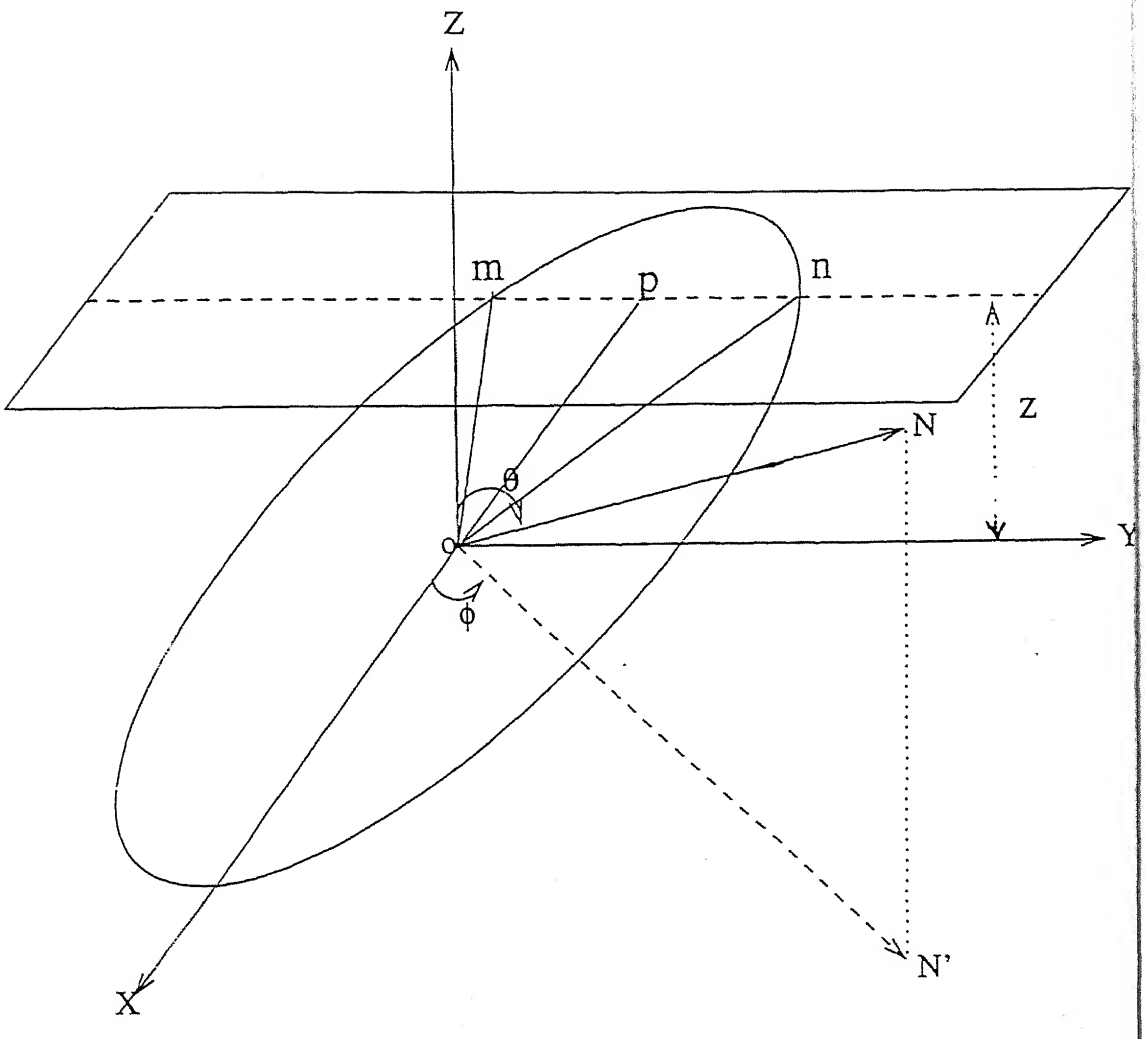

Figure 4.2 : Intersection of a disc by a plane at height z from centre of the disc.

perpendicular drawn from the origin to the line mn. The perpendicular (op) bisects the line mn. Length of the perpendicular op is given by.

$$op = \frac{z}{\sin\theta} \tag{4.5}$$

The length of line mp can be written as

$$mp = \sqrt{R^2 - \left(\frac{z}{\sin\theta}\right)^2} \tag{4.6}$$

Length of line mn is given by

$$l(\theta,\phi) = 2\sqrt{R^2 - \left(\frac{z}{\sin\theta}\right)^2} \tag{4.7}$$

It may be noted that length $l(\theta,\phi)$ is independent of angle ϕ. Now the average intersection length is given by(using equation (2.4)).:

$$\bar{l} = \frac{1}{4\pi}\int_0^{2\pi}\cdot\int_0^{\pi} l(\theta,\phi).d\theta.d\phi \tag{4.8}$$

$$\bar{l} = \frac{\pi R}{2} \tag{4.9}$$

The average value of reciprocals of line length (harmonic mean) for a circular disc of size R has also been given (without derivation) by [19].

$$\left(\frac{\bar{1}}{l}\right) = \frac{\pi}{4R} \tag{4.9 b}$$

4.1.1.4 Probability density of line lengths

Rearranging equation (4.7) as:

$$l(\theta,\phi) = \frac{2}{\sin\theta}\sqrt{R^2\sin^2\theta - z^2} \tag{4.10}$$

Differentiating the above equation with respect to z.

$$\frac{dl}{dz} = \frac{-2z}{\sin\theta}\frac{1}{\sqrt{R^2\sin^2\theta - z^2}} \tag{4.11}$$

$$dz = -\frac{l.\sin^2\theta}{4z}dl \tag{4.12}$$

Negative sign shows that the value of dz decreases with an increases in the value of dl. Taking the absolute value of dz

$$dz = \frac{l\sin^2\theta}{4z}dl \tag{4.13}$$

Rewriting equation (4.10) as:

$$z = \sin\theta\sqrt{R^2 - \frac{l^2}{4}} \tag{4.14}$$

Substituting z from above equation in equation (4.13) :

$$dz = \frac{l\sin\theta}{4\sqrt{R^2 - \frac{l^2}{4}}}dl \tag{4.15}$$

Fig (4.3) shows a disc of size 'R' and orientation (θ,ϕ). The centre of the disc lies at the origin of XYZ coordinate system. A plane perpendicular to Z-axis intersect the disc at a height z from the origin. If a plane perpendicular to Z-axis lies within the range of tangent diameter (from -Rsinθ to Rsinθ), an intersection of the disc with the plane occurs.

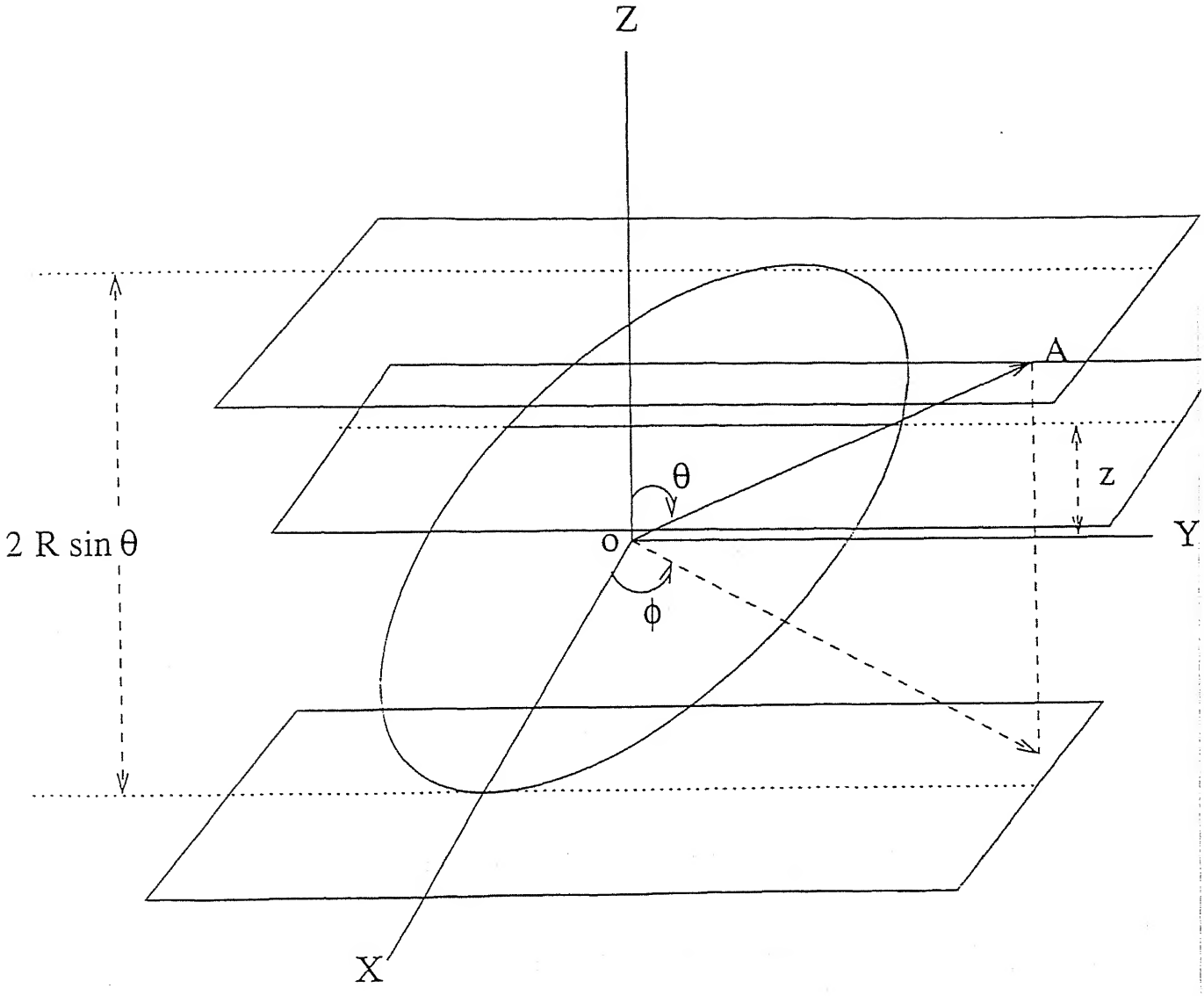

Figure 4.3 : Probability of intersecting of a circular disc.

Probability of finding a random plane perpendicular to Z-axis, which intersects the disc between height z to z+dz from origin , is given by

$$P_r(z) = \frac{dz}{Tangent\ Diameter} \tag{4.16}$$

or

$$P_r(z) = \frac{dz}{2R\sin\theta} \tag{4.17}$$

The length of lines obtained from the intersection of disc and plane at a height in between z and z+dz are l+dl and l respectively. The length of lines are also found between l and l+dl for a plane intersecting the disc between height -z and -z+dz. So the probability of line lengths lying between l to l+dl is given by.

$$P_r(l) = \frac{dz}{R\sin\theta} \tag{4.18}$$

Substituting the value of dz from equation ( ), expression for probability density of line lengths can be written as

$$p(l) = \frac{l}{4R\sqrt{R^2 - \frac{l^2}{4}}} \tag{4.19}$$

Average length of lines can also be determined by using probability density of line lengths

$$\mu = \bar{l} = \int_0^{2R} l\,p(l)dl \tag{4.20}$$

From equation (4.19), the equation for average length can be written as:

$$\bar{l} = \frac{\pi R}{2} \tag{4.21}$$

The average length is same as already derived in section (4.1.1.3).

Standard deviation (σ^2) of the line length distribution is given by

$$\sigma^2 = \int_o^{2R} \frac{(l - \mu)^2 l}{4R\sqrt{R^2 - \frac{l^2}{4}}} dl$$

$$= \frac{1}{4}\int_o^{2R} \frac{l^2}{\sqrt{R^2 - \frac{l^2}{4}}} dl - \mu^2 \qquad (4.22)$$

4.1.2 Circular Discs of Various Sizes

The interfaces in any sample would generally have different sizes. These interfaces can be approximated by thin circular discs of various sizes. The parameters such as average length and standard deviation depend on the size distribution of circular discs. The profile of lines obtained from intersection of a random plane with discs is analyzed to obtain the distribution of discs.

4.1.2.1 Average length

If the size of discs varies from R_{min} to R_{max} , the average length of lines can be written as:

$$\bar{l} = \frac{\int_{R_{min}}^{R_{max}} Probability.density.of.discs * Probability.of.cutting * Average.length.\ dR}{\int_{R_{min}}^{R_{max}} Probability.of.cutting.dR} \qquad (4.23)$$

Standard deviation of lines can also be given by

$$\sigma^2 = \int_{R_{min}}^{R_{max}} (l - \bar{l}) * probability.density.of.\ lines\ dl \qquad (4.24)$$

Example

For random uniform distribution of discs where the size of the discs varies from 0 to R_{max}. The value of average length is given by

$$\bar{l} = \frac{\int_0^{R_{max}} \frac{l}{R_{max}} \frac{4R}{\pi L} \frac{\pi R}{2} dR}{\int_0^{R_{max}} \frac{4R}{\pi L} dR} \qquad (4.25)$$

$$\bar{l} = \frac{\pi R}{3} \qquad (4.26)$$

4.1.2.2 Derivation of disc size distribution from a measured distribution of line lengths

Size distribution of discs is obtained from the measurements of line lengths. The elliptical discs are contained in a cubic volume of unity. Two types of methods are used to derive the relationship between n_A and n_V.

Method 1. Continuous Method

Let the probability distribution of the disc sizes have density $n_V(R)$, so that $\mathbf{n_V(R)\ dR}$, is the number of discs per unit volume whose radii lie in the range (R/ R+dR). Probability density of lines lying in the range (l/ l+dl) after cutting a disc of size 'R' is given from equation (4.19). If the probability distribution of the lines have density $n_A(l)$, so that $\mathbf{n_A(l)\ dl}$. is the number of lines/area, whose lengths lie in the range (l/ l+dl). The relationship between $n_A(l)$ and $n_V(R)$ can be written by using equation (2.43)

$$n_A(l)dl = \int_{l/2}^{\infty} n_V(R)\frac{4R}{\pi}\frac{l}{4R\sqrt{R^2-l^2/4}}\,dl\,dR \qquad (4.27)$$

or,

$$n_A(l) = \frac{l}{\pi}\int_{l/2}^{\infty}\frac{n_V(R)}{\sqrt{R^2-l^2/4}}\,dR \qquad (4.28)$$

Substituting l/2 by x in the above equation

$$n_A(l) = \frac{2x}{\pi}\int_{x}^{\infty}\frac{n_V(R)}{\sqrt{R^2-x^2}}\,dR \qquad (4.29)$$

which is an integral equation of Abel's type whose solution is given by [21]

$$n_V(l) = \frac{4\pi * 2x}{\pi}\int_{x}^{\infty}\frac{R\dfrac{d(n_A(R)/R)\,dR}{dR}}{(R^2-x^2)^{1/2}} \qquad (4.30)$$

or,

$$n_V(l) = 8x \int_x^\infty \frac{R \frac{d}{dR}\left(\frac{n_A(R)}{R}\right) dR}{(R^2 - x^2)^{1/2}} \tag{4.31}$$

Integrating the above equation (Integration by parts).

$$n_V(l) = 8x\left\{\frac{n_A(R)}{(R^2 - x^2)^{1/2}}\Big|_x^\infty - \int_x^\infty \frac{n_A(R)dR}{R(R^2 - x^2)^{1/2}} + \int_x^\infty \frac{R^2 n_A(R)}{(R^2 - x^2)^{1/2}} dR\right\} \tag{4.32}$$

or

$$n_V(R) = 8x\left\{\frac{n_A(l)}{(l^2 - x^2)^{1/2}}\Big|_x^\infty - \int_x^\infty \frac{n_A(l)dl}{l(l^2 - x^2)^{1/2}} + \int_x^\infty \frac{l^2 n_A(l)}{(l^2 - x^2)^{1/2}} dl\right\} \tag{4.33}$$

For solution of practical problems replace ∞ by $l_{max}/2$, where l_{max} is the maximum line length obtained in the microstructure and also replace x by l/2. If the length distribution $n_A(l)$ is known, the above equation can be used to unfold the distribution of circular discs $n_V(r)$

Examples

1. The following equations can be derived for random distribution of discs. where size of discs varies between 0 to R_{max}

$$n_A(l) = \frac{l}{\pi} \int_{l/2}^{R_{max}} \frac{n_V(R)dR}{\sqrt{R^2 - \frac{l^2}{4}}}$$

Say, $n_V(r) = C = \text{Constant}$

$$n_A(l) = \frac{lC}{\pi} [\, log(\sec\theta + \tan\theta) \,]_{R=l/2}^{R=R_{max}}$$

$$n_A(l) = \frac{lC}{\pi} [\, log(\frac{2R}{l} + \sqrt{\frac{4R^2}{l^2} - 1}) \,]_{R=l/2}^{R=R_{max}}$$

$$n_V(R) = \frac{\pi\, n_A(l)}{l[\, log(2\frac{R_{max}}{l} + \sqrt{\frac{4R_{max}^2}{l^2} - 1})\,]}$$

2. If the distribution of line lengths is given by equation: $n_A(l) = l\, e^{-l}$ such that : $n_A(0) = 0$ and $n_A(\infty) = 0$. Substituting the value of $n_A(l)$ in the equation (4.33)

$$n_V(R) = 8x[\int_x^\infty \frac{e^{-l}\, dl}{(l^2 - x^2)^{1/2}} - \int_x^\infty \frac{l\, e^{-l}\, dl}{(l^2 - x^2)^{1/2}} - \int_x^\infty \frac{e^{-l}\, dl}{(l^2 - x^2)^{1/2}}]$$

Thus ,the size distribution of the discs is given by

$$n_v(R) = -8x\int_x^{\infty} \frac{l.e^{-l}}{(l^2 - x^2)^{1/2}}\, dl$$

In general, equation (4.33) will need to be solved numerically. Often the approach of assuming continuous distributions can be tedious and therefore, it may be easier to discretise the distribution, as discussed below.

Method 2. Discrete Method

The actual distribution of discs is approximated as discrete distribution where the disc sizes are divided in several classes. All the discs in a particular class can then be assumed to be the same size. Let the size of the discs varies from 0 to R_{max}. The discs are divided in `M' classes and the width of each class is

$$\Delta R = R_{max}/M \qquad (4.34)$$

So the i^{th} class will contain all the discs whose radii lie in between $(i-1)\Delta R$ and $i\Delta R$ and the value of i varies from 1 to M. The maximum length of line which can be obtained from the distribution of the discs will be the diameter of the largest size disc. So the length of lines will vary between 0 and $2R_{max}$.

The length of lines are also divided in 'M' classes and the width of each class is

$$2\Delta R = 2\, R_{max}/M \qquad (4.35)$$

So the j^{th} class will contain all the lines whose length lie in between $(j-1)2\Delta P$ and $j.2\Delta R$ and the value of j also varies from 1 to M.

Assumption

The distribution of disc sizes is assumed to be discrete i.e. a particular class has a particular size only. The size of the discs in a particular class has been chosen as the largest size in that class. However, the intersection lengths are considered to assume a continuous distribution which are also then broken up into classes, as given in table 4.1:

Table (4.1) Distribution of discs and lines in various classes

Class No.	Size	Numerical Density
CIRCULAR DISCS		
1	ΔR	N_{v1}
2	$2\Delta R$	N_{v2}
3	$3\Delta R$	N_{v3}
i	$i\Delta R$	N_{vi}
m	$m\Delta R$	N_{vm}
Profile (Lines)		
1	0 to $2\Delta R$	N_{A1}
2	$2\Delta R$ to $4\Delta R$	N_{A2}
3	$3\Delta R$ to $6\Delta R$	N_{A3}
j	$2(j-1)\Delta R$ to $2j\Delta R$	N_{Ai}
m	$2(m-1)\Delta R$ to $2m\Delta R$	N_{AM}

Since the size of the discs in the i^{th} class is $i\Delta R$,the probability of cutting a disc in the i^{th} class is given by (from equation (2.28)):

$$P_i = \frac{4\, i\, \Delta R}{\pi L} \qquad (4.36)$$

For L = 1,

$$P_i = \frac{4\, i\, \Delta R}{\pi} \qquad (4.37)$$

Probability of lines lying in the j^{th} class after cutting the discs of ith class ($i \geq j$) is given by (from equation (4.19))

$$P_i^j = \frac{l\,dl}{4R\sqrt{R^2 - l^2/4}} \qquad (4.38)$$

IN the above equation the value of l is taken as the mid point of a particular class and therefore, P_i^j becomes :

$$P_i^j = \frac{\left[\frac{(j-1)2\Delta R + j2\Delta R}{2}\right].2\Delta R}{4i\Delta R\sqrt{(i\Delta R)^2 - \left[\frac{(2j-1)\Delta R}{4}\right]^2}} \qquad (4.39)$$

or,

$$P_i^j = \frac{(2j-1)}{i\sqrt{4i^2 - (2j-1)^2}} \qquad (4.40)$$

The number per unit area of lines in j^{th} class contributed from the discs of ith class is given by

$$P_i * N_V(i) * P_i^j \qquad (4.41)$$

Therefore, the total number of lines per unit area in j^{th} class is given by

$$n_{A_j} = P_m * N_{V_m} * P_m^j + P_{m-1} * N_{V_{m-1}} * P_{m-1}^i + \ldots\ldots + P_j * N_{V_j} * P_j^i \quad (4.42)$$

or,

$$N_{A_j} = \sum_{i=j}^{m} P_i . N_{V_i} . P_i^j \quad (4.43)$$

Above equation can be expanded to 'm' simultaneous equations with 'm' unknowns, i.e, n_{V1}, n_{V2} , ... n_{Vm} :

For j = m

$$N_{A_m} = \frac{4M}{\pi} \Delta R * N_{V_m} * \frac{2m-1}{m\sqrt{4m-1}} \quad (4.44)$$

or

$$N_{A_m} = \frac{4(2m-1)}{\pi\sqrt{4m-1}} \Delta R\_ N_{V_m} \quad (4.45)$$

For j = m-1

$$N_{A_{m-1}} = \frac{4m}{\pi} \Delta R * N_{V} * \frac{2m-3}{\sqrt{3}\sqrt{4m-3}} + \frac{4(m-1)}{\pi} \Delta R * N_{V_{m-1}} * \frac{(2m-3)}{(m-1)\sqrt{4m-5}}$$

$$N_{A_{m-1}} = \frac{4(2m-3)}{\sqrt{3}\pi\sqrt{4m-3}} \Delta R\ N_{V_m} + \frac{4(2m-3)}{\pi\sqrt{4m-5}} \Delta R\ N_{V_{m-1}} \quad (4.47)$$

The number of lines in other classes can also be written in similar fashion. The set of m equations given by equation (4.43) can be easily solved to determine m unknowns. Thus knowing the values of N_{A1} - ..... N_{Am}, one can calculate the values of N_{V1} ..... N_{Vm}.

4.2 Elliptical Discs

All the discs are assumed to have elliptical shape. The stereological relationships for various parameters are obtained in the same fashion as were obtained for circular discs. First elliptical discs of constant size are considered. Subsequently discs of varying sizes are analyzed. However, the shape of elliptical discs are assumed to be a constant, i.e., the ratio of major axis to minor axis is kept constant.

4.2.1 Discs of Constant Size

The distribution of discs is assumed to have all the discs of single size. A disc from the distribution is chosen randomly. Let he semi-major and semi-minor axes of the elliptical disc are `a' and `b' respectively. The orientation of the disc is given by θ,ϕ and ξ, as shown in figure 4.4. It is necessary to define an extra parameter (ξ) for the orientation of elliptical disc because the rotation of disc about its normal changes the position of the disc. While the rotation of a circular disc about its normal has no effect on the position of the disc. The following parameters are obtained for the disc mentioned above.

4.2.1.1 Average tangent diameter

Tangent Diameter of the elliptical disc is taken as the distance between tangent planes parallel to XY plane, as shown in Figure (4.4). There is no effect of angle o on the tangent diameter $H(\theta,\phi,\xi)$ because change in ϕ merely results in the rotation of discs about the Z-axis. The tangent diameter of an elliptical disc having orientation θ , ϕ and ξ can be written as

$$H(\theta, \phi, \xi) = H(\theta = \frac{\pi}{2}, \xi) \sin \theta \qquad (4.55)$$

where, $H(\theta = \pi/2, \xi)$ is the maximum value of tangent diameter at $\theta = \pi/2$ and at a constant value of ξ

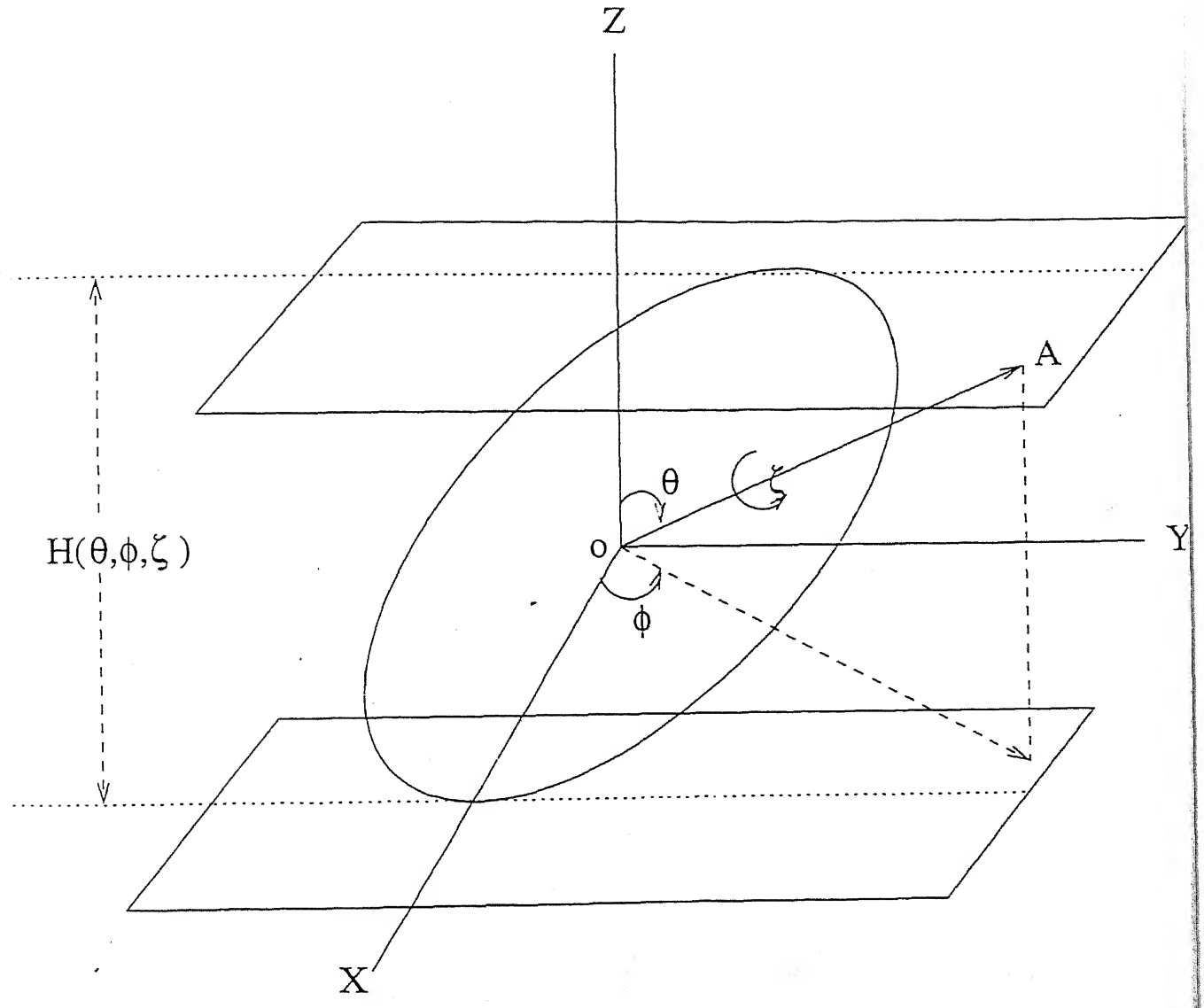

Figure 4.4 : Tangent diameter of an elliptical disc at a particular orientation (θ,ϕ).

In order to determine the value of H($\theta=\pi/2$, ξ), the ellipse is fixed in XYZ-coordinates in such a way that its major and minor axes lie along X and Y axes respectively. The equation of ellipse in XYZ-coordinates is then given by

$$\frac{x^2}{a^2} + \frac{y^2}{b^2} = 1$$
$$and \qquad (4.56)$$
$$z = 0$$

Instead of rotating ellipse by ($\theta=\pi/2$, ξ) in anti-clockwise direction, the axes are rotated clockwise by the same amount. After the rotation, XYZ coordinate system is changed to X'Y'Z'. The parallel planes which are tangent to the disc and perpendicular to the new Z' axis represent lines AB and A'B' in XY-plane as shown in figure (4.5).

Equation of line AB in XY coordinates is given by

$$y = tan\ (90+\xi)x + c$$
$$or \qquad (4.57)$$
$$y = -cot\ \xi.x + c$$

where, c is the intercept of the line AB on the Y-axis.

Substituting equation (4.57) in equation (4.56) and rearranging :

$$x^2(b^2 + a^2\ cot^2\ \xi) + x(-2a^2\ c.cot\ \xi) + a^2(c^2 - b^2) = 0 \qquad (4.58)$$

Since the line AB just touches the ellipse, the solution of equation (4.58) should give a single value of x and y. The two roots of the equation (4.58) can be made equal by using the following property

$$4a^4c^2\ cot^2\xi = 4(b^2 + a^2\ cot^2\xi).\ a^2(c^2-b^2)$$

or

$$c = (a^2 cos^2\xi + b^2 sin^2\xi)^{1/2} / sin\xi \qquad (4.59)$$

Substituting c from above equation in equation (4.57), the equation of line AB becomes :

$$y = -\cot\xi . x + (a^2 \cos^2\xi + b^2 \sin^2\xi)^{1/2} / \sin\xi \qquad (4.60)$$

Figure (4.5) shows that the line CD, which is perpendicular to the pair of lines AB and AB' and passing through origin, is along the new Z'-axis. This line intersects the lines AB and AB' at C and D respectively. The tangent diameter of the ellipse having orientation ($\theta = \pi/2$, ξ) is nothing but the length of line CD. The equation of the line CD is obviously given by

$$y = \tan\xi . x \qquad (4.61)$$

From equations (4.57) and (4.59), the coordinates (x,y) of point C is given by

$$x = -\cos\xi (a^2 \cos^2\xi + b^2 \sin^2\xi)^{1/2} \qquad (4.62)$$

and

$$y = \sin\xi (a^2 \cos^2\xi + b^2 \sin^2\xi)^{1/2} \qquad (4.63)$$

Length of line CD. i.e.. $H(\theta=\pi/2, \xi)$, is simply given by

$$H(\theta = \pi/2, \xi) = 2(x^2 + y^2)^{1/2} = (a^2 \cos^2\xi + b^2 \sin^2\xi)^{1/2} \qquad (4.64)$$

Thus, from equation (4.55), tangent Diameter $H(\theta,\phi,\xi)$ is given by

$$H(\theta,\phi,\xi) = 2(a^2 \cos^2\xi + b^2 \sin^2\xi)^{1/2} . \sin\theta \qquad (4.65)$$

The average tangent diameter ($\overline{H}$) can be written as:

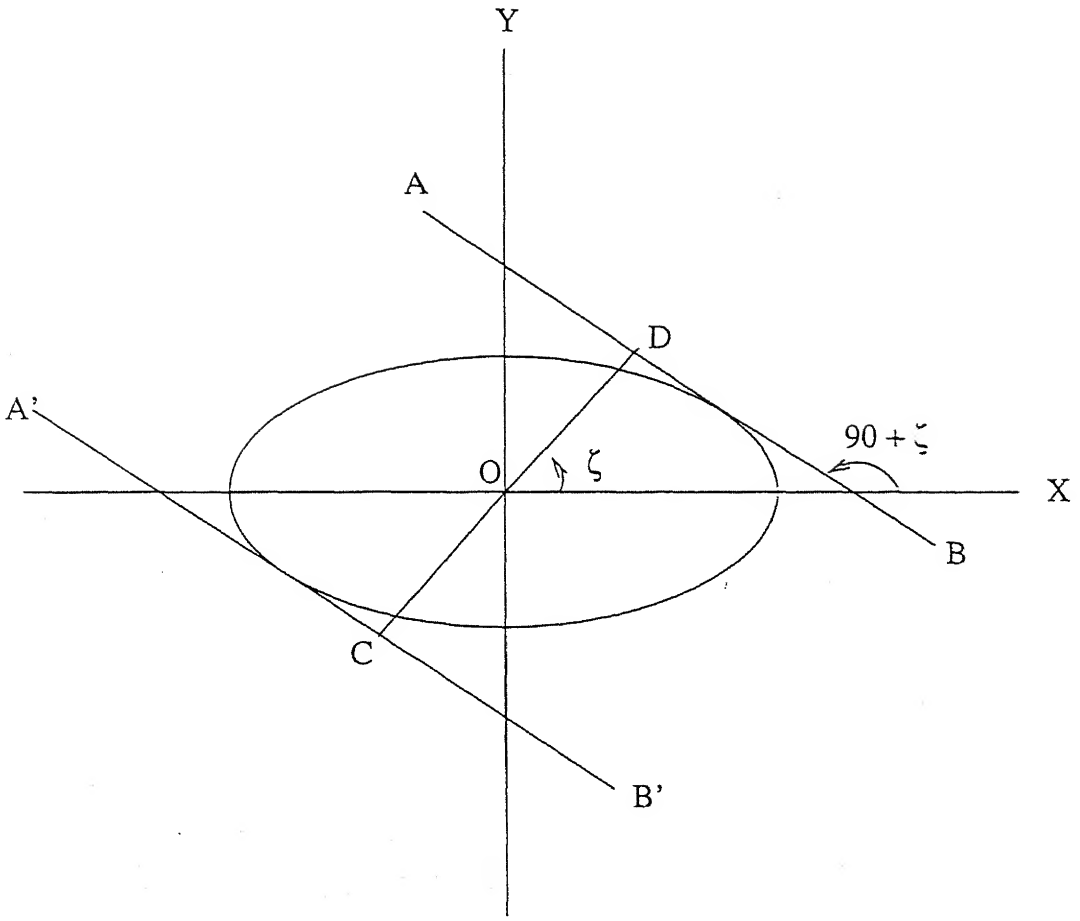

Figure 4.5 : Projection of tangent planes on (AB and A′B′) on XY plane.

$$\overline{H} = \frac{\int_0^{2\pi}\int_0^{2\pi}\int_0^{\pi} H(\theta,\phi,\xi)\, d\theta d\phi d\xi}{\int_0^{2\pi}\int_0^{2\pi}\int_0^{\pi} d\theta d\phi d\xi}$$

$$= \frac{\int_0^{\pi}\int_0^{2\pi} (a^2\cos^2\xi + b^2\sin^2\xi)^{1/2}\, d\xi\, \sin\theta\, d\theta}{\pi^2} \qquad (4.66)$$

Suppose

$$I = \int_0^{2\pi} (a^2\cos^2\xi + b^2\sin^2\xi)^{1/2} d\xi$$
$$= \left(\frac{a^2+b^2}{2}\right)^{1/2} \int_0^{2\pi} \left\{1+\frac{a^2-b^2}{a^2+b^2}\cos 2\xi\right\}^{1/2} d\xi \qquad (4.67)$$

The solution of the integral(I) can only be written in the series form[20].

$$I = 2\pi\left(\frac{a^2+b^2}{2}\right)^{1/2}\left\{1-\frac{t^2}{16}-\frac{15}{2^{10}}t^4-\ldots\ldots\ldots\right\} \qquad (4.68)$$

where $t = (a^2-b^2)/(a^2+b^2)$

Therefore, the average tangent diameter is given by. the following relationship :

$$\overline{H} = \frac{4}{\pi}\left(\frac{a^2+b^2}{2}\right)^{1/2}\left(1-\frac{1}{2^4}t^2-\frac{15}{2^{\cdot\cdot}}t^4-\ldots.\right) \qquad (4.69)$$

For the case when a = b = R (i.e., circular disc), the equation of average tangent diameter for elliptical disc reduces to equation (4.2) which is identical to the equation of average tangent diameter derived for circular disc of radius R.

4.2.1.2 Probability of cutting a disc by the plane of polish

From equation (2.28), probability of cutting a randomly oriented elliptical disc by a horizontal plane of polish within a cube of dimension L is given by

$$P_r = \frac{\overline{H}}{L} = \frac{4}{\pi L}\left(\frac{a^2+b^2}{2}\right)^{1/2}\left(1 - \frac{1}{2^4}t^2 - \frac{15}{2^{10}}t^4 - \ldots\right) \qquad (4.70)$$

where $t = (a^2-b^2)/(a^2+b^2)$

4.2.1.3 Average length of lines

The elliptical disc whose semi-major and semi-minor axes are `a' and `b' and has the orientation (θ,ϕ,ξ) with respect to X-Y-Z frame, is cut by a plane perpendicular to Z-axis at a height z from the origin as shown in figure (4.6).

Consider the frame X'Y'Z', which is obtained from XYZ frame by following operations in sequence.

1. Rotation of Z-axis by an angle θ in anticlockwise direction
2. Rotation of new Y-axis by an angle ϕ in anticlockwise direction
3. Rotation of new Z-axis by an angle ξ in anticlockwise direction.

Since the orientation of the normal of the disc is defined by (θ,o,ξ) in XYZ frame and the orientation of X'Y'Z' can also be given by (θ,ϕ,ξ) with respect to XYZ frame. So, the normal of the disc will lie along Z'-axis and the disc will lie in X'Y' plane, as shown in figure 4.7. The equation of ellipse in X'Y'Z' frame is given by

$$\frac{x'^2}{a^2} + \frac{y'^2}{b^2} = 1 \qquad (4.71)$$

In the figure (4.7), axis Z' is coming out of the plane of paper . Line AB is the intersecting line between elliptical disc and sectioning plane and line OD is perpendicular to line AB. The length of line OD is given by

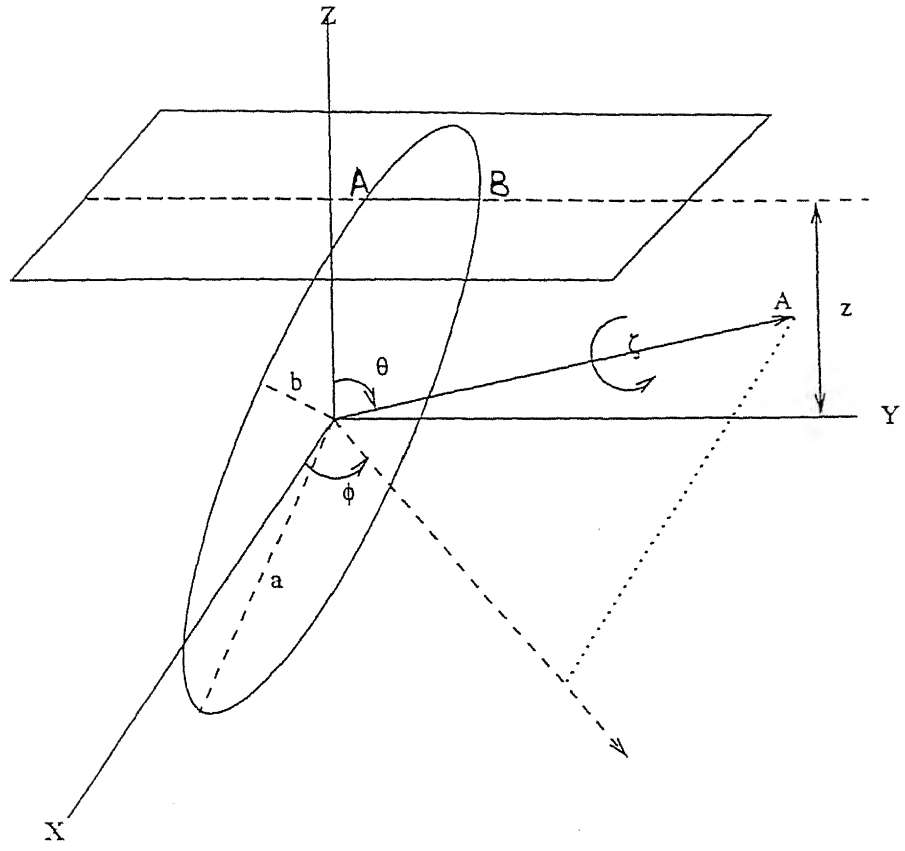

Fig 4.6 Intersection of Elliptical Disc by a Plane

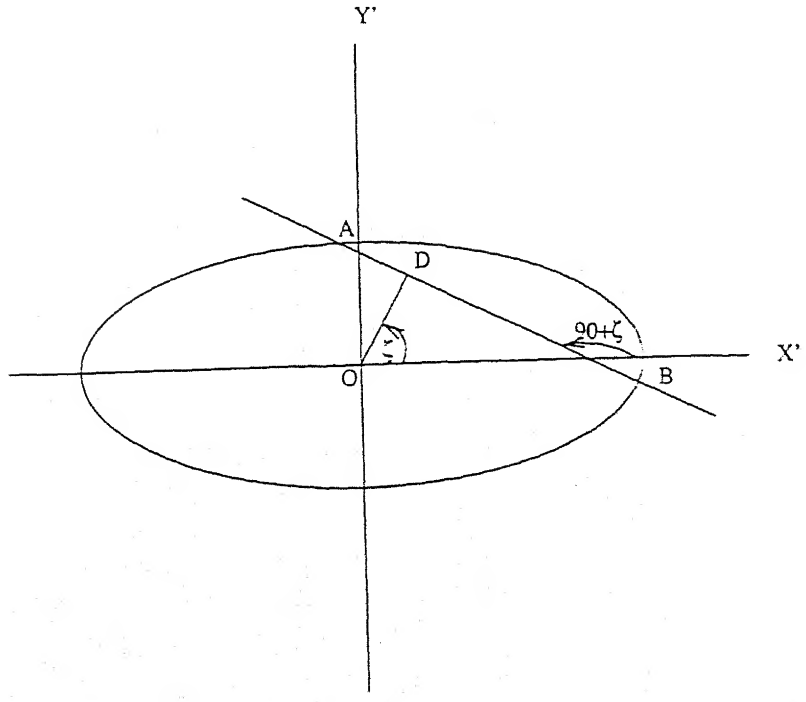

Fig 4.7 Projection of Elliptical Disc
and Plane of Polish on X'Y' Plane

$$OD = \frac{z}{\sin\theta} \tag{4.72}$$

Equation of line AB in X'Y' frame is given by

$$y' = \tan(90+\xi)\,x' + \frac{z}{\sin\theta\,\sin\xi} \tag{4.73}$$

Substituting equation (4.73) in equation (4.71) :

$$(m^2a^2+b^2)x'^2 + (2ma^2c)x' + a^2(c^2-b^2) = 0 \tag{4.74}$$

where m = tan (90+ξ) and c = z/sinθ sinξ.

Let x_1 and x_2 be the two roots of the quadratic equation (4.74), one can write the following identity :

$$(x_1 - x_2)^2 = (x_1 + x_2)^2 - 4x_1x_2 \tag{4.75}$$

Using the properties of summation and multiplication of roots[@] ,one can write the following equation by using equation (4.75) :

$$(x_1-x_2)^2 = 4a^2b^2(a^2m^2+b^2-c^2)/(m^2a^2+b^2)^2 \tag{4.76}$$

From equation (4.73), one can write the following equation

$$x' = \frac{y'}{m} - \frac{c}{m} \tag{4.77}$$

where m = tan (90+ξ) and c = z/sinθ sinξ.

A quadratic equation in terms of y' can be obtained from equations (4.71) and (4.77) :

[@] If x_1 and x_2 are the two roots of equation $ax^2 + bx + c = 0$, the following identities hold good

$x_1 + x_2 = -b/a$;

and

$x_1.x_2 = c/a$.

$$(m^2a^2+b^2)y'^2 - (2b^2c)y' + b^2(c^2-a^2) = 0 \qquad (4.78)$$

If y1 and y2 are the roots of the above equation ,then the square of the difference of the roots is given by

$$(y_1 - y_2)^2 = \frac{4a^2b^2m^2(a^2m^2+b^2-c^2)}{(m^2a^2+b^2)^2} \qquad (4.79)$$

Therefore, the intersection length between the ellipse and the plane of polish , i.e., the length AB in figure 4.7 is given by

$$l(\theta,\phi,\xi) = \{(x_1 - x_2)^2 + (y_1 - y_2)^2\}^{1/2} \qquad (4.80)$$

or

$$l(\theta,\phi,\xi) = \frac{2ab}{\sin\theta(a^2\cos^2\xi + b^2\sin^2\xi)} \cdot \{a^2\sin^2\theta\cos^2\xi + b^2\sin^2\theta\sin^2\xi - z^2\}^{1/2} \qquad (4.81)$$

By putting a = b = R (i.e., case of circular disc) equation (4.81) reduces to the equation (4.10) which was derived for circular disc.

Average length of lines in the microstructure is obtained by averaging over θ.o and ξ as follows

$$\bar{l} = \frac{\int_0^{\pi}\int_0^{2\pi}\int_{-H(\theta.o,\xi)}^{H(\theta.o,\xi)} l\, dz\, d\xi\, d\theta}{\int_0^{\pi}\int_0^{2\pi}\int_{-H(\theta.o,\xi)}^{H(\theta.o,\xi)} dz\, d\xi\, d\theta} \qquad (4.82)$$

or

$$\bar{l} = \frac{I}{4\pi^2 H(\theta,\phi,\xi)} \int_0^{\pi}\int_0^{2\pi}\int_{-H(\theta.o,\xi)}^{H(\theta.o,\xi)} l\, dz d\xi d\theta \qquad (4.83)$$

4.2.1.4 Probability Density of Line Lengths

Rearranging equation (4.81) as :

$$z = \frac{\sin\theta}{2ab}\{a^2\cos^2\xi + b^2\sin^2\xi\}^{1/2}\{4a^2b^2 - l^2(a^2\cos^2\xi + b^2\sin^2\xi\}^{1/2} \qquad (4.84)$$

Differentiating the above equation with respect to l

$$dz = \frac{(a^2\cos^2\xi + b^2\sin^2\xi)^{3/2}.l\ \sin\theta dl}{2ab\{4a^2b^2 - l^2(a^2\cos^2\xi + b^2\sin^2\xi)\}^{1/2}} \qquad (4.85)$$

The following expression of probability of lines lying between l to l+dl can be obtained in an analogous manner as in the case of circular disc (See section 4.1.1.4).

$$P_r(l) = 2dz / H(\theta,\phi,\xi) \qquad (4.86)$$

or

$$p(l)\{\xi\} = \frac{(a^2\cos^2\xi + b^2\sin^2\xi)l\ dl}{2ab\{4a^2b^2 - l^2(a^2\cos^2\xi + b^2\sin^2\sin^2\xi)\}^{1/2}} \qquad (4.87)$$

where P(l){ξ} is the probability density function of line lengths at a particular value of ξ. The probability density of line lengths can be obtained by integrating over the range of ξ is given by

$$P(l) = \frac{1}{2\pi}\int_0^{2\pi} P(l)\{\xi\}\ d\xi \qquad (4.88)$$

4.2.2 Elliptical Discs of Various Sizes

The interfaces in any sample generally have different sizes. In some cases these microstructures are found to have a shape close to the elliptical shape. In order to analyze the distribution of such microstructural elements, the microstructure can be approximated by thin elliptical discs of various sizes. The ratio of semi-minor and semi-major axes (b/a=k) is assumed to be constant (i.e, the shape of elliptical discs is kept constant). The discs are analyzed using a similar approach as used for circular discs.

4.2.2.1 Derivation of disc size distribution from a measured distribution of profile sizes

When a cubic volume filled with elliptical discs of various sizes is intersected by a random plane, the lines of different lengths are obtained on the plane of polish. Distribution of the discs inside the cubic volume is obtained from the measurements of line lengths distribution. The elliptical discs are contained in a cubic volume of unity. Two approaches are used as discussed below :

Method 1. Continuous Method

Let the probability distribution of the semi-major axis have density $n_v(a)$, so that $\mathbf{n_v(a)\ da}$, is the number of elliptical discs per unit volume whose semi major axes lie in the range (a/a+da). From equation (4.69) and noting that cube dimension is unit (L = 1), the probability of cutting the elliptical disc of semi-major and semi-minor axes a and b respectively, is given by

$$P_r = \frac{4a}{\pi}\left(\frac{1+k^2}{2}\right)^{1/2}\left\{1 - \frac{t^2}{16} - \frac{15}{2^{10}}t^4 - \ldots.\right\} \qquad (4.89)$$

where k = b/a.

Probability density of lines lying in the range (l/ l+dl) after cutting a disc of size a is given by equation (4.88).

$$p(l) = \frac{1}{2\pi}\int_0^{2\pi} p(l)(\xi)\, d\xi \qquad (4.90)$$

Let the probability distribution of lines have density $n_A(l)$ per unit area. so that $\mathbf{n_A(l)\ dl}$ is the number of lines/area, whose lengths lie in the range (l/ l+dl). The relationship between $n_A(l)$ and $n_v(a)$ can be written by using equation (2.43)

$$n_A(l)\, dl = \int_{l/2}^{\infty} n_v(a).\overline{H}.P(l)\, da \qquad (4.91)$$

or

$$n_A(l) = \frac{1}{2\pi}\int_{l/2}^{\infty} n_v(a) * \frac{4a}{\pi}\left(\frac{1+k^2}{2}\right)^{1/2} - \{1 - \frac{t^2}{16} - \frac{15}{2^{10}}t^4 - \ldots\ldots\} * \int_0^{2\pi} \frac{(a^2\cos^2\xi + b^2\sin^2\xi)l}{2ab\{4a^2b^2 - l^2(a^2\cos^2\xi + b^2\sin^2\xi)\}^{1/2}}\, d\xi \qquad (4.92)$$

The above equation can only be solved numerically by assuming some kind of a distribution for $N_v(a)$. As will be shown below, by assuming discrete distributions instead of the continuous distributions, one can obtain a much simpler solution for practical problems.

Method 2. Discrete Method

The actual distribution of discs is approximated as discrete distribution where the discs are divided in several classes. All the discs in a particular class are assumed to have the same size. Let the size of the disc varies from 0 to a_{max}. And the discs are divided in M classes such that the width of each class is

$$\Delta a = \frac{a_{max}}{M} \qquad (4.93)$$

Therefore, the i^{th} class will contain all the discs whose size lie in between $(i-1).\Delta a$ and $i.\Delta a$ and the value of i varies from 1 to M.

The length distribution obtained from these discs will have the length of lines varying between 0 and $2\Delta a_{max}$. The maximum length of line being the length of major axis of the largest size disc. The length distribution of lines are also divided in M classes such that the width of each class is

$$2\Delta a = \frac{2\,a_{max}}{M} \qquad (4.94)$$

So the j^{th} class will contain all the lines whose length lie in between $2(j-1).\Delta a$ and $2j.\Delta a$ and the value of j will vary from 1 to M.

Assumption:

The distribution of the disc sizes is assumed to be discrete i.e. a particular class has a particular size only. The size of the discs in a particular class has been chosen as the largest size in that class. However, the intersection lengths are considered to assume a continuous distribution which are also then broken up into classes, as given in table 4.2.

Table 4.2 . Distribution of elliptical discs and lines in various classes

Class No.	Size	Numerical Density
ELLIPTICAL DISCS		
1	Δa	N_{v1}
2	$2\Delta a$	N_{v2}
3	$3\Delta a$	N_{v3}
i	$i\Delta a$	N_{vi}
m	$m\Delta a$	N_{vm}
Profile (Lines)		
1	0 to $2\Delta a$	N_{A1}
2	$2\Delta a$ to $4\Delta a$	N_{A2}
3	$3\Delta a$ to $6\Delta a$	N_{A3}
j	$2(j-1)\Delta a$ to $2j\Delta a$	N_{Ai}
m	$2(m-1)\Delta a$ to $2m\Delta a$	N_{Am}

Since the size of the discs in the i^{th} class is $i\Delta a$, the probability of cutting a disc in the i^{th} class is given by (from equation (4.70)) :

$$P_i = \frac{4.i.\Delta a}{\pi}\left(\frac{1+K^2}{2}\right)^{1/2}\left\{1-\frac{t^2}{16}-\frac{15}{2^{10}}t^4-.....\right\} \qquad (4.95)$$

Probability of lines lying in the jth class after cutting the discs of ith class ($i \geq j$) is given from equations (4.87) and (4.88)

$$P_i^j = \frac{(2j-1)}{2\pi . i . K} \int_0^{2\pi} \frac{(\cos^2\xi + K^2 \sin^2\xi)\, d\xi}{\{4i^2K^2 - (2j-1)^2(\cos^2\xi + K^2\sin^2\xi)\}^{1/2}} \quad (4.96)$$

The number of lines in j^{th} class contributed from the discs of ith class is given by

$$P_i * N_v(i) * P_i^j \quad (4.97)$$

Total number of lines per uniy area in j^{th} class is:

$$N_{Aj} = P_m * N_{v_m} * P_m^i + P_{m-1} * N_{v_{m-1}} * P_{m-1}^j + \ldots\ldots + P_j * N_{v_j} * P_j^j \quad (4.98)$$

or,

$$N_{Aj} = \sum_{i=j}^{M} P_i * N_{v_i} * P_i^j \quad (4.99)$$

For different values of j (from 1 to M) equation (4.99) will give m simultaneous equations, which can be solved for M unknowns (N_{v_1}, N_{v_2}, ..., N_{v_m}).

CHAPTER 5

MICROSTRUCTURAL SIMULATION

Simulation was used for evolving a model which represented the real sample. Since it is difficult to perform the experiments on real samples, microstructures containing circular and elliptical discs were simulated. The simulated microstructure were used for testing the equations developed in the previous chapter (see appendices C-1 to C-4).

Consider a cube of dimension 1, containing circular or elliptical discs. If the cube has N_V number of discs per unit volume, then N_V is the number of discs inside the cube of dimension 1. In order to simulate a 3-D structure n_V number of discs are then randomly distributed (which also have random orientations) inside the unit cubic volume. Finally, random sections of the cube are taken to generate microstructures on the plane of polish.

A disc of size a_1 (semi-major axis) with orientation (θ_1, ϕ_1, ξ_1) is generated at any random position inside the cube. Another discs of size a_2 (semi-major axis) with orientation (θ_2, ϕ_2, ξ_2) is also generated at some other location inside the cube. Suppose the centres of the first and second discs are at (x_1, y_1, z_1) and (x_2, y_2, z_2) respectively.

5.1 Generation of Distribution of Discs in 3-D Space

In order to generate a random position and random orientation of a disc the following procedure was adopted :

- A random position of the disc was obtained by generating 3 uniform random numbers corresponding to the x,y,z coordinates which denoted the centre of the disc.

- For random orientation θ and ϕ were generated for circular discs and θ,ϕ and ξ were generated for elliptical discs. It should be noted that ϕ and ξ are uniformly distributed from 0 to 2π and in the case of θ, $\cos\theta$ is uniformly distributed over -1 to +1 (i.e., θ going from 0 to π).

During the generation process described above it was ensured that no overlap of discs occured. For this the conditions of overlap between two discs have been discussed in the next section If an overlap occurs, the position and orientation of the last disc was generated again.

5.1.1 Condition for Overlap of Two Discs

Let the positions of the centres of two discs be (x_1,y_1,z_1) and (x_2,y_2,z_2) respectively. The orientation of the two discs are given by (θ_1 ,ϕ_1) and (θ_2 ,ϕ_2) for circular discs and (θ_1,ϕ_1,ξ_1) and (θ_2 ,ϕ_2,ξ_2) for elliptical discs. For the case of circular discs, the radii of the two discs are denoted by R_1 and R_2 respectively. For the case of elliptical discs the semi-major and semi-minor axes of the discs are denoted by (a_1,b_1) and (a_2,b_2).

Suppose

$$\Delta x = x_2 - x_1$$

$$\Delta y = y_2 - y_1$$

$$\Delta z = z_2 - z_1$$

Condition 1.

If $|\Delta x|$ or $|\Delta y|$ or $|\Delta z| > a_1 + a_2$, there is no overlap between the discs.

Condition 2.

If $d_1 <= b_1$ and $d_2 <= b_2$ the two discs overlap each other. Otherwise , there is no overlap between the discs. It may be noted that for the circular discs, $a_1 = b_1 = R_1$ and $a_2 = b_2 = R_2$. The expressions for d_1 and d_2 are complex and therefore they are given in appendix-B.

Here d_1 and d_2 are the distances from the centers of first and second disc to the intersecting line between the disc planes respectively.

5.2 Generation of Microstructure on the Plane of Polish

In order to generate 2-D microstructures exhibiting lines of varying lengths, the cube of unit dimension containing randomly distributed discs was sectioned randomly by planes parallel to the XY-plane. The position of the plane of polish along the Z-axis is chosen randomly.

The length of line intersected between a disc and the random plane is given by

$$l = [(x_1 - x_2)^2 + (y_1 - y_2)^2]^{1/2} \qquad (5.1)$$

where (x_1,y_1) and (x_2,y_2) are the end points of the line. The expressions for x_1 , y_1 , x_2 and y_2 are derived in appendices A-1and A-2.

For each simulated distribution of discs, the cube was sectioned randomly 10 to 20 times to obtain 10 ,to 20 microstructures of lines of the type shown in figure 3.1(b).

CHAPTER 6

DISCUSSION

Using the methodology discussed in the previous chapter, discs of various shapes (i.e., different ratios of the minor axis (b) to the major axis (a) of ellipse, k=b/a) and sizes were generated in a cubic volume. The cube was sectioned by random planes (or the so called plane of polish) and on each section a microstructure consisting of straight line segments of varying lengths were obtained. From the microstructure consisting of straight lines, the values of 2-D stereological parameters : number of intercepts per unit length(N_L), length of lines per unit area (L_A), number of lines per unit area (N_A), average line lengths($\bar{l}$) and length distribution of lines were obtained. Using the values of these parameters for the simulated microstructures, 3-D stereological parameters were calculated, namely, surface area of discs per unit volume (S_V) and number of discs per unit volume (N_V). Tables (6.1) and (6.2) compares the calculated values of S_V and N_V with their actual values for structures consisting of discs of different size distribution and shapes (circular shape with k=1 to elongated ellipse shape with k=0.1).

Table (6.1) : Data for surface area per unit volume

Disc Shape k	Actual surface area per unit volume S_V (mm^2/mm^3)	Calculated S_V $S_V = 2*N_L$ (mm^2/mm^3)	Calculated S_V $S_V = 4*L_A/\pi$ (mm^2/mm^3)
Discs of constant size (semi-major axis = 0.1mm; N_V = 400)			
1.0	1.57	1.51	1.49
0.9	1.41	1.38	1.40
0.8	1.26	1.18	1.10
0.7	1.10	1.11	1.00
0.6	0.94	0.93	0.88
0.5	0.78	0.70	0.72

Table 6.1 continued :

Disc Shape k	Actual surface area per unit volume S_V (mm^2/mm^3)	Calculated S_V $S_V = 2*N_L$ (mm^2/mm^3)	Calculated S_V $S_V = 4*L_A/\pi$ (mm^2/mm^3)
0.4	0.63	0.60	0.58
0.3	0.47	0.47	0.42
0.2	0.31	0.34	0.32
0.1	0.16	0.18	0.15
Uniform random distribution of disc sizes (semi-major axis between 0 and 0.1; $N_V = 400$)			
1.0	0.50	0.49	0.44
0.9	0.49	0.44	0.45
0.8	0.42	0.40	0.38
0.7	0.33	0.31	0.36
0.6	0.31	0.28	0.30
0.5	0.24	0.22	0.22
0.4	0.20	0.18	0.18
0.3	0.14	0.13	0.16
0.2	0.11	0.13	0.11
0.1	0.06	0.06	0.05
Normal distribution of disc sizes ($\mu = 0.2$; $\sigma = 0.06$; $N_V = 100$)			
1.0	14.26	13.20	12.94
0.9	12.19	12.08	11.67
0.8	11.42	10.86	10.89
0.7	9.72	9.31	9.33
0.6	7.55	7.54	7.00
0.5	6.91	7.02	6.38
0.4	6.11	5.99	5.88
0.3	4.23	4.08	3.92
0.2	2.81	2.77	2.67
0.1	1.29	1.31	1.22

Table 6.2 : Data for number of lines per unit area

Disc shape k = b/a	Actual number of discs per unit volume N_V	Calculated N_V $N_V = N_A / \overline{H}$
Discs of constant size (semi-major axis = 0.1mm)		
1.0	400	425
0.9	400	412
0.8	400	392
0.7	400	409
0.6	400	410
0.5	400	405
0.4	400	391
0.3	400	355
0.2	400	432
0.1	400	395
Uniform random distribution of disc sizes (semi-major axis between 0 and 0.1)		
1.0	400	391
0.9	400	415
0.8	400	420
0.7	400	400
0.6	400	431
0.5	400	374
0.4	400	383
0.3	400	386
0.2	400	405
0.1	400	410
Normal distribution of disc sizes ($\mu = 0.2 ; \sigma = 0.06$)		
1.0	100	105
0.9	100	101

Table 6.2 continued :

Disc shape k = b/a	Actual number of discs per unit volume N_V	Calculated N_V $N_V = N_A / \overline{H}$
0.8	100	104
0.7	100	99
0.6	100	95
0.5	100	101
0.4	100	106
0.3	100	103
0.2	100	96
0.1	100	95

It is clear from tables 6.1 and 6.2 that there is good agreement between the calculated and actual values of S_V and N_V. Since, equations (2.13) and (2.31) (used for calculating S_V and N_V) are fundamental relationships in stereology, the methodology used for generating simulated microstructures is valid. The value of mean tangent diameter, $\overline{H}$ (used in calculating N_V) was estimated from equations (4.2) for circular discs (k=1) and equation (4.69) for elliptical discs (k<1). From the self-consistent results, it may be concluded that the above equations for $\overline{H}$ are valid.

The mean ($\bar{l}$) and harmonic mean $\overline{\left(\frac{1}{l}\right)}$ of line lengths can also be obtained ("measured") from the line segments on 2-D microstructures. Equations (4.9) and (4.9b) were used to calculate the mean and the harmonic mean of line lengths respectively for circular discs. A comparison of the "measured" and calculated values are shown in table (6.3)

Table 6.3 : Data for mean and harmonic mean of line lengths

Constant size (radius) of circular discs (mm)	"Measured" from microstructure $\bar{l}$ (mm)	Calculated from equation (4.9) $\bar{l} = \pi R/2$ (mm)	"Measured" from microstructure $\left(\frac{\bar{1}}{l}\right)$ (1/mm)	Calculated from equation (4.9b) $\left(\frac{\bar{1}}{l}\right) = \pi/4R$ (1/mm)
0.1	0.1599	0.1571	8.1117	7.8540
0.2	0.2918	0.3142	4.5637	3.9270
0.3	0.4794	0.4712	2.4137	2.6181
0.4	0.6423	0.6283	1.6984	1.9635
0.5	0.7720	0.7854	1.6370	1.5708
0.6	0.9436	0.9425	1.2509	1.3090
0.7	1.1311	1.0996	1.1040	1.1220
0.8	1.2383	1.2567	0.9552	0.9817
0.9	1.3713	1.4137	0.9115	0.8727
1.0	1.5312	1.5708	0.7321	0.7854

From the above table, it is clear that the equations (4.9) and (4.9 b) hold good for circular discs simulated in 3-D structure within reasonable limits. However, the average value obtained for reciprocal lengths (harmonic mean) is more prone to measurement error because small errors in the smaller line segments can be magnified many-fold. While the same error will not be magnified in the case of mean lengths. If the chances of error in the measurement are higher or the profile has many small line segments, it is recommended that for the calculation of the average disc size, equation (4.9) be used instead of the equation (4.9b).

The 3-D structure simulated for certain distribution of interfaces (discs) can be unfolded using the length distribution of lines obtained from 2-D microstructure by using the methodologies described

The 3-D structure simulated for certain distribution of interfaces (discs) can be unfolded using the length distribution of lines obtained from 2-D microstructure by using the methodologies described in chapter 4. Figures (6.1), (6.2) and (6.3) compare the actual distribution of discs as simulated in 3-D space with the unfolded distributions of discs. The nature of the unfolded distribution remains more or less same as compared to the actual distribution shown in these figures. The values of the calculated μ and σ are found to be very close to the actual values as shown in table 6.4.

Table 6.4 : Actual and calculated data for μ and σ

Disc shape k=b/a	Actual distribution parameters from 3-D structure		Calculated distribution parameters after unfolding the microstructure	
	μ	σ	μ	σ
Discs of constant size				
1.0	0.1	0	0.0.995	0.0005
0.9	0.1	0	0.0912	0.0103
0.8	0.1	0	0.0904	0.0293
0.7	0.1	0	0.0913	0.0408
0.6	0.1	0	0.0892	0.0612
Uniform random distribution of disc sizes				
1.0	1.0	0.3	1.0313	0.2620
0.9	1.0	0.3	0.9316	0.3351
0.8	1.0	0.3	0.9447	0.2665
0.7	1.0	0.3	0.9532	0.3116
Normal distribution of disc sizes				
1.0	1.45	1.5	1.4978	1.5186
0.9	1.45	1.5	1.3556	1.3382
0.8	1.45	1.5	1.4616	1.5750
0.7	1.45	1.5	1.5612	1.6823

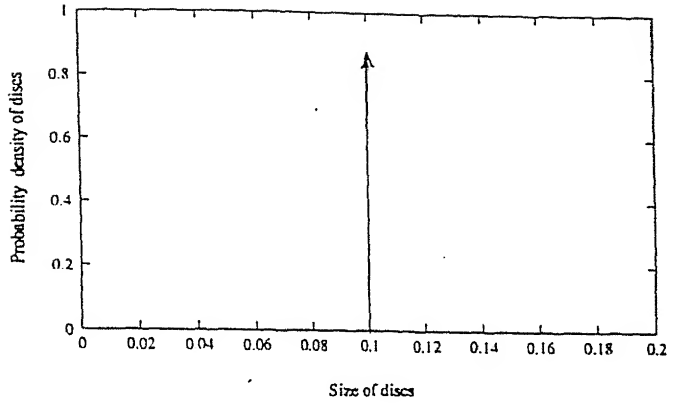

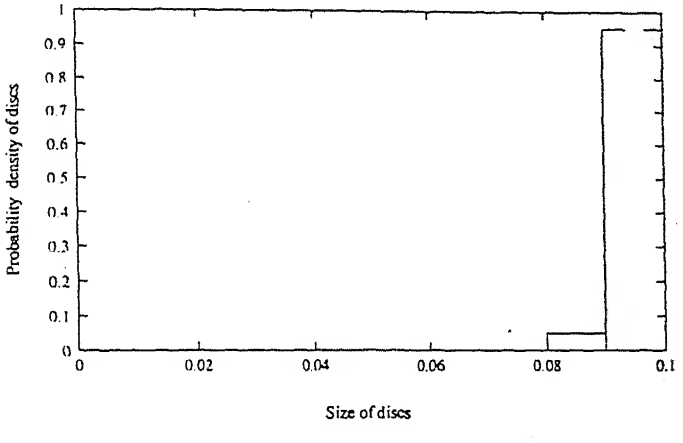

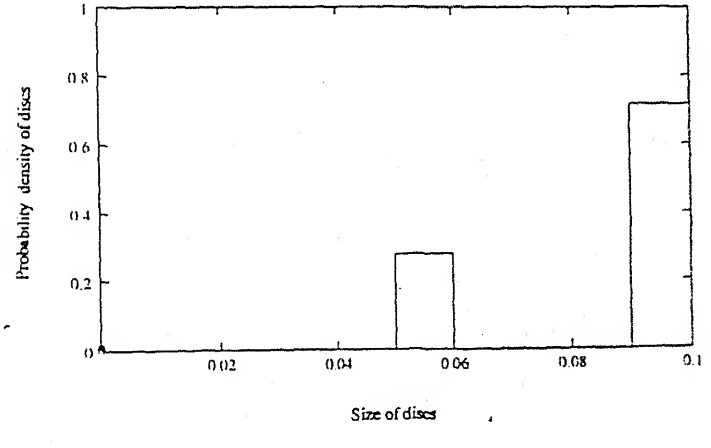

Figure 6.1 : Distribution of discs of constant size
(a) Actual distribution for both k=1 and k=0.6
(b) unfolded distribution for k=1
(c) unfolded distribution for k=0.6

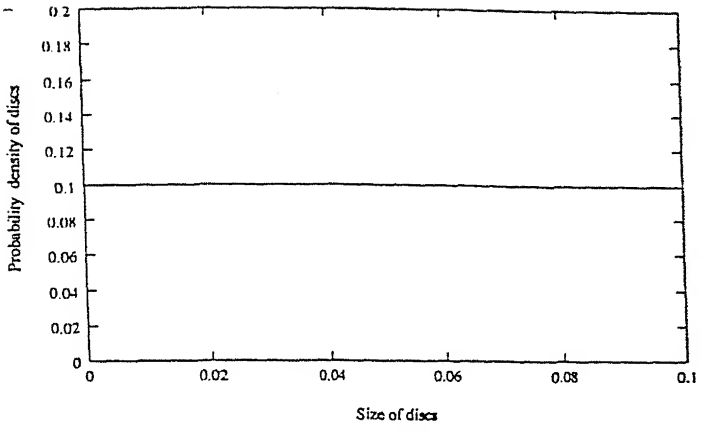

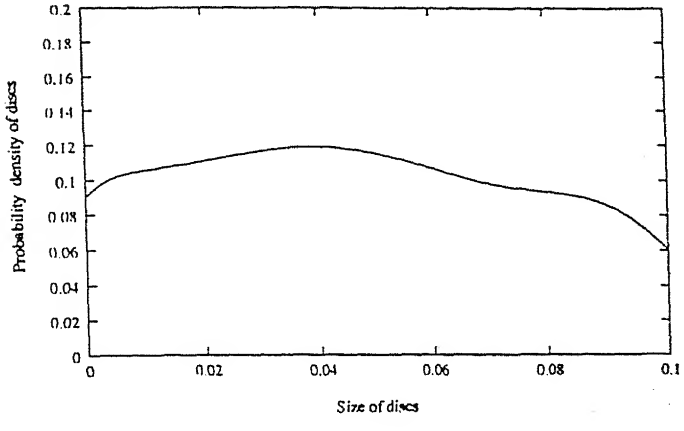

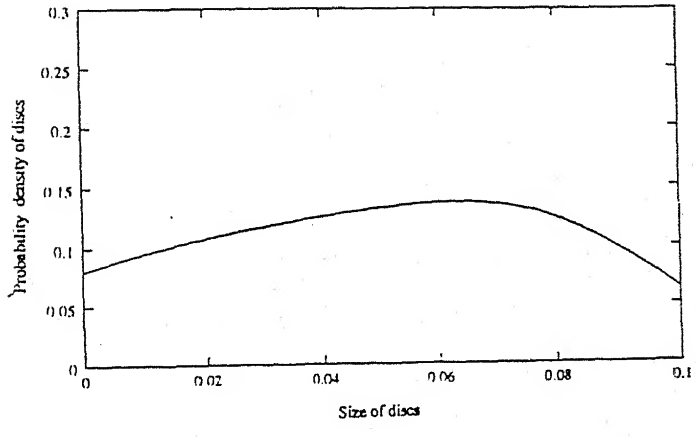

Figure 6.2 : Uniform random distribution of disc size
(a) Actual . distribution for both k=1 and k=0.6
(b) unfolded distribution for k=1
(c) unfolded distribution for k=0.6

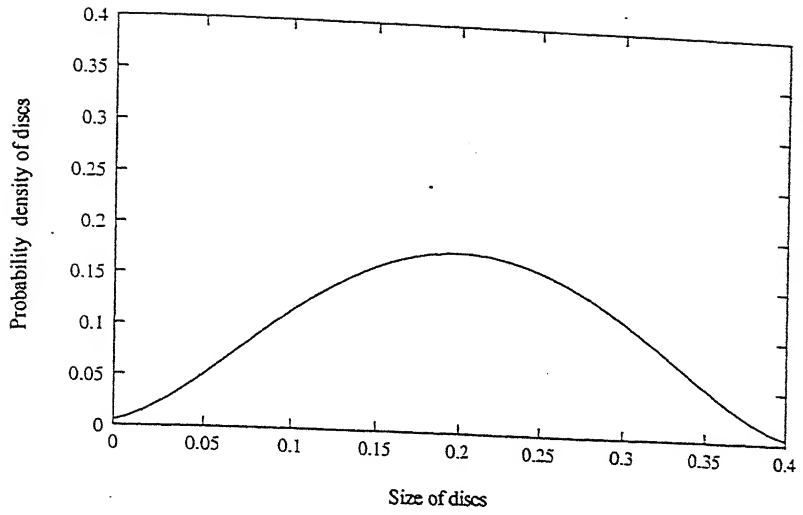

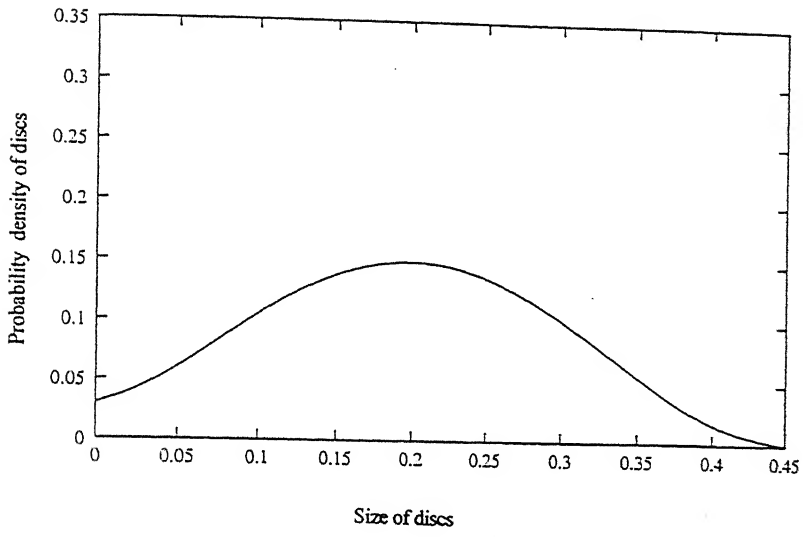

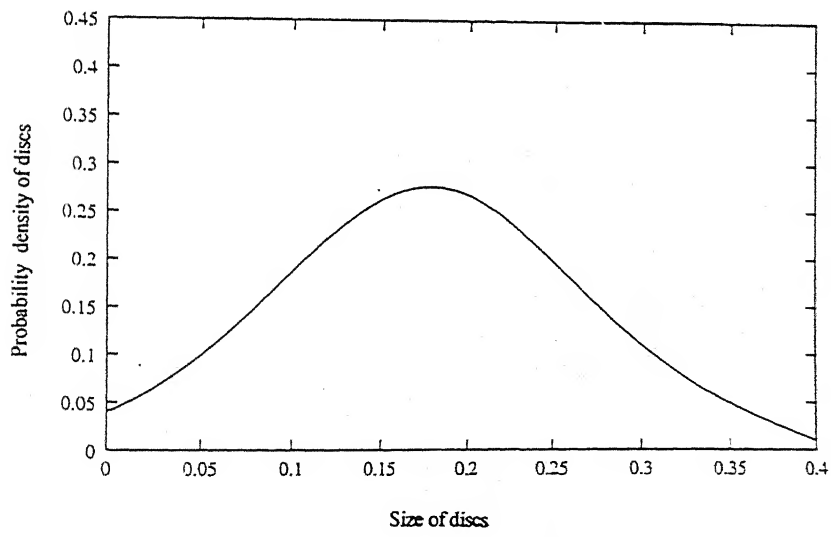

Figure 6.3 : Normal distribution of disc size
(a) Actual distribution for both k=1 and k=0.6
(b) unfolded distribution for k=1
(c) unfolded distribution for k=0.6

It is not always possible to unfold the distribution as one may not have the complete shape information (which is usually lost) from the 2-D microstructure. In order to describe the distribution of elliptical discs completely, it is necessary to know the distribution of both semi-major and semi-minor axes or the distribution of one of the axis and their ratio. This is a bi-variate problem and in order to solve it, bi-variate information is needed, but the section profile provides only uni-variate information (lines are uni-variate). So, from the profile of lines, it would generally be impossible to determine the distribution of both the axes. In order to determine the distribution of both the axes of the elliptical discs, some extra information like the nature of the distribution of discs , the disc shape (k) etc., is required. Equation (4.99) consists of m equations in terms of m+1 unknowns (N_{V1},N_{V2},.....N_{Vm} and k) which can only be solved for m unknowns. In order to reduce the number of unknowns to m, some techniques are proposed to determine the shape factor, k. The methods assume a constant (as a first approximation an average value) shape factor, k, as inclusion of a distribution of shapes would introduce far too many unknowns and the problem would become intractable.

Equation (4.99) can be solved for different values of the shape factor, k to unfold the various possible size distributions of discs. The different size distributions exhibit different characteristics for the appropriate value of k as give in table 6.5.

Table 6.5 : Characteristics of various distributions

Distribution of discs	Characteristics
1. Constant size	All the discs lie in the last class
2. Uniform random	The discs are evenly distributed among the classes
3. Normal	The discs are distributed normally
4. Log normal	Log normal distribution for the discs is obtained
5. Others	Distribution similar to the initial distribution appears for the appropriate value of k

Figures 6.4 to 6.7 show various plots for probability density of lines versus length of lines. A similar plot can also be obtained from the 2-D profile of lines. The plot thus obtained can then be superimposed on these figures. The value of k for which a plot in the respective figure is found close to the plot obtained from the 2-D profile, is the appropriate value of k. However, such a superimposition may result in multiple possibilities.

The coefficient of variation defined as the ratio, σ/μ was calculated for the unfolded size distributions of discs over a range of k varying from 1.0 (for circular case) down to small values. The variation of the calculated σ/μ was plotted as a function of k, as shown in figures (6.8), (6.9) and (6.10). Figures (6.8), (6.9) and (6.10) correspond to actual distributions: normal, log-normal and gamma distributions respectively. In each figure there are several plots corresponding to actual shape of discs given by k=1.0, 0.9, 0.8 and 0.7. It may be noted that the curves in these figures are plotted only up to a certain minimum value of k. The calculations showed that beyond a certain minimum k, the N_V of discs in certain size classes become negative. Since negative values of N_V has no physical significance, the cut off value of k can be determined. Thus, it may be concluded that it is possible to determine a range of values of the shape factor, k from the distribution of line lengths.

The values of N_V in some classes start appearing negative below a certain value of k as discussed above. In the figures 6.8 to 6.10, the only values of k for which all the classes have some positive value of N_V are shown in appendix D-1. For a value of k larger than the actual value, one needs less number of discs in higher classes to get the required number of lines and their contribution to lower classes never exceeds. While below a certain value of k, one needs more number of discs to generate required number of lines in higher classes[3]. The extra discs which are required to fulfill the number of lines in the last few classes contribute more for the lower classes (i.e. generate large number of small lines). As one goes to lower classes, the contribution in a lower class from other higher classes is more than the actual strength of that particular class. In order to compensate these excess number of lines, a negative value to N_V for that particular class gets generated.

---

[3] For an elliptical disc, the probability to find a larger line is lower than that of a circular disc.

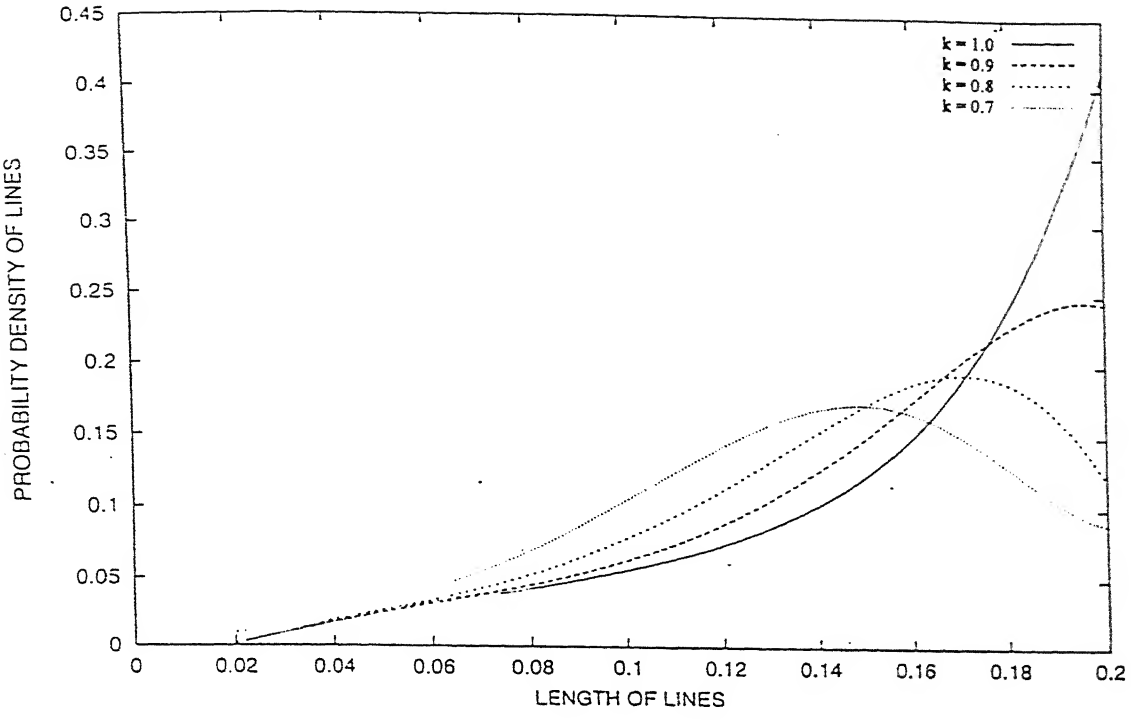

Figure 6.4 : Distribution of lines for discs of constant size.

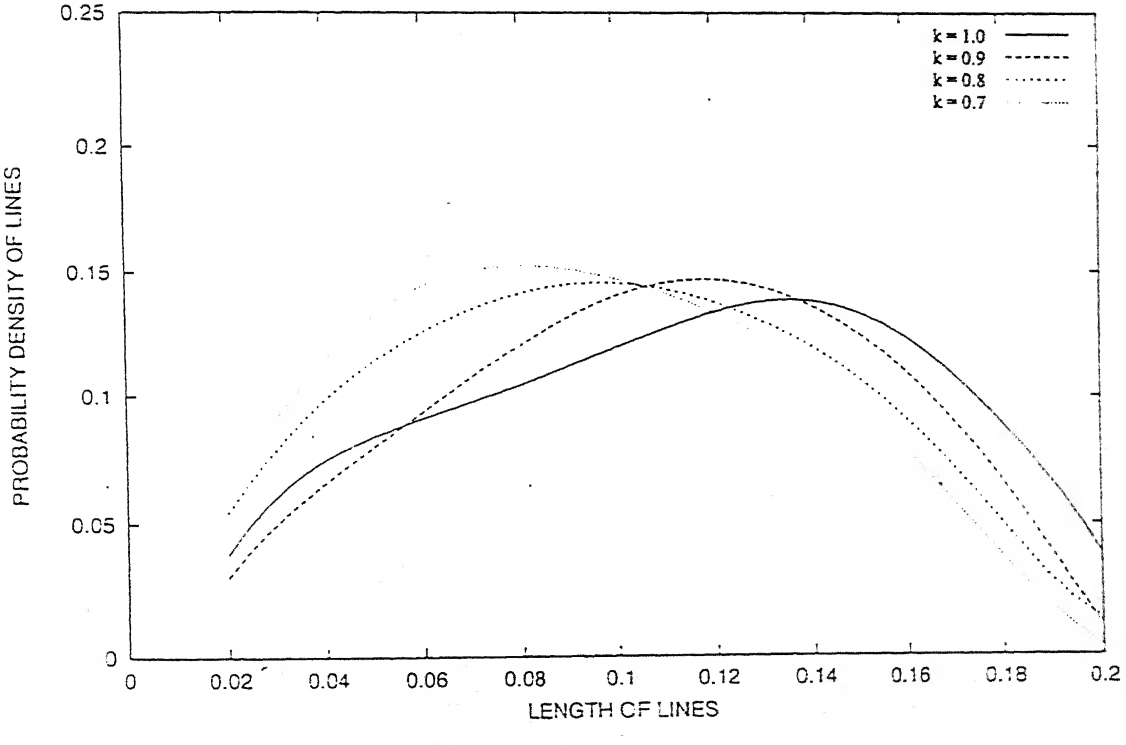

Figure 6.5 : Distribution of lines for uniform random distribution of discs.

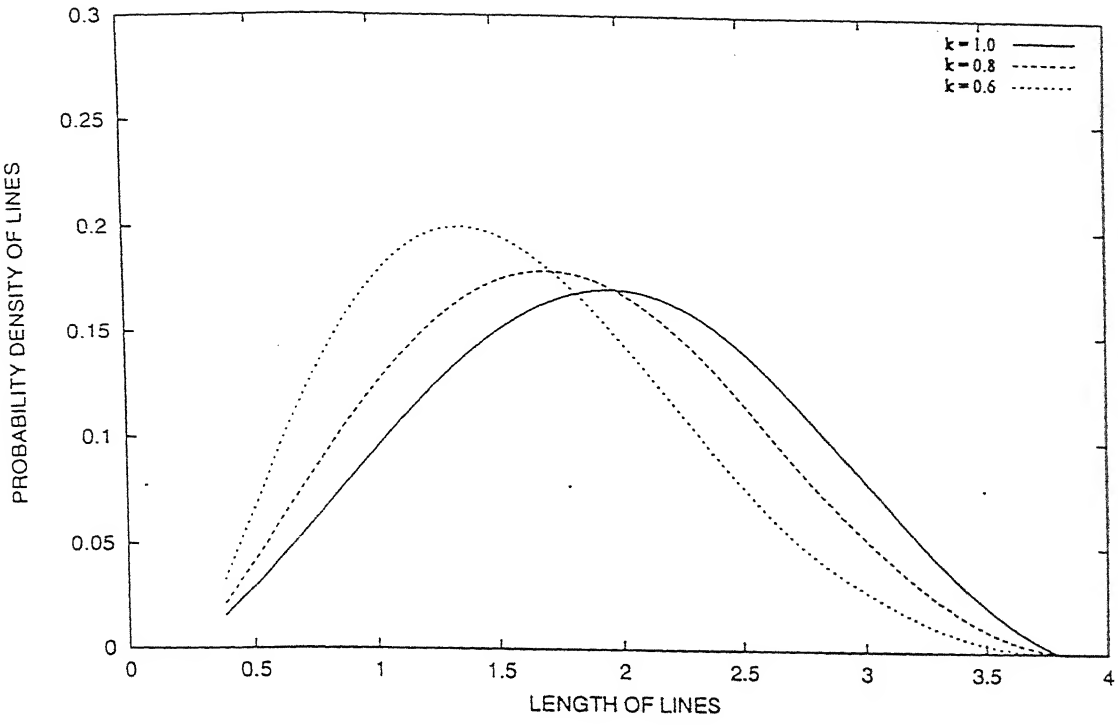

Figure 6.6 : Distribution of lines for normal distribution of discs.

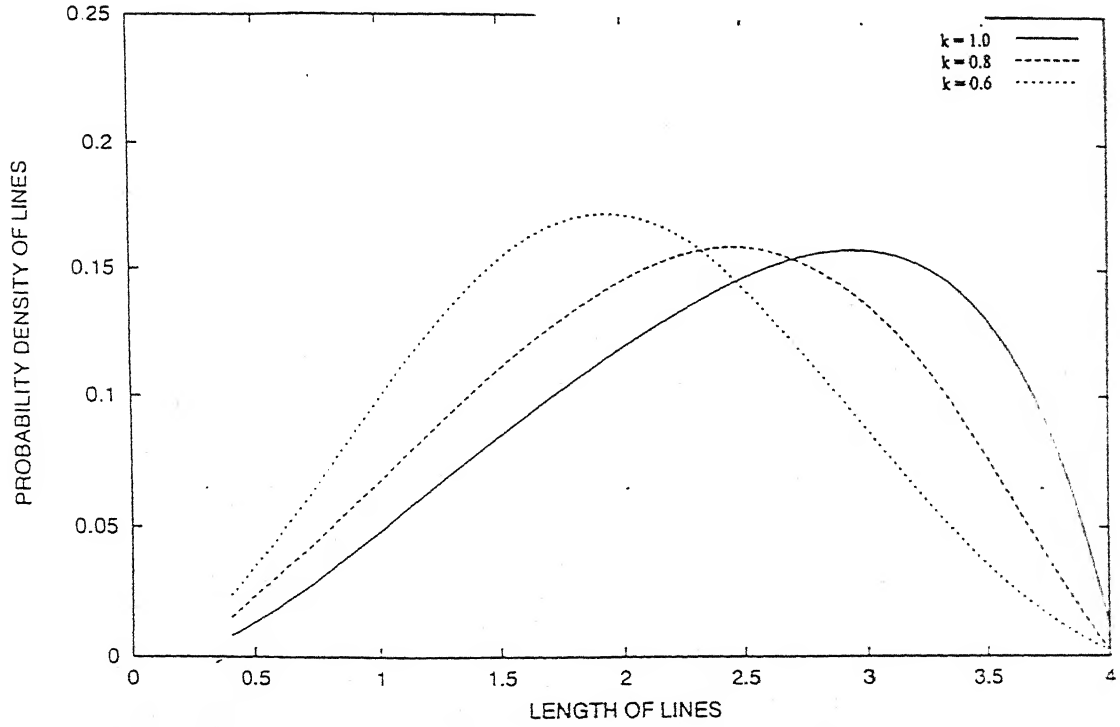

Figure 6.7 : Distribution of lines for beta distribution of discs.

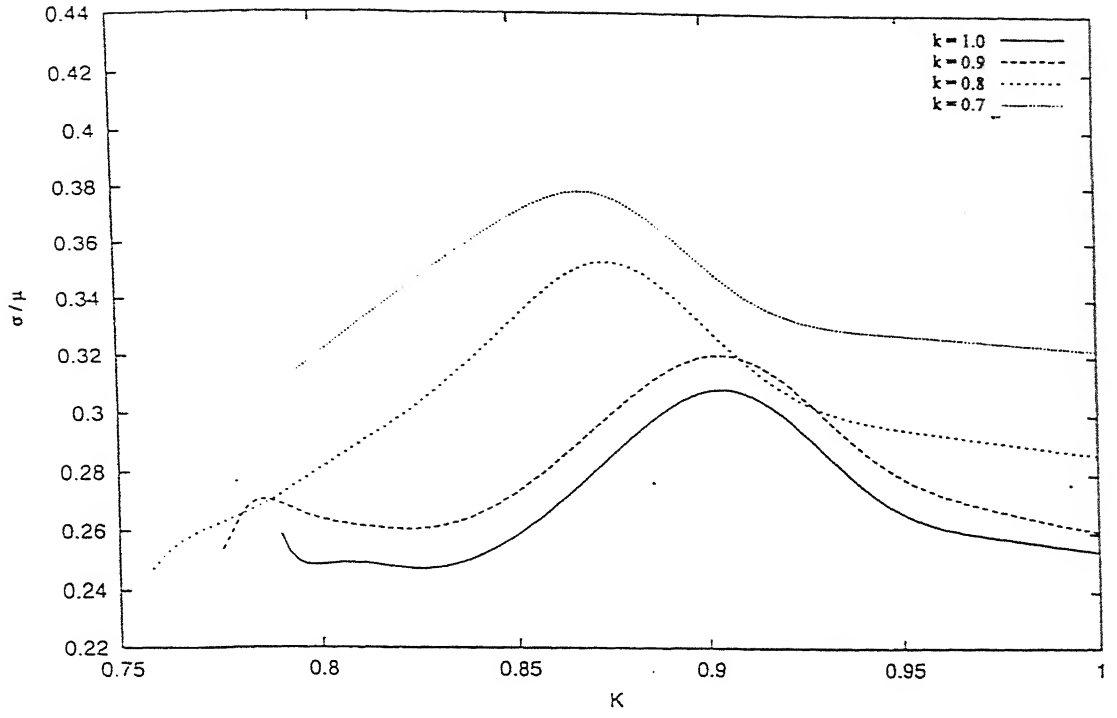

Figure 6.8 : Variation of σ/μ for normal distribution of discs.

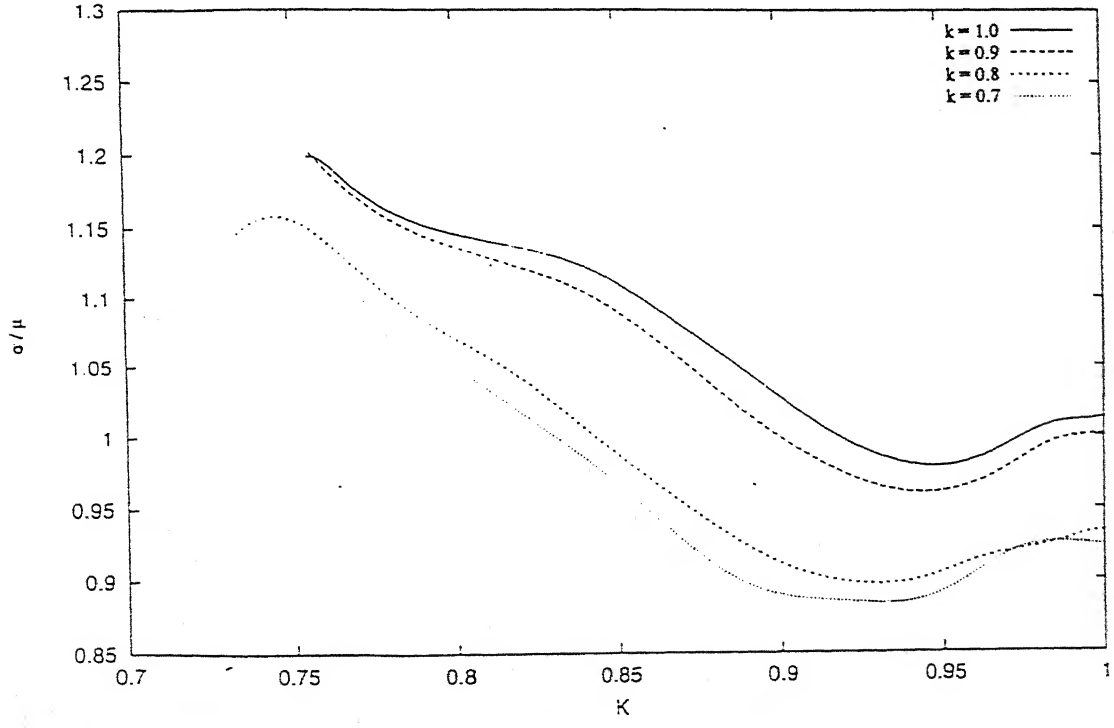

Figure 6.9 : Variation of σ/μ for log normal distribution of discs.

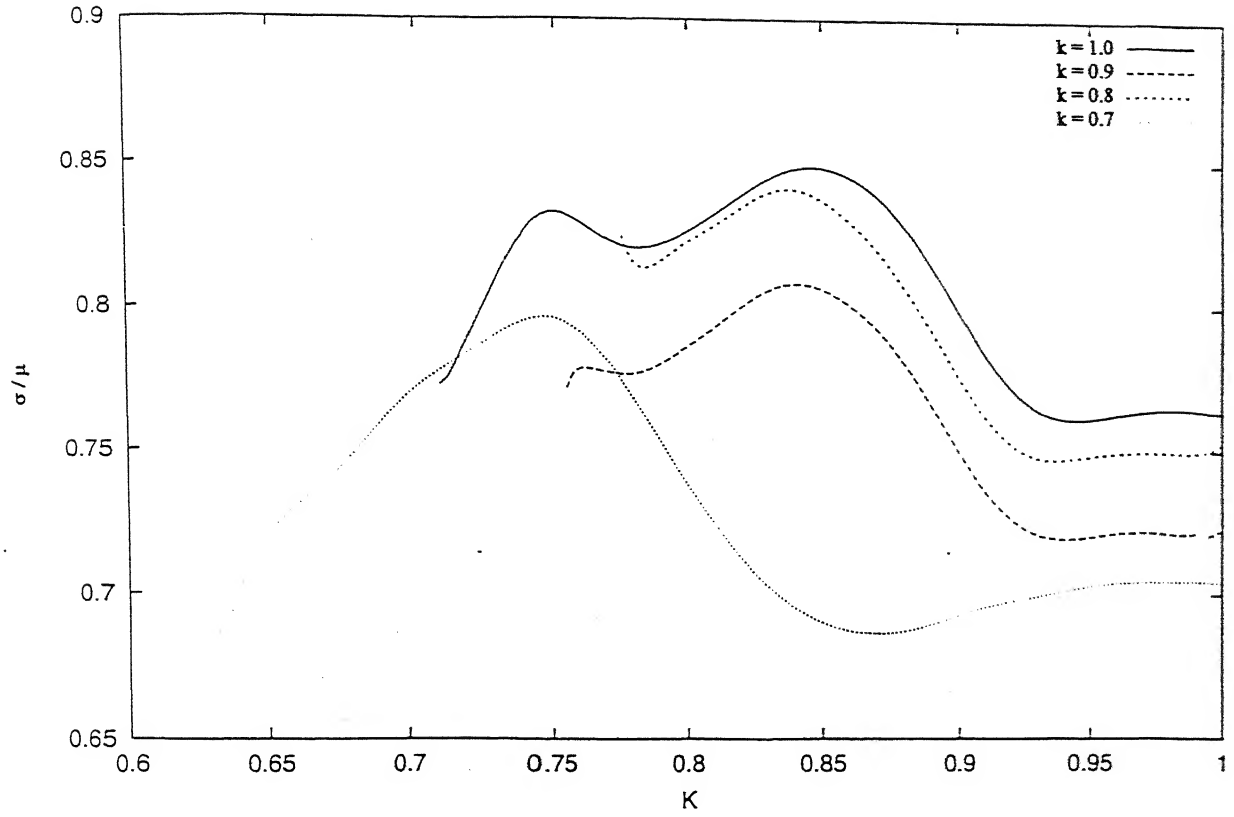

Figure 6.10 : Variation of σ/μ for gamma distribution of discs.

If it is possible to assume a certain distribution of disc sizes then the shape and size of the discs can be completely determined. For example, figure 6.8 shows that for normally distributed discs, the peak in the σ/μ versus k curves coincide with the actual value of k. Such an assumption may be reasonable in view of the fact that many natural processes produce normal distributions.

CHAPTER 7

CONCLUSION

The major conclusions of this study are summarized below.

1. Relationships for mean tangent diameter of circular and elliptical discs have been derived. The validity of these equations were also tested using simulated data.

2. The expected length distribution of line segments in the 2-D microstructure has been determined from a known size distribution and shape of interfaces (modelled as circular and elliptical discs) between particles.

3. Conversely, a methodology for transforming the "measured" line length distribution from observed microstructures to size distribution of discs, assuming circular or elliptical shapes.

4. Without any prior knowledge of shape (circular or elliptical in this case), it has been shown that it is possible to extract some limited information on shape of interfaces from the length distribution of line segments in the 2-D microstructure.

REFERENCES

1. V.Raghavan; "Materials Science and Engineering" 3rd Edition, PRENTICE HALL OF INDIA PRIVATE LIMITED, NEW DELHI P. 266

2. M. Sujata; "Microstructural Evolution of $TiAl_3$ and $TiAl_3$-based Compounds Formed by Reaction Synthesis" , A PhD.Thesis Submitted to The Department of Materials and Metallurgical Engineering, I.I.T Kanpur, Feb 1996 P.194

3. J.E.Burke; "Recrystallization and Sintering in Ceramics" **Sintering Key Papers ;** ELSEVIER SCIENCE PUBLISHERS LONDON , P.30

4. D.Kolar; "Sintering in Chemically Heterogeneous Systems" **SINTERING '85;** Ed..G.c.Kuczynski and M.M.Ristic P 247

5. S.Bhargava and S.Sangal; Pressure Sintering Microstructural Evolution and Deformation of Snows; **"PROCEEDINGS"** Snowsymp-94, Snow and Avalanche Study Establishment Manali(H.P); 26-28 Sept(1994) P.105

6. E.E.Adams, D.C.Vandervoort, M.Q.Edens, R.M.Lang; Ice Grain Orientation in Processed Snow; **"PROCEEDINGS"** Snowsymp-94, Snow and Avalanche Study Establishment Manali(H.P); 26-28 Sept(1994) P.99

7. P.R.Kry; Quantitative Stereological Analysis of Grain Bonds in Snow; **J. Glacial V.14**(1975a) P.72

8. M.G.Edens, R.L.Brown; Measurement of Microstructure from Surface Section; **"PROCEEDINGS"** Snowsymp-94, Snow and Avalanche Study Establishment Manali(H.P); 26-28 Sept(1994) P.64

9. K.C.Agrawal and R.K.Mittal; Influence of Microstructure on Mechanical Properties **"PROCEEDINGS"** Snowsymp-94, Snow and Avalanche Study Establishment Manali(H.P); 26-28 Sept(1994) P.83-84

10. S.Bhargava and S.Sangal; Pressure Sintering, Microstructural Evolution and Deformation of Snows; **"PROCEEDINGS"** Snowsymp-94, Snow and Avalanche Study Establishment Manali(H.P); 26-28 Sept(1994) P.111

11. E.R.Weibel; Stereological Methods; ACADEMIC PRESS , NEW YORK, TORONTO, SYDNEY, SAN FRANCISCO **V.2** (1980) P.2

12. R.E.Miles and P.Davy; Probabilistic Foundations of Stereology. In **"Proceedings of the Fourth International Congrss for Stereology"** ; U.S.GOVERNMENT PRINTING OFFICE, WASHINGTON (1976a) P.443

13. E.R.Weibel; Stereological Methods; ACADEMIC PRESS , NEW YORK, TORONTO, SYDNEY, SAN FRANCISCO **V.2** (1980) P.42

14. R.E.Miles and P.Davy; Precise and General Conditions for the Validity of a Comprehensive Set of Stereological Formuae. **J. Microscopy 107**(1976b) P.211

15. E.R.Weibel; Stereological Methods; ACADEMIC PRESS , NEW YORK, TORONTO, SYDNEY, SAN FRANCISCO **V.2** (1980) P.71

16. E.R.Weibel; Stereological Methods; ACADEMIC PRESS , NEW YORK, TORONTO, SYDNEY, SAN FRANCISCO **V.2** (1980) P.154-155

17. R.T.Dehoff and F.N.Rhines: Determination of the Number of Particles Per Unit Volume from Measurements Made on Random Plane Sections: **Trans AIME 221**(1961) P.975

18. E.R.Weibel; Stereological Methods; ACADEMIC PRESS , NEW YORK, TORONTO, SYDNEY, SAN FRANCISCO **V.2** (1980) P.141-142

19. "Quantitative Microscopy", Ed.. R.T.Dehoff and F.N.Rhines; McGRAW-HILL BOOK COMPANY (1968) P.141

20. G.Prasad; Text-Book on Integral Calculas and Elementary Differential Equations, 12th Edition. POTHISHALA (PRIVATE) LIMITED, ALLAHABAD. P.106

21. E.R.Weibel; Stereological Methods; ACADEMIC PRESS , NEW YORK, TORONTO, SYDNEY, SAN FRANCISCO **V.2** (1980) P.187

APPENDIX

APPENDIX A-1

1. Equation of circle in 3-dimension

Consider a frame XYZ, which contains a circle of radius R. The center of the circle is at the origin of the coordinates. The circle lies on the XY plane and its normal is along Z-axis. Equation of circle in the above frame is given by

$$x^2 + y^2 = R^2 \tag{1}$$

and

$$z = 0 \tag{2}$$

Rotation of coordinates

Frame $X_1Y_1Z_1$ is obtained by rotating frame XYZ by an angle θ (clockwise) around Y-axis.

Frame $X_2Y_2Z_2$ is obtained by rotating frame $X_1Y_1Z_1$ by an angle ϕ (clockwise) around Z_1-axis.

So the transformation of coordinates can be written as :

$$\begin{aligned} x &= x_1 \cos\theta - z_1 \sin\theta \\ y &= y_1 \\ z &= x_1 \sin\theta + z_1 \cos\theta \end{aligned} \tag{3}$$

and

$$\begin{aligned} x_1 &= x_2 \cos\phi - y_2 \sin\phi \\ y_1 &= x_2 \sin\phi + y_2 \cos\phi \\ z_1 &= z_2 \end{aligned} \tag{4}$$

From equations (3) and (4), the overall transformation can be written as :

$$
\begin{aligned}
x &= \cos\theta\cos\phi\, x_2 - \cos\theta\sin\phi\, y_2 - \sin\theta\, z_2 \\
y &= \sin\phi\, x_2 +\_\cos\phi\, y_2 \\
z &= \sin\theta\cos\phi\, x_2 - \sin\theta\sin\phi\, y_2 + \cos\theta\, z_2
\end{aligned} \tag{5}
$$

Substituting the above value of x, y and z in equations (1) and (2) and writting x_2, y_2, z_2 as x, y, z respectively.

$$
\begin{aligned}
&\cos^2\theta\cos^2\phi\, x^2 - 2\cos^2\theta\sin\phi\cos\phi xy - 2\sin\theta\cos\theta\cos\phi xz \\
&+ \cos^2\theta\sin^2\phi\, y^2 + w\sin\theta\cos\theta\sin\phi yz + \sin^2\theta\, z^2 \\
&+ \sin^2\phi\, x^2 + 2\sin\phi\cos\phi xy + \cos^2\phi\, y^2 \\
&= R^2
\end{aligned} \tag{6}
$$

or,

$$
\begin{aligned}
&x^2(\cos^2\theta\cos^2\phi + \sin^2\phi) + y^2(\cos^2\theta\sin^2\phi + \cos^2\phi) \\
&+ z^2\sin^2\theta + 2xy\sin\phi\cos\phi(1-\cos^2\theta) \\
&+ 2\sin\theta\cos\theta\sin\phi zy - 2\sin\theta\cos\theta\cos\phi xz \\
&= R^2
\end{aligned} \tag{7}
$$

and

$$
\sin\theta\cos\phi\, x - \sin\theta\sin\phi\, y + \cos\theta\, z = 0 \tag{8}
$$

If the centre of the circle is at (x_0, y_0, z_0), the equation of circle in 3-dimension can be written as

$$
\begin{aligned}
&(x-x_0)^2(\cos^2\theta\cos^2\phi + \sin^2\phi) + (y-y_0)^2(\cos^2\theta\sin^2\phi + \cos^2\phi) \\
&(z-z_0)^2\sin^2\theta + 2(x-x_0)(y-y_0)\sin\phi\cos\phi(1-\cos^2\theta) \\
&2(y-y_0)(z-z_0)\sin\theta\cos\theta\sin\phi - 2(x-x_0)(z-z_0).\sin\theta\cos\theta\cos\phi \\
&= R^2
\end{aligned} \tag{9}
$$

and

$$(x - x_0)\sin\theta\cos\phi - (y - y_0)\sin\theta\sin\phi + (z - z_0)\cos\theta = 0 \qquad (10)$$

2. Expression for end points of the intersecting line

From equations (9) and (10), coefficient of various terms can be denoted as :

$$a_1 = \cos^2\theta\cos^2\phi + \sin^2\phi$$
$$a_2 = \cos^2\theta\sin^2\phi + \cos^2\phi$$
$$a_3 = (z - z_0)\sin^2\theta$$
$$a_4 = \sin 2\phi\sin^2\theta$$
$$a_5 = (z - z_0)\sin 2\theta\sin\phi$$
$$a_6 = -(z - z_0)\sin 2\theta\cos\phi$$

and

$$b_1 = \tan\phi$$
$$b_2 = -(z - z_0)\cos\theta / \sin\theta\cos\phi$$

The equations (9) and (10) can be rewritten in the following form :

$$a_1 x'^2 + a_2 y'^2 + a_3 z'^2 + a_4 x'y' + a_5 y' + a_6 x' = R^2 \qquad (11)$$

$$x' = b_1 y' + b_2 \qquad (12)$$

where $x' = x - x_0$; $y' = y - y_0$ and $z' = z - z_0$

Equation of a plane at height h from the origin and parallel to x-y plane is given by

$$z = h \qquad (13)$$

From equations (9), (10) and (13), one can write a equation in terms of y′ as:

$$y'^2(a_1 b_1^2 + a_2 + a_4 b_1) + y'(2a_1 b_1 b_2 + a_4 b_2 + a_5 + a_6 b_1) = R^2 - a_3 - a_1 b_2^2 - a_6 b_2 \qquad (14)$$

or

$$Ay'^2 + By' - C = 0 \tag{15}$$

where $A = a_1b_1^2 + a_2 + a_4b_1$, $B = 2a_1b_1b_2 + a_4b_2 + a_5 + a_6b_1$ and $C = R^2 - a_3 - a_1b_2^2 - a_6b_2$.

If y_1' and y_2' are the roots of equation (15), the values of roots can be written as :

$$y_{1'}' = \frac{-B + \sqrt{B^2 + 4AC}}{2A} \tag{16}$$

and

$$y_{2'}' = \frac{-B - \sqrt{B^2 + 4AC}}{2A} \tag{17}$$

Since (x_0 , y_0) is the centre of the disc , the y-coordinates of end-points of the intersecting line can be written as :

$$\begin{aligned} y_1 &= y'_{1'} + y_0 \\ y_2 &= y'_{2'} + y_0 \end{aligned} \tag{18}$$

Similarily the x-coordinates of end-points of the intersecting line can be written as :

$$\begin{aligned} x_1 &= b_1 y'_{1'} + b_2 + x_0 \\ x_2 &= b_2 y'_{2'} + b_2 + x_0 \end{aligned} \tag{19}$$

APPENDIX A-2

1. Equation of ellipse in 3-dimension

Consider a frame xyz which contains an ellipse whose semi-major and semi-minor axes are given by 'a' and 'b' respectively. The ellipse is oriented in such a manner that its major and minor axes lie along x and y-axes of xyz coordinates respectively. The normal of the ellipse lies along z-axis and the centre of the ellipse is cosidered at the centre of the coordinates. Equation of the ellipse in this frame is given by

$$\frac{x^2}{a^2} + \frac{y^2}{b^2} = 1 \tag{1}$$

and

$$z = 0 \tag{2}$$

Rotation of Coordinates

Frame $x_1y_1z_1$ is obtained by rotating frame xyz by an angle ξ (clock wise) around z-axis.

Frame $x_2y_2z_2$ is obtained by rotating frame $x_1y_1z_1$ by an angle θ (clock wise) around y_1-axis.

Frame $x_3y_3z_3$ is obtained by rotating frame $x_2y_2z_2$ by an angle ϕ (clock wise) around z_2-axis.

Transformation of co-ordinates

$$\begin{aligned} x &= \cos\xi\, x_1 - \sin\xi\, y_1 \\ y &= \sin\xi\, x_1 + \cos\xi\, y_1 \\ z &= z_1 \end{aligned} \tag{3}$$

and

$$
\begin{aligned}
x_1 &= \cos\theta\, x_2 - \sin\theta\, z_2 \\
y_1 &= y_2 \\
z_1 &= \sin\theta\, x_2 + \cos\theta\, z_2
\end{aligned}
\tag{4}
$$

and

$$
\begin{aligned}
x_2 &= \cos\phi\, x_3 - \sin\phi\, y_3 \\
y_2 &= \sin\phi\, x_3 + \cos\phi\, y_3 \\
z_2 &= z_3
\end{aligned}
\tag{5}
$$

From equations (3), (4) and (5), the overall transformation can be written as :

$$
\begin{aligned}
x = {} & (\cos\theta\cos\phi\cos\xi - \sin\phi\sin\xi)\, x_3 \\
& - (\sin\xi\cos\phi + \sin\phi\cos\theta\cos\xi)\, y_3 - \sin\theta\cos\xi\, z_3
\end{aligned}
\tag{6}
$$

$$
\begin{aligned}
y = {} & (\sin\xi\cos\theta\cos\phi + \cos\xi\sin\phi)\, x_3 \\
& + (\cos\phi\cos\xi - \sin\xi\sin\phi\cos\theta)\, y_3 - \sin\xi\sin\theta\, z_3
\end{aligned}
\tag{7}
$$

$$
z = \sin\theta\cos\phi\, x_3 - \sin\theta\sin\phi\, y_3 + \cos\theta\, z_3 \tag{8}
$$

The equation of ellipse in 3-dimension is obtained by substituting the above values of x, y and z in equations (1) and (2)

$$x_3^2\left(\frac{(\cos\theta\cos\phi\cos\xi - \sin\phi\sin\xi)^2}{a^2} + \frac{(\sin\xi\cos\theta\cos\phi + \cos\xi\sin\phi)^2}{b^2}\right)$$

$$+ y_3^2\left(\frac{(\sin\xi\cos\phi + \sin\phi\cos\theta\cos\xi)^2}{a^2} + \frac{(\cos\xi\cos\phi - \sin\xi\sin\phi\cos\theta)^2}{b^2}\right)$$

$$+ z_3^2\left(\frac{\cos^2\xi}{a^2} + \frac{\sin^2\xi}{b^2}\right)\sin^2\theta$$

$$+ 2x_3y_3\left(\frac{(\sin\phi\sin\xi - \cos\theta\cos\phi\cos\xi)(\sin\xi\cos\phi + \sin\phi\cos\theta\cos\xi)}{a^2}\right.$$

$$\left. + \frac{(\sin\xi\cos\theta\cos\phi + \cos\xi\sin\phi)(\cos\xi\cos\phi - \sin\xi\sin\phi\cos\theta)}{b^2}\right)$$

$$+ 2y_3z_3\left(\frac{\sin\xi\cos\phi + \sin\phi\cos\theta\cos\xi)\cos\xi}{a^2} + \frac{\sin\xi(\sin\xi\sin\phi\cos\theta - \cos\xi\cos\phi)}{b^2}\right)\sin\theta$$

$$+ 2x_3z_3\left(\frac{(\sin\phi\sin\xi - \cos\theta\cos\phi\cos\xi)\cos\xi}{a^2} - \frac{(\sin\xi\cos\theta\cos\phi + \cos\xi\sin\phi)\sin\xi}{b^2}\right)\sin\theta$$

$$= 1 \qquad (9)$$

and

$$\sin\theta\cos\phi\ x_3 - \sin\theta\sin\phi\ y_3 + \cos\theta\ z_3 = 0 \qquad (10)$$

2. Expression for end points of the intersecting line

Equation (9) can be rewritten as :

$$a_1x_3^2 + a_2y_3^2 + a_3z_3^2 + a_4x_3y_3 + a_5y_3z_3 + a_6x_3z_3 = 1 \qquad (11)$$

where $x_3 = x - x_0$; $y_3 = y - y_0$; $z_3 = z - z_0$; and $a_1, a_2 \ldots\ldots a_6$ are the coefficients of x_3^2, y_3^2 .... and x_3z_3 respectively.

Similarily equation (10) can be rewritten as :

$$x_3 = b_1y_3 + b_2 \qquad (12)$$

where $b_1 = \tan\phi$ and $b_2 = -z_3/\cos\phi\tan\theta$

Equation of a plane in xyz frame which is perpendicular to z-axis and is at a height h from the origin. is given by

$$z = h \tag{13}$$

From equations (9), (10) and (13), one can write a equation in terms of y_3 as:

$$(a_1b_1^2 + a_2 + a_4b_1)y_3^2 + (2a_1b_1b_2 + a_4b_2 + a_5 + a_6b_1)\, y_3 = 1 - a_3 - a_1b_2^2 - a_6b_2$$

$$or \tag{14}$$

$$A\,y_3^2 + B\,y_3 - C = 0$$

where

$$A = a_1b_1^2 + a_2 + a_4b_1$$
$$B = 2a_1b_1b_2 + a_4b_2 + a_5 + a_6b_1$$
$$C = 1 - a_3 - a_1b_2^2 - a_6b_2$$

If y'_1 and y'_2 are the two roots of equation (14) ,the value of roots can be written as:

$$y'_1 = \frac{-B + \sqrt{B^2 + 4AC}}{2A} \tag{15}$$

$$y'_2 = \frac{-B + \sqrt{B^2 + 4AC}}{2A} \tag{16}$$

If (x_0, y_0) is the centre of the disc, the y-coordinates of the end points of the intersecting line can be written as :

$$y_1 = y'_1 + y_0 \tag{17}$$

and

$$y_2 = y'_2 + y_0 \tag{18}$$

Similarily the x-coordinates of end points of intersecting line can be written as :

$$x_1 = b_1 y'_1 + b_2 + x_0 \tag{19}$$

and

$$x_2 = b_2 y'_2 + b_2 + x_0 \tag{20}$$

APPENDIX B

Expressions for d_1 and d_2 defined in section 5.1.1

General equation of a plane in XYZ coordinates is given by

$$Ax + By + Cz + D = 0 \tag{1}$$

where the direction of normal to the plane is [A, B, C] and the magnitude of the normal is given by

$$(A^2 + B^2 + C^2)^{1/2} \tag{2}$$

Equation of a plane passing through any point $q(x_o, y_o, z_o)$, whose normal is along the direction [A, B, C] is given by

$$A(x - x_o) + B(y - y_o) + C(z - z_o) = 0 \tag{3}$$

or

$$Ax + By + Cz - (Ax_o + By_o + Cz_o) = 0 \tag{4}$$

From equations (1) and (4), one can write equation for D as:

$$D = -(Ax_o + By_o + Cz_o) \tag{5}$$

Figure B.1 shows a plane whose normal is given by [A, B, C]. The normal makes an angle θ with Z -axis and the projection of normal on XY plane makes angle ϕ with X-axis. Consider a unit vector $\hat{n}$ parallel to the normal [A, B, C]. The equation for the unit vector can be written as :

$$\hat{n} = i \sin\theta\cos\phi + \hat{j} \sin\theta\sin\phi + \hat{k} \cos\theta \tag{6}$$

where $\hat{i}$, $\hat{j}$, $\hat{k}$ are unit vectors parallel to x, y, z axes respectively.

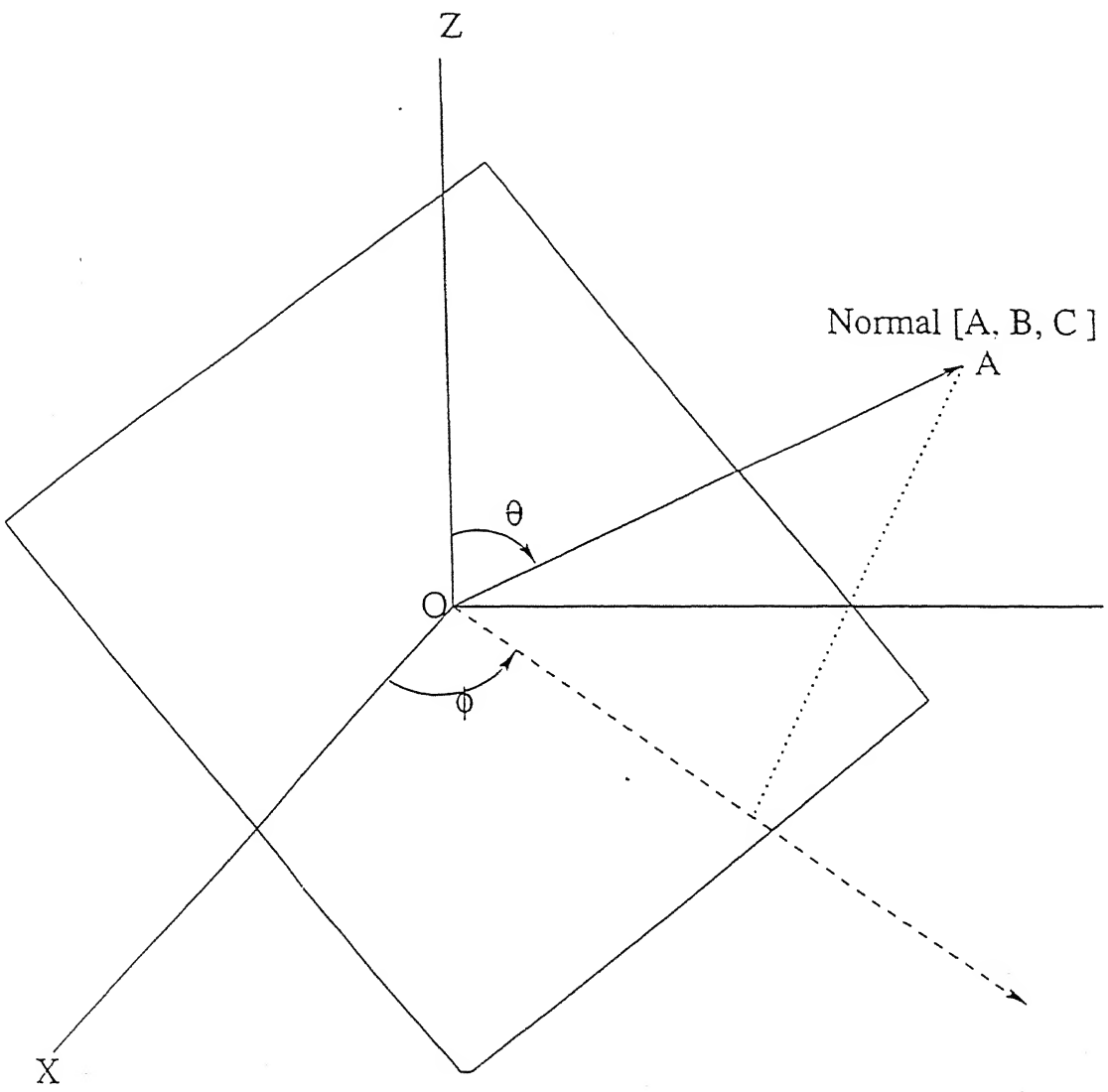

Figure B.1 : Plane of orientation [A, B, C]

The vector oq in figure B1 is given by

$$\overline{oq} = \hat{i}\, x_o + \hat{j}\, y_o + \hat{k}\, z_o \tag{7}$$

Magnitude of vector normal to the plane can be written as:

$$\overline{oq}.\hat{n} = x_o \sin\theta\cos\phi + y_o \sin\theta\sin\phi + z_o\cos\theta$$

Let α, β, γ be the angles which the normal makes with X, Y and Z axes respectively. The direction cosines are given by

$$\begin{aligned} \cos\alpha &= \hat{n}.\hat{i} = \sin\theta\cos\phi \\ \cos\beta &= \hat{n}.\hat{j} = \sin\theta\sin\phi \\ \cos\gamma &= \hat{n}.\hat{k} = \cos\theta \end{aligned} \tag{9}$$

From equations (1) and (9), the values of A, B, C and D can be written as :

$$\begin{aligned} A &= (A^2 + B^2 + C^2)^{1/2}\cos\alpha \\ B &= (A^2 + B^2 + C^2)^{1/2}\cos\beta \\ C &= (A^2 + B^2 + C^2)^{1/2}\cos\gamma \end{aligned} \tag{10}$$

The length of normal from the origin to the plane containing first disc is given by

$$p_1 = x_1 \sin\theta_1\cos\phi_1 + y_1\cos\theta_1\sin\phi_1 + z_1\cos\theta_1 \tag{11}$$

where (x_1, y_1, z_1) and (θ_1, ϕ_1) are the centre and orientation of first disc respectively

The length of normal from the origin to the plane containing second disc is given by

$$p_2 = x_2 \sin\theta_2\cos\phi_2 + y_2\cos\theta_2\sin\phi_2 + z_2\cos\theta_2 \tag{12}$$

where (x_2, y_2, z_2) and (θ_2, ϕ_2) are the centre and orientation of second disc respectively

The Equations of planes containing first and second discs can be written as :

$$A_1x + B_1y + C_1z + D_1 = 0 \tag{13}$$

and

$$A_2x + B_2y + C_2z + D_2 = 0 \tag{14}$$

where

$$A_1 = p_1 \sin\theta_1 \cos\phi_1;$$
$$B_1 = p_1 \sin\theta_1 \sin\phi_1;$$
$$C_1 = p_1 \cos\theta_1$$

$$A_2 = p_2 \sin\theta_2 \cos\phi_2;$$
$$B_2 = p_2 \sin\theta_2 \sin\phi_2;$$
$$C_2 = p_2 \cos\theta_2$$

and

$$D_1 = -(A_1 x_1 + B_1 y_1 + C_1 z_1)$$
$$D_2 = -(A_2 x_2 + B_2 y_2 + C_2 z_2)$$

The equation of the line obtained by intersection of the two planes can be given by the combined equation of the planes as follows :

$$A_1 x + B_1 y + C_1 z + D_1 = 0$$
$$\textit{and} \qquad (15)$$
$$A_2 x + B_2 y + C_2 z + D_2 = 0$$

Distances from the centre of discs to the intersecting line can now be written as :

$$d_1 = \left[\frac{[Z(y_1 - y_o) - Y(z_1 - z_o)]^2 + [X(z_1 - z_o) - Z(x_1 - x_o)]^2 + [Y(x_1 - x_o) + X(y_1 - y_o)]^2}{X^2 + Y^2 + Z^2}\right]^{1/2}$$

and

$$d_2 = \left[\frac{[Z(y_2 - y_o) - Y(z_2 - z_o)]^2 + [X(z_2 - z_o) - Z(x_2 - x_o)]^2 + [Y(x_2 - x_o) + X(y_2 - y_o)]^2}{X^2 + Y^2 + Z^2}\right]^{1/2}$$

where $X = B_1C_2 - C_1B_2$, $Y = C_1A_2 - A_1C_2$, $Z = A_1B_2 - B_1A_2$ and x_0, y_0, z_0 can be obtained by using one of the following equations.

For $X \neq 0$

$$x_o = 0; \quad y_o = \frac{C_1 D_1 - C_2 D_1}{X}; \quad z_o = \frac{B_1 D_2 + B_2 D_1}{X} \qquad (18)$$

or,

For $Y \neq 0$

$$x_o = \frac{C_1 D_2 - C_2 D_1}{Y}; \quad y_o = 0; \quad z_o = \frac{A_2 D_1 - A_1 D_2}{Y} \qquad (19)$$

or,

For $Z \neq 0$

$$x_o = \frac{B_1 D_2 - B_2 D_1}{Z}; \quad y_o = \frac{A_2 D_1 - A_1 D_2}{Z}; \quad z_o = 0 \qquad (20)$$

APPENDIX C-1

This Program Gives the Coordinates of End Points of Lines Obtained from Intersection of Discs and Plane

```
#include <stdio.h>
#include <math.h>
#include <stdlib.h>

#define pi 3.14159

/* This program generates the co-ordinates of lines which are stored in
   a file (sample) */

int i,j,c,k,n,nv,t;
float A,B,C,ML,MM,x1,x2,y1,y2,x01,x02,y01,y02;
float kk,f1,f2,f3,f4,f5,f6,g1,g2,l,h,n1,randno;
float sv,sv0,lina,lin0,sintheta,dx,dy,dz,rr,p1,p2;
float a1,a2,b1,b2,c1,c2,d1,d2,xx,yy,zz,x0,y0,z0,m,p,o,den,dist;
float x[1000],y[1000],z[1000],ra[1000],rb[1000],theta[1000],fi[1000],
      zi[1000],len[1000];

main()
{
FILE *fpt;
fpt= fopen("sample","w");
printf("enter the length of the cube\n");
scanf("%f",&l);
printf("No. of discs/volume\n");
scanf("%d",&nv);
/* Total no of discs in cube */
n1 = l*l*l*nv;
n = n1/1;
printf("the value of n= %d \n",n);
/* 'n' will be an integer */
printf("Give ratio b/a\n");
scanf("%f",&kk);
h=0;
t=0;
c=0;
lin0=0;
sv0=0;
```

```
for(i=1; i<=n; ++i)

{
randno =(float)rand()/(float)RAND_MAX ;
 ra[i] =randno/10.0;
 rb[i]=kk*ra[i];
 sv= pi*ra[i]*rb[i];
 sv0=sv0+sv;
 }
 for(i=1; i<=n; ++i)
 {
 found:
x[i] = l*((float)rand()/(float)RAND_MAX) ;
y[i] = l*((float)rand()/(float)RAND_MAX);
z[i] = l*((float)rand()/(float)RAND_MAX) ;

sintheta =((float)RAND_MAX-2*(float)rand())/(float)RAND_MAX ;
theta[i] = asin(sintheta)+pi/2;
fi[i] = 2*pi*(float)rand()/(float)RAND_MAX ;
zi[i] = 2*pi*(float)rand()/(float)RAND_MAX ;

switch (i)
{
case 1:
break;

default:
for(j=1; j<i; ++j)
{
dx = x[i] - x[j];
dy = y[i] - y[j];
dz = z[i] - z[j];
rr = ra[i] + rb[j];
          if(abs(dx)>rr || abs(dy)>rr || abs(dz)>rr)
 i=i;
                        else
                                {
/* distance from the center of the disc to the line */
  p1=x[i]*sin(theta[i])*cos(fi[i]) + y[i]*cos(theta[i])*sin(fi[i])
     + z[i]*cos(theta[i]);

  p2 = x[j]*sin(theta[j])*cos(fi[j]) + y[j]*cos(theta[j])*sin(fi[j])
       + z[j]*cos(theta[j]);

a1 = p1*sin(theta[i])*cos(fi[i]);
```

```
a2 = p2*sin(theta[j])*cos(fi[j]);
b1 = p1*sin(theta[i])*sin(fi[i]);
b2 = p2*sin(theta[j])*sin(fi[j]);
c1 = p1*cos(theta[i]);
c2 = p2*cos(theta[j]);
d1 = -(a1*x[i]+b1*y[i]+c1*z[i]);
d2 = -(a2*x[j]+b2*y[j]+c2*z[j]);

xx = b1*c2 - c1*b2;
yy = c1*a2-a1*c2;
zz = a1*b2-b1*a2;

if(xx==0.0)
if(yy==0.0)
if(zz==0.0)
  printf(" not possible\n");
   else
    {
     x0=(b1*d2-b2*d1)/zz;
     y0=(a2*d1-a1*d2)/zz;
     z0=0.0;
     }
      else
  {
  x0=(c1*d2-c2*d1)/yy;
  y0=0.0;
  z0=(a2*d1-a1*d2)/yy;
  }
   else
       {
       x0=0.0;
       y0=(c1*d2-c2*d1)/xx;
       z0=(b2*d1-b1*d2)/xx;
       }

/* Distance of the line from the centre of the disc */

   m=pow((zz*(y[i]-y0)-yy*(z[i]-z0)),2);
   p=pow((xx*(z[i]-z0)-zz*(x[i]-x0)),2);
   o=pow((yy*(x[i]-x0)-xx*(y[i]-y0)),2);

   den = pow(xx,2)+pow(yy,2)+pow(zz,2);

    dist=sqrt(m+p+o)/den;
```

```
if(dist>ra[i])
 i=i;
   else
   {
   if(dist<rb[i]){
   ++t;
   goto found;
   }
   else{
   m=pow((zz*(y[j]-y0)-yy*(z[j]-z0)),2);
   p=pow((xx*(z[j]-z0)-zz*(x[j]-x0)),2);
   o=pow((yy*(x[j]-x0)-xx*(y[j]-y0)),2);
   dist=sqrt(m+p+o)/den;
    if(dist<rb[j]){
    ++t;
    goto found;
    }
    else
    i=i;
    }
    }

   }}}}

for(h=0; h<l; h=h+l/10)
{
for(k=1; k<=n; ++k)
{
f1=(pow((cos(theta[k])*cos(fi[k])*cos(zi[k])-sin(fi[k])*sin(zi[k])),2)
    /(ra[k]*ra[k])) + (pow((sin(zi[k])*cos(theta[k])*cos(fi[k])+cos(zi[k])
    *sin(fi[k])),2)/(rb[k]*rb[k]));
f2=(pow((cos(theta[k])*sin(fi[k])*cos(zi[k])+cos(fi[k])*sin(zi[k])),2)
    /(ra[k]*ra[k])) + (pow((-sin(zi[k])*cos(theta[k])*sin(fi[k])+cos(zi[k])
    *cos(fi[k])),2)/(rb[k]*rb[k]));

f3=pow((h-z[k]),2)*pow(sin(theta[k]),2)*((pow(cos(zi[k]),2)/(ra[k]*ra[k]))
   +(pow(sin(zi[k]),2)/(rb[k]*rb[k])));

f4=2*((((sin(fi[k])*sin(zi[k])-cos(theta[k])*cos(fi[k])*cos(zi[k]))*(sin(zi[k]
    *cos(fi[k])+sin(fi[k])*cos(theta[k])*cos(zi[k])))/(ra[k]*ra[k]))
    + (((sin(zi[k])*cos(theta[k])*cos(fi[k])+cos(zi[k])*sin(fi[k]))*(cos(zi[k]
    *cos(fi[k])-sin(zi[k])*sin(fi[k])*cos(theta[k])))/(rb[k]*rb[k])));

f5=2*sin(theta[k])*(h-z[k])*((((cos(fi[k])*sin(zi[k])+cos(theta[k])*sin(fi[k])
    *cos(zi[k]))*cos(zi[k]))/(ra[k]*ra[k])) + (((sin(zi[k])*cos(theta[k])
```

```
    *sin(fi[k])-cos(zi[k])*cos(fi[k]))*sin(zi[k]))/(rb[k]*rb[k])));

f6=2*sin(theta[k])*(h-z[k])*((((sin(fi[k])*sin(zi[k])-cos(theta[k])*cos(fi[k])
    *cos(zi[k]))*cos(zi[k]))/(ra[k]*ra[k])) - (((sin(zi[k])*cos(theta[k])
    *cos(fi[k])+cos(zi[k])*sin(fi[k]))*sin(zi[k]))/(rb[k]*rb[k])));

g1=tan(fi[k]);

g2=-((h-z[k])*cos(theta[k]))/(sin(theta[k])*cos(fi[k]));

A=f1*g1*g1+f2+f4*g1;
B=2*f1*g1*g2+f4*g2+f5+f6*g1;
C=1-f3-f1*g2*g2-f6*g2;
ML=B*B+4*A*C;
if(ML>=0)
{
MM=sqrt(ML);
y1=(-B+MM)/(2*A);
y01=y1+y[k];
x1=(g1*y1+g2);
x01=x1+x[k];
y2=-(B+MM)/(2*A);
y02=y2+y[k];
x2=(g1*y2+g2);
x02=x2+x[k];
 fprintf(fpt,"%f  %f  \n",x01,y01);
fprintf(fpt,"%f  %f  \n",x02,y02);
len[k]=sqrt(pow((x01-x02),2)+pow((y01-y02),2));
lin0=lin0+len[k];
++c;
}
else
len[k]=0;
}
}
printf("No. of lines or discs cutting the plane= %d\n",c);
}
```

APPENDIX C-2

This Program Calculates the Length of Various Profile Lines

```
#include <stdio.h>
#include <math.h>
#include <stdlib.h>

#define pi 3.14159

/* This program calculates the  length of lines */

int i,j,c,k,n,nv,t,q,mm,option,class[50];
float both,lx,fo,fo1,ff,fx1,fx2,v,mu,sigma,min,max,maxsize;
float A,B,C,ML,MM,x1,x2,y1,y2,x01,x02,y01,y02;
float kk,f1,f2,f3,f4,f5,f6,g1,g2,l,h,n1,randno;
float sv,sv0,lina,lin0,sintheta,dx,dy,dz,rr,p1,p2;
float a1,a2,b1,b2,c1,c2,d1,d2,xx,yy,zz,x0,y0,z0,m,p,o,den,dist;
float x[2000],y[2000],z[2000],ra[2000],rb[2000],theta[2000],fi[2000],
      zi[2000],len[2000];
float gamma(int pp);
main()
{
FILE *fpt;
fpt= fopen("out","w");
printf("enter the length of the cube\n");
scanf("%f",&l);
printf("No. of discs/volume\n");
scanf("%d",&nv);
/* Total no of discs in cube */
n1 = l*l*l*nv;
n = n1/1;
printf("the value of n= %d \n",n);
/* 'n' will be an integer */
printf("Give ratio b/a\n");
scanf("%f",&kk);
h=0;
t=0;
c=0;
lin0=0;
sv0=0;
printf("Enter the corresponding # for the type of distribution\n");
```

```
printf(" 1-normal  2-log normal 3-gamma 4-beta 5-weibull \n");
 scanf("%d",&option);
switch (option) {
case 1:
printf("It takes normal distribution\n");
printf("the value of mu\n");
scanf("%f",&mu);
printf("The value of SIGMA\n");
scanf("%f",&sigma);
for(i=1; i<=n; ++i)
{
lx=0;
ff=sigma*sqrt(2*pi)*((float)rand()/(float)RAND_MAX);
for(fo1=0; ff>fo1; fo1=fo1+fo)
{
v=-pow(((lx-mu)/sigma),2)/2;
fx1=exp(v);
lx=lx+((mu+3*sigma)/100);
v=-pow(((lx-mu)/sigma),2)/2;
fx2=exp(v);
fo=((mu+3*sigma)/100)*(fx1+fx2)*0.5;
}
 ra[i] =lx;
 rb[i]=kk*ra[i];
 sv= pi*ra[i]*rb[i];
 sv0=sv0+sv;
 }
 break;
 case 2:
 printf("It gives log normal distribution\n");
printf("the value of alfa\n");
scanf("%f",&mu);
printf("The value of beta\n");
scanf("%f",&sigma);
for(i=1; i<=n; ++i)
{
lx=(mu+3*sigma)/100;
ff=sigma*sqrt(2*pi)*((float)rand()/(float)RAND_MAX);
for(fo1=0; ff>fo1; fo1=fo1+fo)
{
v=-pow(((log(lx)-mu)/sigma),2)/2;
fx1=exp(v)/lx;
lx=lx+((mu+3*sigma)/100);
v=-pow(((log(lx)-mu)/sigma),2)/2;
fx2=exp(v)/lx;
```

```
fo=((mu+3*sigma)/100)*(fx1+fx2)*0.5;
}
 ra[i] =lx;
 rb[i]=kk*ra[i];
 sv= pi*ra[i]*rb[i];
 sv0=sv0+sv;
 }
 break;
case 3:
 printf("It gives  gamma distribution\n");
printf("the value of alfa\n");
scanf("%f",&mu);
printf("The value of beta\n");
scanf("%f",&sigma);
for(i=1; i<=n; ++i)
{
lx=(mu+3*sigma)/100;
ff=pow(sigma,mu)*gamma(mu)*((float)rand()/(float)RAND_MAX);
for(fo1=0; ff>fo1; fo1=fo1+fo)
{
v=-lx/sigma;
fx1=exp(v)*pow(lx,mu-1);
lx=lx+((mu+3*sigma)/100);
v=-lx/sigma;
fx2=exp(v)*pow(lx,mu-1);
fo=((mu+3*sigma)/100)*(fx1+fx2)*0.5;
}
 ra[i] =lx;
 rb[i]=kk*ra[i];
 sv= pi*ra[i]*rb[i];
 sv0=sv0+sv;
}
break;
case 4:
 printf("It gives  beta  distribution\n");
printf("the value of alfa\n");
scanf("%f",&mu);
printf("The value of beta\n");
scanf("%f",&sigma);
for(i=1; i<=n; ++i)
{
lx=(mu+3*sigma)/100;
ff=gamma(mu)*gamma(sigma)*((float)rand()/(float)RAND_MAX)/gamma(both);
for(fo1=0; ff>fo1; fo1=fo1+fo)
{
```

```
v=pow(1-lx,sigma-1);
fx1=pow(lx,mu-1);
lx=lx+((mu+3*sigma)/100);
v=pow(1-lx,sigma-1);
fx2=pow(lx,mu-1);
fo=((mu+3*sigma)/100)*(fx1+fx2)*0.5;
}
 ra[i] =lx;
 rb[i]=kk*ra[i];
 sv= pi*ra[i]*rb[i];
 sv0=sv0+sv;
}
break;
case 5:
 printf("It gives  weibull  distribution\n");
printf("the value of alfa\n");
scanf("%f",&mu);
printf("The value of beta\n");
scanf("%f",&sigma);
for(i=1; i<=n; ++i)
{
lx=(mu+3*sigma)/1000;
ff=((float)rand()/(float)RAND_MAX)/(mu*sigma);
for(fo1=0; ff>fo1; fo1=fo1+fo)
{
v=-mu*pow(lx,sigma);
fx1=pow(lx,sigma-1)*exp(v);
lx=lx+((mu+3*sigma)/100);
v=-mu*pow(lx,sigma);
fx2=pow(lx,sigma-1)*exp(v);
fo=((mu+3*sigma)/100)*(fx1+fx2)*0.5;
}
 ra[i] =lx;
 rb[i]=kk*ra[i];
 sv= pi*ra[i]*rb[i];
 sv0=sv0+sv;
}
break;
default:
printf("Absurd value\n");
break;
}
 for(i=1; i<=n; ++i)
 {
 found:
```

```
x[i] = 1*((float)rand()/(float)RAND_MAX) ;
y[i] = 1*((float)rand()/(float)RAND_MAX);
z[i] = 1*((float)rand()/(float)RAND_MAX) ;

sintheta =((float)RAND_MAX-2*(float)rand())/(float)RAND_MAX ;
theta[i] = asin(sintheta)+pi/2;
fi[i] = 2*pi*(float)rand()/(float)RAND_MAX ;
zi[i] = 2*pi*(float)rand()/(float)RAND_MAX ;

switch (i)
{
case 1:
break;

default:
for(j=1; j<i; ++j)
{
dx = x[i] - x[j];
dy = y[i] - y[j];
dz = z[i] - z[j];
rr = ra[i] + rb[j];
         if(abs(dx)>rr || abs(dy)>rr || abs(dz)>rr)
 i=i;
                        else
                                {
/* distance from the center of the disc to the line */
  p1=x[i]*sin(theta[i])*cos(fi[i]) + y[i]*cos(theta[i])*sin(fi[i])
     + z[i]*cos(theta[i]);

  p2 = x[j]*sin(theta[j])*cos(fi[j]) + y[j]*cos(theta[j])*sin(fi[j])
       + z[j]*cos(theta[j]);

a1 = p1*sin(theta[i])*cos(fi[i]);
a2 = p2*sin(theta[j])*cos(fi[j]);
b1 = p1*sin(theta[i])*sin(fi[i]);
b2 = p2*sin(theta[j])*sin(fi[j]);
c1 = p1*cos(theta[i]);
c2 = p2*cos(theta[j]);
d1 = -(a1*x[i]+b1*y[i]+c1*z[i]);
d2 = -(a2*x[j]+b2*y[j]+c2*z[j]);

xx = b1*c2 - c1*b2;
yy = c1*a2-a1*c2;
zz = a1*b2-b1*a2;
```

```
if(xx==0.0)
if(yy==0.0)
if(zz==0.0)
  printf(" not possible\n");
   else
    {
     x0=(b1*d2-b2*d1)/zz;
     y0=(a2*d1-a1*d2)/zz;
     z0=0.0;
     }
      else
  {
  x0=(c1*d2-c2*d1)/yy;
  y0=0.0;
  z0=(a2*d1-a1*d2)/yy;
  }
   else
       {
       x0=0.0;
       y0=(c1*d2-c2*d1)/xx;
       z0=(b2*d1-b1*d2)/xx;
       }

/* Distance of the line from the centre of the disc */

   m=pow((zz*(y[i]-y0)-yy*(z[i]-z0)),2);
   p=pow((xx*(z[i]-z0)-zz*(x[i]-x0)),2);
   o=pow((yy*(x[i]-x0)-xx*(y[i]-y0)),2);

   den = pow(xx,2)+pow(yy,2)+pow(zz,2);

    dist=sqrt(m+p+o)/den;

 if(dist>ra[i])
  i=i;
    else
    {
    if(dist<rb[i]){
    ++t;
    goto found;
    }
    else{
    m=pow((zz*(y[j]-y0)-yy*(z[j]-z0)),2);
    p=pow((xx*(z[j]-z0)-zz*(x[j]-x0)),2);
    o=pow((yy*(x[j]-x0)-xx*(y[j]-y0)),2);
```

```
    dist=sqrt(m+p+o)/den;
     if(dist<rb[j]){
     ++t;
     goto found;
     }
     else
     i=i;
     }
     }

    }}}}

for(h=0; h<l; h=h+l/10)
{
for(k=1; k<=n; ++k)
{
f1=(pow((cos(theta[k])*cos(fi[k])*cos(zi[k])-sin(fi[k])*sin(zi[k])),2)/(ra[k]
    *ra[k])) + (pow((sin(zi[k])*cos(theta[k])*cos(fi[k])+cos(zi[k])
    *sin(fi[k])),2)/(rb[k]*rb[k]));
f2=(pow((cos(theta[k])*sin(fi[k])*cos(zi[k])+cos(fi[k])*sin(zi[k])),2)/(ra[k]
    *ra[k])) + (pow((-sin(zi[k])*cos(theta[k])*sin(fi[k])+cos(zi[k])
    *cos(fi[k])),2)/(rb[k]*rb[k]));

f3=pow((h-z[k]),2)*pow(sin(theta[k]),2)*((pow(cos(zi[k]),2)/(ra[k]*ra[k]))
   +(pow(sin(zi[k]),2)/(rb[k]*rb[k])));

f4=2*((((sin(fi[k])*sin(zi[k])-cos(theta[k])*cos(fi[k])*cos(zi[k]))*(sin(zi[k])
    *cos(fi[k])+sin(fi[k])*cos(theta[k])*cos(zi[k])))/(ra[k]*ra[k]))
    + (((sin(zi[k])*cos(theta[k])*cos(fi[k])+cos(zi[k])*sin(fi[k]))*(cos(zi[k])
    *cos(fi[k])-sin(zi[k])*sin(fi[k])*cos(theta[k])))/(rb[k]*rb[k])));

f5=2*sin(theta[k])*(h-z[k])*((((cos(fi[k])*sin(zi[k])+cos(theta[k])*sin(fi[k])
    *cos(zi[k]))*cos(zi[k]))/(ra[k]*ra[k])) + (((sin(zi[k])*cos(theta[k])
    *sin(fi[k])-cos(zi[k])*cos(fi[k]))*sin(zi[k]))/(rb[k]*rb[k])));

f6=2*sin(theta[k])*(h-z[k])*((((sin(fi[k])*sin(zi[k])-cos(theta[k])*cos(fi[k])
    *cos(zi[k]))*cos(zi[k]))/(ra[k]*ra[k])) - (((sin(zi[k])*cos(theta[k])
    *cos(fi[k])+cos(zi[k])*sin(fi[k]))*sin(zi[k]))/(rb[k]*rb[k])));

g1=tan(fi[k]);

g2=-((h-z[k])*cos(theta[k]))/(sin(theta[k])*cos(fi[k]));

A=f1*g1*g1+f2+f4*g1;
B=2*f1*g1*g2+f4*g2+f5+f6*g1;
```

```
C=1-f3-f1*g2*g2-f6*g2;
ML=B*B+4*A*C;
if(ML>=0)
{
MM=sqrt(ML);
y1=(-B+MM)/(2*A);
y01=y1+y[k];
x1=(g1*y1+g2);
x01=x1+x[k];
y2=-(B+MM)/(2*A);
y02=y2+y[k];
x2=(g1*y2+g2);
x02=x2+x[k];
fprintf(fpt,"%f  %f  \n",x02,y02); */
len[k]=sqrt(pow((x01-x02),2)+pow((y01-y02),2));
fprintf(fpt,"%f \n",len[k]);
lin0=lin0+len[k];
++c;
}
else
len[k]=0;
}
}
printf("No. of lines or discs cutting the plane= %d\n",c);
lina=lin0/(l*l);
sv0=sv0/(l*l*l);
lina=(4*lina)/pi;
lin0=lin0/c;
printf("Average value of line length is= %f\n",lin0);
printf("4*La/pi = %f\n",lina/10);
printf("S.area/vol = %f\n",sv0);
printf("In how many classes you want to classify the discs\n");
scanf("%d",&mm);
printf("Maximum size of discs\n");
scanf("%f",&maxsize);
for(q=1; q<=mm; ++q)
class[q]=0;
min=0;
max=maxsize/mm;
for(q=1; q<=mm; ++q)
{
for(i=1; i<=n; ++i)
{
if(ra[i]>=min && ra[i]<=max)
++class[q];
```

```
else
i=i;
}
min=min+maxsize/mm;
max=max+maxsize/mm;
printf("No. of discs in %d class = %d\n",q,class[q]);
}
}

float gamma(pp)
int pp;
{
int i;
float t;
t=1.0;
if(pp>1)
{
for(i=1; i<=pp-1; ++i)
t=t*i;
}
else
t=1;
return(t);
}
```

APPENDIX C-3

This Program Calculates Number of Intercepts Per Unit Length(NL) on a Random Line

```
#include<stdio.h>
#include<math.h>
#include<stdlib.h>

#define pi 3.14159

/* This program is used to find the no of intercepts per unit length(NL)
   This program reads the coordinates from a file(sample) and use them
   to find out the value of 'NL'  */
main()
{
FILE *fpt;
int i,j,k,n,intpt;
float c,l,theta,totlen,m1,x0,nl,x[1000],y[1000],m2[500];

fpt=fopen("sample","r");
printf("Enter the no. of lines\n");
scanf("%d",&n);
for(i=1; i<=2*n; ++i)
{
fscanf(fpt,"%f",&x[i]);
fscanf(fpt,"%f",&y[i]);
}
printf("Enter the length of cube\n");
scanf("%f",&l);
totlen=18*l;
theta=0;
intpt=0;
for(j=1; j<=18; ++j)
{
m1=tan(theta);
for(k=1; k<=n; ++k)
{
m2[k]=(y[2*k]-y[2*k-1])/(x[2*k]-x[2*k-1]);
x0=(m2[k]*x[2*k-1]-m1*l/2-y[2*k-1]+l/2)/(m2[k]-m1);
if(x[2*k]>x[2*k-1])
{
```

```
if(x0>=x[2*k-1] && x0<=x[2*k])
++intpt;
else
 intpt=intpt;
 }
   else
     {
     if(x0>=x[2*k] && x0<=x[2*k-1])
       ++intpt;
else
  intpt=intpt;
}
}
theta=theta+(10/180.0)*pi;
}
nl=intpt/totlen;
printf("2*no.of intercept/lengh(nl)= %f\n",2*nl/10);
/* 2*nl is divided by 10 because in cord2.c we have taken lines
from 10 sections  */
}
```

APPENDIX C-4

This Program Obtains the Discrete Distribution of Discs

```
#include<stdio.h>
#include<math.h>
#include<stdlib.h>

# define pi 3.14159

/* This program finds out the distribution of discs from the
   distribution of lines  */
/* This program calculates for various possible values of b/a
   starting from b/a=1 */

float dr,kk;

main()
{
int i,j,m,n,na0,tot,maxno;
int na[200],nv[200],np[200];
float nn,sv,coeff,av,sigma,avg,avgv,sig,sigm,sv0,maxlength;
float min,max,sum,sum1,length[8000];
float kron(int i, int j);
float pc(int i);

FILE *fpt;
FILE *ft;
FILE *ft1;
fpt=fopen("out","r");
ft=fopen("fo","a");
ft1=fopen("lo","w");
printf("Enter the no. of lines\n");
scanf("%d",&n);
nn=n;
printf("The value of n= %d\n",n);
for(i=1; i<=n; ++i)
{
 fscanf(fpt,"%f",&length[i]);
 }
printf("Enter the maxlength of lines\n");
scanf("%f",&maxlength);
```

```
printf("Enter the no of classes\n");
scanf("%d",&m);
na0=0;
tot=0;
dr=maxlength/m;
min=0;
max=dr;
for(i=1; i<=m; ++i)
{
na[i]=0;
}
for(i=1; i<=m; ++i)
{
for(j=1; j<=n; ++j)
{
if(length[j]>=min && length[j]<=max)
++na[i];
  else
    i=i;
        }
min  = min+dr;
max  =max+dr;
na[i]=na[i];
}
for(i=1; i<=m; ++i)
{
printf("na[%d]=%d\n",i,na[i]);
fprintf(ft1,"%f \t  %f\n",maxlength*i/10,na[i]/nn);
}
na0=0;
for(i=1; i<=m; ++i)
na0  =na0+na[i];
fprintf(ft," b/a     \t   mu     \t    sigma     \t  sigma/mu  \n\n");
printf("Total no. of lines=%d\n",na0);
/* na0 must be equal to n */
/* kron(i,j) is defined as a function*/
for(kk=1; kk>=0; kk=kk-0.005)
{
tot=0;
for(j=m; j>0; --j)
{
sum1=0;
for(i=m; i>j; --i)
{
sum  = nv[i]*kron(i,j)*pc(i);
```

```
sum1=sum1+sum;
}
i=j;
nv[i] =(na[j]-sum1)/(kron(i,j)*pc(i));
if(nv[i]>0)
{  np[i]=nv[i];
   nv[i]=nv[i];
                }
     else
        {
          np[i]=nv[i];
          nv[i]=0;}
sv0=0;
for(i=1; i<=m; ++i)
{
sv=nv[i]*pi*kk*i*i*dr*dr/4;
sv0=sv0+sv;
}
avgv=0;
for(i=1; i<=m; ++i)
{
avg=nv[i]*(2*i-1)*0.5*dr*0.5;
avgv=avgv+avg;
}
sigm=0;
for(i=1; i<=m; ++i)
{
sig=nv[i]*pow(((2*i-1)*0.5*dr*0.5 - avgv/tot),2);
sigm=sigm+sig;
}
coeff=sqrt(sigm/tot)/(avgv/tot);
maxno=0;
for(i=1; i<=m; ++i)
{
if(np[i]>maxno)
maxno=np[i];
else
  maxno=maxno;
s }
for(i=1; i<=m; ++i)
{
 if(np[i] < -maxno/10)
 goto last;
 else
   np[i]=np[i];
```

```
}
av=avgv/tot;
sigma=sqrt(sigm/tot);
fprintf(ft," %1.3f \t\t%f       \t  %f   \t  %f \n",kk,av,sigma,coeff);
            }
for(i=1; i<=m; ++i)
printf("termimation k=%f\n",kk);
}
float kron(i,j)
int i,j;
{
/* This complete calculates p(i,j)(prob of lines lying in jth
class after cutting the discs of ith class) */
float k,l,m,m01,m02,th,m0;
m01=0;
m02=0;
for(th=0; th<=pi/2; th=th+pi/100)
{
k=((cos(th)*cos(th)+pow((kk*sin(th)),2))*(2*j-1));
if ((4*i*i*kk*kk - k*(2*j-1)) >0)
{
l=kk*i*sqrt(4*i*i*kk*kk - k*(2*j-1));
m=k/l;
}
else
 m=0;
m01=m01+m;
}
for(th=0; th<=pi/2; th=th+pi/2)
{
k=((cos(th)*cos(th)+pow((kk*sin(th)),2))*(2*j-1));
if ((4*i*i*kk*kk - k*(2*j-1)) >0)
{
l=kk*i*sqrt(4*i*i*kk*kk - k*(2*j-1));
m=k/l;
}
else
 m=0;
m02=m02+m;
}
m0=m01-m02/2;
m0=m0/50;
return(m0);
}
float pc(i)
```

```
int i;
{
float p,t;
p=(1-kk*kk)/(1+kk*kk);
t=4*i*dr*sqrt((1+kk*kk)/2)*(1-p*p/16-15*p*p*p*p/1024)/pi;
return(t);
}
```

APPENDIX D-1

Data for Sigma and Mu Values

The only values of b/a for which any class has more than 10% of the discs of the class which has max no of discs are listed

NORMAL DISTRIBUTION
mu=1 sigma=0.3

actual b/a=1

b/a	mu	sigma	sigma/mu
1.000	1.031283	0.261989	0.254042
0.995	1.028964	0.262205	0.254824
0.990	1.026608	0.262403	0.255602
0.985	1.024167	0.262655	0.256457
0.980	1.020961	0.262854	0.257457
0.975	1.017840	0.262960	0.258351
0.970	1.014654	0.263029	0.259231
0.965	1.010353	0.262797	0.260104
0.960	1.005964	0.262817	0.261259
0.955	1.001018	0.262255	0.261988
0.950	0.993738	0.261284	0.262931
0.945	0.983989	0.258871	0.263083
0.940	0.975867	0.262051	0.268532
0.935	0.969017	0.267029	0.275567
0.930	0.960623	0.273348	0.284553
0.925	0.967177	0.285523	0.295213
0.920	0.971258	0.297394	0.306194
0.915	0.963067	0.307800	0.319604
0.910	0.976605	0.305130	0.312440
0.905	1.002877	0.314780	0.313877
0.900	0.998370	0.347921	0.348489
0.895	1.028552	0.313246	0.304550
0.890	1.034022	0.311973	0.301709
0.885	1.028191	0.312443	0.303876
0.880	1.053045	0.298192	0.283171
0.875	1.070309	0.307699	0.287486
0.870	1.074917	0.293238	0.272801

0.865	1.049284	0.293704	0.279909
0.860	1.073475	0.290772	0.270870
0.855	1.084835	0.282114	0.260053
0.850	1.085137	0.277140	0.255396
0.845	1.085476	0.272699	0.251226
0.840	1.084487	0.259468	0.239254
0.835	1.071921	0.273909	0.255531
0.830	1.087645	0.262454	0.241305
0.825	1.100000	0.262686	0.238805
0.820	1.094122	0.274197	0.250610
0.815	1.042289	0.261252	0.250652
0.810	1.093786	0.273181	0.249758
0.805	1.099341	0.276005	0.251064
0.800	1.104042	0.278119	0.251910
0.795	1.099872	0.261770	0.238001
0.790	1.103040	0.285756	0.259062

actual b/a=.9

b/a	mu	sigma	sigma/mu
1.000	0.968871	0.252741	0.260862
0.995	0.966860	0.252941	0.261611
0.990	0.963991	0.253683	0.263159
0.985	0.961202	0.253947	0.264198
0.980	0.957972	0.254713	0.265887
0.975	0.954412	0.255599	0.267808
0.970	0.950903	0.255909	0.269122
0.965	0.946410	0.256502	0.271026
0.960	0.941646	0.257257	0.273199
0.955	0.935762	0.256795	0.274423
0.950	0.929178	0.256381	0.275922
0.945	0.920016	0.253658	0.275710
0.940	0.912391	0.256601	0.281240
0.935	0.906130	0.261366	0.288443
0.930	0.898544	0.266416	0.296497
0.925	0.904028	0.277021	0.306429
0.920	0.907298	0.288308	0.317766
0.915	0.899303	0.297700	0.331035
0.910	0.912196	0.295950	0.324437
0.905	0.936741	0.305094	0.325698
0.900	0.931569	0.335110	0.359727
0.895	0.960893	0.305109	0.317526
0.890	0.965760	0.304252	0.315039
0.885	0.959939	0.304389	0.317092
0.880	0.984035	0.292996	0.297749

0.875	1.000361	0.303678	0.303568
0.870	1.004831	0.289547	0.288154
0.865	0.980745	0.288517	0.294182
0.860	1.003552	0.286486	0.285472
0.855	1.014767	0.278360	0.274309
0.850	1.015880	0.274297	0.270009
0.845	1.015605	0.269020	0.264887
0.840	1.015442	0.256865	0.252959
0.835	1.001990	0.269749	0.269213
0.830	1.018466	0.259007	0.254311
0.825	1.031512	0.258294	0.250403
0.820	1.024892	0.270369	0.263803
0.815	0.975703	0.256643	0.263034
0.810	1.026060	0.266720	0.259946
0.805	1.028568	0.273956	0.266347
0.800	1.034924	0.271550	0.262386
0.795	1.033118	0.260549	0.252196
0.790	1.035256	0.277759	0.268299
0.785	1.015261	0.300973	0.296449
0.780	1.045363	0.273916	0.262029
0.775	1.037518	0.263029	0.253518

actual b/a=.8

b/a	mu	sigma	sigma/mu
1.000	0.879920	0.252464	0.286917
0.995	0.878650	0.252696	0.287596
0.990	0.876706	0.252605	0.288130
0.985	0.874868	0.253280	0.289507
0.980	0.872737	0.253230	0.290157
0.975	0.870708	0.253162	0.290754
0.970	0.868378	0.253603	0.292042
0.965	0.866140	0.253566	0.292754
0.960	0.863455	0.253624	0.293732
0.955	0.860710	0.253384	0.294389
0.950	0.857633	0.253227	0.295263
0.945	0.853778	0.252972	0.296298
0.940	0.850257	0.252836	0.297364
0.935	0.845179	0.251618	0.297710
0.930	0.839642	0.249038	0.296601
0.925	0.835464	0.250441	0.299762
0.920	0.828983	0.250140	0.301743
0.915	0.821286	0.248136	0.302131
0.910	0.822083	0.255815	0.311180
0.905	0.819707	0.263974	0.322034

0.900	0.780247	0.257581	0.330127
0.895	0.824518	0.278272	0.337497
0.890	0.828145	0.282920	0.341631
0.885	0.822386	0.285390	0.347027
0.880	0.837177	0.302439	0.361260
0.875	0.811232	0.336772	0.415137
0.870	0.846788	0.317680	0.375159
0.865	0.854457	0.295889	0.346289
0.860	0.868918	0.301493	0.346975
0.855	0.887829	0.297513	0.335102
0.850	0.890256	0.307211	0.345081
0.845	0.909906	0.288198	0.316734
0.840	0.921826	0.290496	0.315131
0.835	0.906392	0.281936	0.311053
0.830	0.929658	0.282172	0.303522
0.825	0.942608	0.278182	0.295120
0.820	0.922425	0.287725	0.311922
0.815	0.925866	0.255888	0.276377
0.810	0.939952	0.265530	0.282493
0.805	0.927987	0.286184	0.308392
0.800	0.944677	0.266509	0.282117
0.795	0.958576	0.255124	0.266149
0.790	0.946556	0.261484	0.276248
0.785	0.931514	0.237734	0.255213
0.780	0.952510	0.259882	0.272839
0.775	0.964517	0.250022	0.259220
0.770	0.959962	0.255992	0.266669
0.765	0.970231	0.246798	0.254370
0.760	0.956265	0.245144	0.256355
0.755	0.976787	0.234511	0.240084

actual b/a=.7

b/a	mu	sigma	sigma/mu
1.000	0.795443	0.256470	0.322423
0.995	0.794187	0.256379	0.322819
0.990	0.792706	0.256508	0.323585
0.985	0.791374	0.256460	0.324069
0.980	0.789391	0.256008	0.324311
0.975	0.787761	0.256224	0.325257
0.970	0.786191	0.256097	0.325744
0.965	0.784291	0.256051	0.326474
0.960	0.782277	0.255948	0.327183
0.955	0.779605	0.255103	0.327221
0.950	0.777099	0.254763	0.327838

0.945	0.774410	0.254666	0.328852
0.940	0.771206	0.253430	0.328615
0.935	0.767935	0.252933	0.329368
0.930	0.763581	0.251222	0.329005
0.925	0.759400	0.250209	0.329483
0.920	0.753913	0.248417	0.329504
0.915	0.747254	0.245206	0.328143
0.910	0.747222	0.251115	0.336065
0.905	0.743468	0.254841	0.342773
0.900	0.710563	0.238761	0.336017
0.895	0.744380	0.265088	0.356118
0.890	0.746858	0.270361	0.361998
0.885	0.741239	0.270697	0.365195
0.880	0.751261	0.286881	0.381866
0.875	0.721995	0.307552	0.425975
0.870	0.755999	0.301357	0.398621
0.865	0.766858	0.287561	0.374986
0.860	0.778712	0.294515	0.378208
0.855	0.796348	0.295318	0.370840
0.850	0.796995	0.305385	0.383170
0.845	0.817260	0.294220	0.360008
0.840	0.828894	0.300791	0.362883
0.835	0.813429	0.292188	0.359205
0.830	0.838558	0.294430	0.351115
0.825	0.851581	0.289811	0.340322
0.820	0.832200	0.292414	0.351375
0.815	0.841534	0.274870	0.326629
0.810	0.853630	0.274923	0.322063
0.805	0.838072	0.289635	0.345596
0.800	0.859541	0.275396	0.320399
0.795	0.873851	0.268160	0.306871
0.790	0.864321	0.272058	0.314765
0.785	0.859267	0.250010	0.290958
0.780	0.868247	0.263959	0.304013
0.775	0.883290	0.260408	0.294816
0.770	0.878484	0.263133	0.299530
0.765	0.887154	0.249350	0.281068
0.760	0.875896	0.245708	0.280522
0.755	0.897114	0.237736	0.265001

LOG NORMAL

avg=1.45 sigma=1.5

actual b/a=1

b/a	mu	sigma	sigma/mu

1.000	1.497808	1.518613	1.013890
0.995	1.489546	1.503778	1.009555
0.990	1.487017	1.504578	1.011810
0.985	1.484466	1.501763	1.011652
0.980	1.485794	1.504152	1.012355
0.975	1.483217	1.504956	1.014657
0.970	1.467933	1.441786	0.982188
0.965	1.463277	1.438575	0.983119
0.960	1.453693	1.420692	0.977299
0.955	1.453846	1.422221	0.978247
0.950	1.444126	1.395788	0.966528
0.945	1.436311	1.390926	0.968402
0.940	1.437482	1.393150	0.969160
0.935	1.439738	1.424441	0.989375
0.930	1.432749	1.418933	0.990358
0.925	1.428824	1.416081	0.991082
0.920	1.417630	1.385031	0.977005
0.915	1.415648	1.404859	0.992379
0.910	1.416766	1.421737	1.003508
0.905	1.426316	1.460801	1.024178
0.900	1.416970	1.459104	1.029736
0.895	1.428767	1.491787	1.044108
0.890	1.428943	1.499353	1.049274
0.885	1.415123	1.477700	1.044220
0.880	1.424961	1.536637	1.078371
0.875	1.382390	1.465495	1.060117
0.870	1.422013	1.559174	1.096456
0.865	1.408861	1.494267	1.060621
0.860	1.426752	1.569002	1.099702
0.855	1.445920	1.620692	1.120873
0.850	1.426010	1.590120	1.115084
0.845	1.456634	1.647179	1.130812
0.840	1.441176	1.621003	1.124778
0.835	1.417355	1.598940	1.128115
0.830	1.456694	1.659685	1.139350
0.825	1.482421	1.684193	1.136110
0.820	1.464489	1.666563	1.137983
0.815	1.444932	1.606367	1.111724
0.810	1.508784	1.743770	1.155745
0.805	1.469520	1.695511	1.153785
0.800	1.502058	1.720663	1.145537
0.795	1.510017	1.713334	1.134645
0.790	1.507317	1.731613	1.148805
0.785	1.531173	1.776814	1.160426
0.780	1.541975	1.794839	1.163987

0.775	1.523971	1.763899	1.157436
0.770	1.541516	1.812773	1.175967
0.765	1.571507	1.862780	1.185347
0.760	1.529630	1.839608	1.202649
0.755	1.554104	1.863350	1.198986

actual b/a=.9

b/a	mu	sigma	sigma/mu
1.000	1.449930	1.452698	1.001909
0.995	1.443258	1.443869	1.000423
0.990	1.438505	1.436752	0.998782
0.985	1.439660	1.439049	0.999576
0.980	1.434851	1.435704	1.000595
0.975	1.432000	1.430306	0.998817
0.970	1.415065	1.360443	0.961400
0.965	1.411111	1.357128	0.961744
0.960	1.408116	1.357221	0.963856
0.955	1.409170	1.359388	0.964673
0.950	1.400000	1.340398	0.957427
B			
0.945	1.398972	1.340398	0.958130
0.940	1.381361	1.291051	0.934622
0.935	1.387537	1.338893	0.964942
0.930	1.385373	1.339590	0.966953
0.925	1.383183	1.353403	0.978470
0.920	1.370393	1.302728	0.950624
0.915	1.365957	1.328057	0.972253
0.910	1.369008	1.339295	0.978296
0.905	1.375269	1.375645	1.000273
0.900	1.355641	1.338155	0.987101
0.895	1.376087	1.394350	1.013271
0.890	1.369375	1.382050	1.009256
0.885	1.361417	1.376956	1.011414
0.880	1.380063	1.458448	1.056798
0.875	1.348562	1.390637	1.031200
0.870	1.379808	1.484787	1.076082
0.865	1.361613	1.405110	1.031945
0.860	1.381818	1.494425	1.081492
0.855	1.396574	1.526985	1.093379
0.850	1.390789	1.531913	1.101470
0.845	1.396529	1.545456	1.106641
0.840	1.395333	1.558967	1.117272
0.835	1.365767	1.507863	1.104041
0.830	1.402365	1.573684	1.122164

0.825	1.422504	1.593435	1.120162
0.820	1.414334	1.584298	1.120172
0.815	1.397586	1.534722	1.098124
0.810	1.455517	1.670810	1.147915
0.805	1.425655	1.636619	1.147977
0.800	1.439298	1.618760	1.124687
0.795	1.453086	1.638811	1.127814
0.790	1.457295	1.684435	1.155864
0.785	1.460215	1.668406	1.142576
0.780	1.475812	1.712450	1.160344
0.775	1.461538	1.683421	1.151814
0.770	1.480074	1.742599	1.177373
0.765	1.493680	1.757754	1.176794
0.760	1.454459	1.732394	1.191092
0.755	1.489675	1.793799	1.204154

actual b/a=.8

b/a	mu	sigma	sigma/mu
1.000	1.468085	1.370270	0.933372
0.995	1.467226	1.371417	0.934701
0.990	1.464586	1.359138	0.928002
0.985	1.458333	1.348702	0.924824
0.980	1.455633	1.339525	0.920236
0.975	1.452907	1.337314	0.920440
0.970	1.449261	1.330651	0.918158
0.965	1.446484	1.328352	0.918331
0.960	1.446429	1.330272	0.919694
0.955	1.446372	1.332207	0.921068
0.950	1.443542	1.329879	0.921261
0.945	1.423965	1.247645	0.876177
0.940	1.423800	1.249327	0.877460
0.935	1.418006	1.237664	0.872820
0.930	1.426292	1.299968	0.911432
0.925	1.426136	1.301856	0.912855
0.920	1.409722	1.257218	0.891819
0.915	1.409483	1.258975	0.893218
0.910	1.412129	1.277448	0.904625
0.905	1.404070	1.265841	0.901551
0.900	1.381271	1.199508	0.868409
0.895	1.392647	1.250758	0.898115
0.890	1.412099	1.340876	0.949562
0.885	1.403862	1.330001	0.947387
0.880	1.397611	1.294688	0.926358
0.875	1.378879	1.305776	0.946983

0.870	1.401817	1.353235	0.965344
0.865	1.392391	1.288546	0.925419
0.860	1.407343	1.374898	0.976946
0.855	1.411092	1.386800	0.982785
0.850	1.408688	1.397255	0.991884
0.845	1.414661	1.416688	1.001433
0.840	1.421679	1.440960	1.013563
0.835	1.383167	1.328498	0.960475
0.830	1.438182	1.518368	1.055755
0.825	1.438071	1.487808	1.034586
0.820	1.436808	1.518599	1.056925
0.815	1.443182	1.534049	1.062963
0.810	1.458333	1.524144	1.045127
0.805	1.451742	1.555130	1.071216
0.800	1.461648	1.574972	1.077532
0.795	1.471667	1.565191	1.063550
0.790	1.474038	1.604396	1.088435
0.785	1.468508	1.585683	1.079792
0.780	1.486816	1.637742	1.101509
0.775	1.459486	1.572491	1.077428
0.770	1.495518	1.712800	1.145289
0.765	1.507530	1.726900	1.145516
0.760	1.451176	1.625682	1.120252
0.755	1.463144	1.625058	1.110661
0.750	1.365761	1.736296	1.271303
0.745	1.499739	1.733397	1.155799
0.740	1.471928	1.735260	1.178903
0.735	1.533996	1.694605	1.104700
0.730	1.505901	1.789793	1.188519
0.725	1.605084	1.805933	1.125133
0.720	1.579449	1.741669	1.102707
0.715	1.633457	1.774163	1.086140
0.710	1.621269	1.745726	1.076766
0.705	1.569568	1.708683	1.088633

actual b/a=.7

b/a	mu	sigma	sigma/mu
1.000	1.450079	1.338959	0.923370
0.995	1.449132	1.340062	0.924734
0.990	1.446315	1.337791	0.924965
0.985	1.445350	1.338897	0.926348
0.980	1.445288	1.340886	0.927764
0.975	1.447115	1.342644	0.927807
0.970	1.438607	1.331664	0.925662

0.965	1.440428	1.333428	0.925716
0.960	1.427032	1.295056	0.907517
0.955	1.417414	1.246707	0.879564
0.950	1.417213	1.248426	0.880902
0.945	1.418997	1.250089	0.880967
0.940	1.411010	1.238125	0.877474
0.935	1.404950	1.221658	0.869538
0.930	1.395903	1.208155	0.865501
0.925	1.404412	1.258157	0.895860
0.920	1.404139	1.259967	0.897324
0.915	1.397920	1.256015	0.898488
0.910	1.391638	1.243602	0.893624
0.905	1.380155	1.217082	0.881844
0.900	1.365484	1.175053	0.860539
0.895	1.374130	1.206324	0.877881
0.890	1.370629	1.215873	0.887091
0.885	1.370167	1.217584	0.888639
0.880	1.376770	1.252783	0.909944
0.875	1.343750	1.196593	0.890488
0.870	1.373656	1.299512	0.946024
0.865	1.366892	1.238888	0.906354
0.860	1.382246	1.331643	0.963390
0.855	1.385949	1.344127	0.969824
0.850	1.385550	1.354741	0.977764
0.845	1.398063	1.389262	0.993705
0.840	1.398699	1.401016	1.001656
0.835	1.361842	1.284968	0.943551
0.830	1.405603	1.421148	1.011060
0.825	1.420841	1.446723	1.018216
0.820	1.406011	1.419472	1.009574
0.815	1.419146	1.457975	1.027361
0.810	1.434730	1.471403	1.025560
0.805	1.429961	1.519097	1.062334
0.800	1.436644	1.483806	1.032828
0.795	1.460630	1.539442	1.053958
0.790	1.459493	1.575886	1.079749
0.785	1.470000	1.588938	1.080910
0.780	1.461869	1.550018	1.060299
0.775	1.447597	1.546021	1.067991
0.770	1.476337	1.641521	1.111888
0.765	1.484959	1.659514	1.117549
0.760	1.457105	1.632675	1.120492
0.755	1.459574	1.615550	1.106864
0.750	1.353700	1.666857	1.231335
0.745	1.478448	1.666599	1.127262

0.740	1.460886	1.677217	1.148082
0.735	1.532667	1.695497	1.106239
0.730	1.488082	1.729798	1.162435
0.725	1.594697	1.764826	1.106684
0.720	1.583424	1.759755	1.111361
0.715	1.610230	1.708015	1.060727
0.710	1.605132	1.693349	1.054959
0.705	1.570205	1.694949	1.079444

GAMMA DISTRIBUTION

AVG=1.6 sigma=1.2

actual b/a=1

b/a	mu	sigma	sigma/mu
1.000	1.712597	1.307424	0.763416
0.995	1.710124	1.305037	0.763124
0.990	1.705334	1.304846	0.765156
0.985	1.698834	1.298396	0.764287
0.980	1.695096	1.296614	0.764921
0.975	1.691318	1.295586	0.766021
0.970	1.682827	1.285583	0.763942
0.965	1.672863	1.275157	0.762260
0.960	1.669595	1.274811	0.763545
0.955	1.663690	1.268447	0.762429
0.950	1.655308	1.263418	0.763252
0.945	1.640776	1.244226	0.758315
0.940	1.628472	1.232318	0.756733
0.935	1.618873	1.222821	0.755353
0.930	1.607458	1.214729	0.755683
0.925	1.604167	1.220945	0.761108
0.920	1.599159	1.226759	0.767127
0.915	1.579299	1.207875	0.764817
0.910	1.584271	1.225495	0.773539
0.905	1.597354	1.262653	0.790465
0.900	1.565278	1.254129	0.801218
0.895	1.606324	1.300264	0.809466
0.890	1.601993	1.306750	0.815703
0.885	1.591447	1.305536	0.820345
0.880	1.600189	1.331216	0.831911
0.875	1.553363	1.340118	0.862720
0.870	1.609110	1.375339	0.854720
0.865	1.610027	1.344321	0.834968
0.860	1.631298	1.382157	0.847274
0.855	1.666570	1.417771	0.850712
0.850	1.649038	1.415390	0.858312

0.845	1.685541	1.437537	0.852864
0.840	1.687698	1.445501	0.856493
0.835	1.652621	1.426269	0.863034
0.830	1.706041	1.453931	0.852225
0.825	1.747231	1.467623	0.839971
0.820	1.712018	1.445000	0.844033
0.815	1.692565	1.389355	0.820858
0.810	1.768840	1.451953	0.820850
0.805	1.731413	1.458644	0.842458
0.800	1.787460	1.478620	0.827219
0.795	1.815731	1.483481	0.817016
0.790	1.802900	1.479101	0.820401
0.785	1.806567	1.464752	0.810793
0.780	1.844672	1.497783	0.811951
0.775	1.839837	1.506424	0.818781
0.770	1.852768	1.517568	0.819081
0.765	1.916701	1.554318	0.810934
0.760	1.874247	1.561174	0.832961
0.755	1.923801	1.562799	0.812350
0.750	1.904756	1.709543	0.897512
0.745	1.928017	1.585772	0.822488
0.740	1.932162	1.644921	0.851337
0.735	1.971341	1.569683	0.796251
0.730	1.905242	1.600071	0.839826
0.725	1.979305	1.543024	0.779578
0.720	1.977972	1.586710	0.802190
0.715	2.005569	1.547634	0.771668
0.710	1.980071	1.530373	0.772888

actual b/a=.9

b/a	mu	sigma	sigma/mu
1.000	1.665432	1.203792	0.722811
0.995	1.659776	1.196039	0.720603
0.990	1.656576	1.195330	0.721567
0.985	1.649215	1.188217	0.720475
0.980	1.648684	1.189202	0.721303
0.975	1.642361	1.185422	0.721779
0.970	1.637134	1.184249	0.723367
0.965	1.629512	1.176730	0.722136
0.960	1.624579	1.172655	0.721821
0.955	1.619164	1.171297	0.723396
0.950	1.611310	1.163366	0.722001
0.945	1.599366	1.145154	0.716005

0.940	1.594095	1.144199	0.717774
0.935	1.579016	1.128659	0.714786
0.930	1.573529	1.129363	0.717726
0.925	1.570434	1.131399	0.720437
0.920	1.556455	1.121729	0.720695
0.915	1.540979	1.105445	0.717365
0.910	1.540101	1.118718	0.726393
0.905	1.550327	1.151817	0.742951
0.900	1.517699	1.131474	0.745519
0.895	1.551254	1.178793	0.759897
0.890	1.542969	1.178188	0.763585
0.885	1.531907	1.181902	0.771523
0.880	1.540185	1.206749	0.783509
0.875	1.478777	1.198674	0.810584
0.870	1.535301	1.235997	0.805052
0.865	1.542407	1.215892	0.788308
0.860	1.563469	1.252661	0.801207
0.855	1.593314	1.284767	0.806349
0.850	1.575689	1.284082	0.814934
0.845	1.612853	1.308070	0.811029
0.840	1.616185	1.324116	0.819285
0.835	1.576838	1.291485	0.819035
0.830	1.639055	1.335520	0.814811
0.825	1.676622	1.346917	0.803352
0.820	1.644494	1.325080	0.805768
0.815	1.634421	1.280550	0.783489
0.810	1.712381	1.340458	0.782804
0.805	1.654767	1.325214	0.800846
0.800	1.726008	1.362148	0.789190
0.795	1.756341	1.367685	0.778713
0.790	1.744300	1.366481	0.783398
0.785	1.759248	1.348030	0.766253
0.780	1.774306	1.371019	0.772708
0.775	1.784884	1.391993	0.779879
0.770	1.783654	1.389782	0.779177
0.765	1.845046	1.419792	0.769516
0.760	1.799613	1.421313	0.789788
0.755	1.856015	1.432171	0.771638

actual b/a=.8

b/a	mu	sigma	sigma/mu
1.000	1.555249	1.170462	0.752588
0.995	1.549826	1.161369	0.749355
0.990	1.542118	1.153376	0.747917

0.985	1.541053	1.154109	0.748909
0.980	1.537725	1.153581	0.750187
0.975	1.534076	1.151461	0.750589
0.970	1.528690	1.146847	0.750216
0.965	1.520670	1.138314	0.748561
0.960	1.516283	1.136338	0.749424
0.955	1.509259	1.131310	0.749580
0.950	1.506815	1.132582	0.751639
0.945	1.495476	1.117767	0.747432
0.940	1.488208	1.112321	0.747423
0.935	1.481089	1.102773	0.744569
0.930	1.468109	1.087360	0.740654
0.925	1.461743	1.085492	0.742601
0.920	1.452063	1.077165	0.741817
0.915	1.439773	1.067834	0.741669
0.910	1.445411	1.090129	0.754200
0.905	1.456064	1.123195	0.771391
0.900	1.433923	1.109337	0.773638
0.895	1.453305	1.142198	0.785932
0.890	1.450325	1.146390	0.790436
0.885	1.435128	1.138922	0.793603
0.880	1.442655	1.168051	0.809654
0.875	1.386518	1.152892	0.831502
0.870	1.439749	1.201142	0.834272
0.865	1.440132	1.171899	0.813745
0.860	1.459214	1.213078	0.831323
0.855	1.485911	1.243524	0.836876
0.850	1.470859	1.246252	0.847295
0.845	1.496076	1.259161	0.841642
0.840	1.496711	1.274879	0.851787
0.835	1.460173	1.237896	0.847773
0.830	1.517578	1.287118	0.848140
0.825	1.558043	1.310218	0.840938
0.820	1.524371	1.283617	0.842063
0.815	1.504471	1.222455	0.812548
0.810	1.589606	1.307239	0.822367
0.805	1.525983	1.276022	0.836196
0.800	1.600931	1.324319	0.827218
0.795	1.623118	1.322966	0.815077
0.790	1.609776	1.319946	0.819956
0.785	1.633100	1.313827	0.804499
0.780	1.638508	1.328368	0.810718
0.775	1.669352	1.376955	0.824844

actual b/a=.7

b/a	mu	sigma	sigma/mu
1.000	1.457544	1.026189	0.704054
0.995	1.457541	1.026929	0.704563
0.990	1.457538	1.027674	0.705076
0.985	1.452740	1.022956	0.704157
0.980	1.452717	1.023694	0.704676
0.975	1.451897	1.023955	0.705253
0.970	1.449446	1.019842	0.703608
0.965	1.447772	1.020343	0.704768
0.960	1.447727	1.021084	0.705301
0.955	1.442767	1.016139	0.704299
0.950	1.442701	1.016871	0.704839
0.945	1.442635	1.017609	0.705382
0.940	1.435897	1.003615	0.698946
0.935	1.431590	0.998846	0.697718
0.930	1.431475	0.999529	0.698251
0.925	1.426301	0.994151	0.697014
0.920	1.424419	0.994494	0.698175
0.915	1.424270	0.995171	0.698723
0.910	1.419787	0.990138	0.697385
0.905	1.417836	0.990451	0.698565
0.900	1.413262	0.985276	0.697165
0.895	1.406016	0.969678	0.689663
0.890	1.401316	0.964142	0.688027
0.885	1.399206	0.964273	0.689157
0.880	1.395198	0.959087	0.687420
0.875	1.380376	0.924559	0.669788
0.870	1.380796	0.935655	0.677620
0.865	1.381221	0.946755	0.685448
0.860	1.376174	0.940575	0.683471
0.855	1.373819	0.945617	0.688313
0.850	1.367448	0.939253	0.686866
0.845	1.367800	0.950657	0.695026
0.840	1.357661	0.937246	0.690338
0.835	1.342427	0.915927	0.682292
0.830	1.351230	0.936864	0.693342
0.825	1.361431	0.957528	0.703325
0.820	1.362562	0.959293	0.704036
0.815	1.357859	0.964037	0.709968
0.810	1.380034	1.009589	0.731568
0.805	1.364407	0.979555	0.717935
0.800	1.376706	1.016815	0.738585
0.795	1.384036	1.041638	0.752609
0.790	1.379340	1.036750	0.751628

0.785	1.385927	1.060964	0.765527
0.780	1.387346	1.063494	0.766568
0.775	1.364247	1.048711	0.768710
0.770	1.365506	1.056507	0.773711
0.765	1.381831	1.105160	0.799780
0.760	1.340149	1.058936	0.790163
0.755	1.348684	1.102165	0.817215
0.750	1.158401	0.992965	0.857186
0.745	1.369782	1.106988	0.808150
0.740	1.336946	1.066716	0.797875
0.735	1.439623	1.147371	0.796994
0.730	1.359406	1.066959	0.784872
0.725	1.511961	1.182563	0.782139
0.720	1.498106	1.152647	0.769403
0.715	1.551887	1.186683	0.764671
0.710	1.566399	1.199250	0.765610
0.705	1.478206	1.225510	0.829052
0.700	1.557261	1.206976	0.775063
0.695	1.587209	1.209630	0.762111
0.690	1.659483	1.247126	0.751515
0.685	1.585500	1.238876	0.781379
0.680	1.617110	1.178241	0.728609
0.675	1.722868	1.267939	0.735947
0.670	1.671092	1.257694	0.752618
0.665	1.705040	1.215641	0.712969
0.660	1.709012	1.279517	0.748688
0.655	1.770916	1.272506	0.718558
0.650	1.700884	1.256257	0.738591
0.645	1.817036	1.284618	0.706985
0.640	1.770094	1.278570	0.722318
0.635	1.835714	1.238256	0.674536
0.630	1.764768	1.209625	0.685430

Date Slip

This book is to be returned on the date last stamped

A 125479
